CHEMICAL REVIEWS

Review

Emulating Human Tissues and Organs: A Bioprinting Perspective Toward Personalized Medicine

Ana Clotilde Fonseca,[∇] Ferry P. W. Melchels,[∇] Miguel J. S. Ferreira, Samuel R. Moxon, Geoffrey Potjewyd, Tim R. Dargaville, Susan J. Kimber, and Marco Domingos*
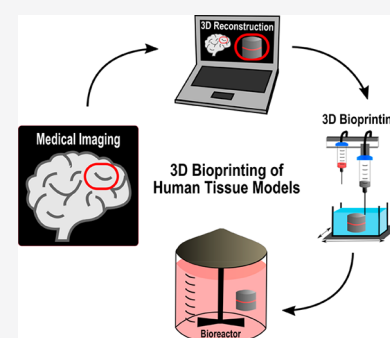
Cite This: https://dx.doi.org/10.1021/acs.chemrev.0c00342

Read Online

ACCESS | Metrics & More | Article Recommendations

ABSTRACT: The lack of in vitro tissue and organ models capable of mimicking human physiology severely hinders the development and clinical translation of therapies and drugs with higher in vivo efficacy. Bioprinting allow us to fill this gap and generate 3D tissue analogues with complex functional and structural organization through the precise spatial positioning of multiple materials and cells. In this review, we report the latest developments in terms of bioprinting technologies for the manufacturing of cellular constructs with particular emphasis on material extrusion, jetting, and vat photopolymerization. We then describe the different base polymers employed in the formulation of bioinks for bioprinting and examine the strategies used to tailor their properties according to both processability and tissue maturation requirements. By relating function to organization in human development, we examine the potential of pluripotent stem cells in the context of bioprinting toward a new generation of tissue models for personalized medicine. We also highlight the most relevant attempts to engineer artificial models for the study of human organogenesis, disease, and drug screening. Finally, we discuss the most pressing challenges, opportunities, and future prospects in the field of bioprinting for tissue engineering (TE) and regenerative medicine (RM).

CONTENTS

ACS Publications   A

1. INTRODUCTION

At present, most of our understanding of human physiology and tissue/organ pathology arises from studies performed on 2D/3D cell culture systems and animal models. While commonly used in vitro 2D culture systems are advantageous for addressing specific experimental questions, they are often oversimplifications that generally ignore the heterogeneity as well as the complexity of the tissue microenvironment. Factors such as tissue architecture, cell–cell and cell–matrix interactions and biophysical cues of the 3D niche are all critical characteristics of the system but are ignored in reductionist 2D and even 3D cell culture systems.[1] Animal models are frequently employed to satisfy regulatory agencies of efficacy and safety by in vivo preclinical testing of human therapies, and, although their usefulness cannot be argued (e.g., wound healing therapies), the truth is that in most cases the lack of genetic, molecular, and physiological relevance to human clinical conditions strongly hinders their success in human predictability.[2,3] Thus, models that more accurately represent the human biology are needed for these purposes. Biofabrication offers a potential route to generate complex 3D biological constructs capable of replicating the functional organization of human tissues while promoting physiologically relevant cellular interactions. This emergent area in tissue engineering (TE) and regenerative medicine (RM) comprises both printing and assembly processes for the automated generation of biologically functional tissue analogues from living cells, biomaterials, and bioactive molecules.[4] Even though it cannot be considered a bioprinting or bioassembly technology on its own, microfluidics play a central role in the field of biofabrication by enabling the handling of materials, cells, and fluids on a small scale and with high precision.[5] This and other areas have witnessed substantial development over the past decade, and several reviews have been published

covering the different aspects related to biofabrication.[6−8] Bioprinting falls under the general umbrella of biofabrication and can be defined as a group of computer-controlled techniques operating in a layer-by-layer fashion that when combined with computer aided design (CAD), or medical imaging, allow the production of patient-specific models/implants with precise 3D spatial positioning of multiple living and nonliving materials.[4,8] Depending on the printing mechanism, bioprinting techniques can be subdivided into four categories, namely, material extrusion, vat photopolymerization, binder/material jetting, and powder bed fusion.[9] Since their introduction in the field of TE, bioprinting techniques have predominantly been used to manufacture 3D acellular scaffolds with precise internal geometries capable of instructing the function of adherent cells both in vitro as well as in vivo.[10−13] However, the combined use of prefabricated constructs, cells, and molecules for direct in vivo implantation or following in vitro tissue maturation process (e.g., incubation), has fallen short of ideal in replicating the hierarchical organization of functional tissues. This can be partially attributed to the fact that bioprinted scaffolds are generally devoid of true 3D nano- and microscale features essential for promoting homogeneous colonization or spatial organization of seeded cells.[14] Various methods have been developed to pattern the surface of engineered scaffolds with chemical or physical cues, and these are comprehensively reviewed elsewhere.[15,16] More recently, the use of bioactive materials as cell-loadable systems has been investigated for the automated manufacturing of 3D constructs with predetermined architectural organization and cellular arrangement.[17−20] This approach requires all components of the final 3D construct (i.e., materials, cells, and bioactive compounds) to be combined in the form of a printable bioink thus further increasing the complexity of the process and in particular of the materials.[21] Their formulation encompasses very stringent and sometimes even antagonistic requirements in order to ensure the printing of well-defined constructs without affecting cell viability and function. It is important that engineered bioinks comply with requirements, including printability, mechanics, bioactivity, and biodegradation.[22] The level of printability of a bioink depends both on its rheological behavior during printing as well as on its ability to retain the predefined shape post printing. Several rheological parameters, including viscosity, shear thinning, recovery, and yield stress, are likely to influence material printability at different stages of the process and are imposed mainly by the printing system.[23] Viscosity is clearly one of the most relevant parameters for bioink design, as it can have a direct effect not only on printability but also on cell viability by shielding the cells from potentially damaging shear stresses. This and other rheological properties are discussed in detail in section 4.1. Mechanical stiffness plays an important role in directing the behavior of encapsulated cells and should mimic the extracellular matrix (ECM) microenvironment of healthy and diseased tissues.[24,25] Further insight into the contribution of mechanical stiffness and network topology of polymeric hydrogels to controlling cell behavior are provided in section 4.2. Encapsulated cells should gradually replace structural materials with newly synthesized ECM. This represents a key step toward the in vitro and in vivo generation of functional tissues and should be facilitated by the enzymatic degradation of bioinks.[26,27] Given the above requirements, it makes sense for hydrogels to be the main candidates for bioprinting of cell-laden constructs. These

hydrophilic and highly hydrated polymers are extremely attractive due to their biomimetic nature, which in many ways replicates the native ECM. Besides allowing for homogeneous cell encapsulation and colonization, most hydrogels also display rheological properties suitable for the manufacturing of 3D constructs without loss of shape fidelity. The growing interest in hydrogels as biomaterials for bioinks has resulted in numerous detailed reviews covering polymer chemistries and their applications.[6,22,28−30] Recent progress in stem cell technology is likely to drive a paradigm shift in RM and disease modeling. The integration of induced pluripotent stem cell (iPSC) technology with advanced bioprinting systems can potentially deliver a new generation of disease models and tissue constructs for the development and testing of personalized therapies with enhanced efficacy and reduced costs.[31,32] This is especially so when combined with incorporation of patient-derived iPSCs carrying heritable mutations. The current review is not aimed at giving another overview of the techniques and materials used for the bioprinting of 3D tissue and organ models and their applications in TE, RM, or disease therapeutics. This has been well covered elsewhere, and we direct the reader to recent review articles.[6,22,33−38] The focus is rather on the different functions of polymeric materials, in particular cell-loadable hydrogels, serving in bioprinting processes, and what properties of the materials are exploited in which way to serve these functions. By relating behavior to structure and properties, this review attempts to unravel why certain materials work well for bioprinting, hence providing a guide toward the selection of appropriate existing materials, and designing tailored matrices that suit both the fabrication and subsequent tissue maturation stages. Importantly, by bringing together two of the major pillars in TE&RM (i.e., bioinks and stem cells) and discussing how these can be effectively integrated using 3D bioprinting, we aim to provide the reader with a unique toolbox for the generation of tissue and organ models, where human developmental pathways or disease mechanisms can be replicated and studied through the adequate incorporation of human pluripotent stem cells (hPSCs) or iPSCs, respectively. After introducing the most relevant bioprinting systems used in the fabrication of cell-laden constructs, we will give an overview of polymeric hydrogels used as biomaterials in bioinks, including both the base polymers and their functional modifications. The dichotomy between the properties required for the fabrication and tissue maturation stages is discussed and how these properties can be decoupled, allowing researchers to engineer suitable bioinks for both stages. We then outline how the combination of stem cell technology with bioprinting opens new avenues for the development of personalized therapies while placing additional requirements on the materials and techniques used for the fabrication of patient-specific tissue models. We review the most recent progress in bioprinted tissue/organ models aimed at tissue regeneration, disease modeling, and drug screening. The latter is not the primary focus of this review, and we direct the reader to a recent article where this topic is covered in detail.[39] Finally, we conclude with a critical overview of the challenges in bioprinting and discuss future prospects for the design and manufacture of realistic tissue models.

2. BIOPRINTING TECHNIQUES

2.1. Material Extrusion-Based Systems

Extrusion bioprinters work on the basis of dispensing a continuous filament of bioink to generate 3D structures in a layer-by-layer fashion.[40] Generally, extrusion systems comprise a material reservoir, a printing head which deposits the bioink, a moveable printing stage, and a positioning system that allows the printing head to move along the x, y, and z axes. Extrusion bioprinters can be classified into pneumatic or mechanical depending on the driving mechanism used to assist the dispensing. The latter can be further divided into piston- or screw-driven systems. Pneumatic and piston mechanisms are, however, often preferred for the extrusion of cell-loadable bioinks, with screw-driven systems commonly applied to the printing of acellular materials.[41−43] Despite sharing the same working principle, the two platforms (pneumatic and piston) utilize different mechanisms for dispensing. Independently of the configuration (i.e., valve-based or valve-free), pneumatic bioprinters use air pressure to promote the extrusion of bioinks through the print head and nozzle. Valve-free configurations are preferred because of their simplicity and ease of operation but are clearly limited by the lack of precise control over the material flow rate. On the other hand, the incorporation of pneumatic valves allows for better pressure control and pulse frequency, which is vital for high-precision applications. Piston-driven systems use positive displacement to trigger extrusion and provide a higher degree of control over the flow rate of bioinks compared to pneumatic set-ups.[44] This review will, therefore, focus on pneumatic and piston driven extrusion systems. For more detailed information on extrusion bioprinting principles and applications, we refer the reader to other excellent recent review papers.[41,45]

2.1.1. Material Requirements. Materials used for extrusion often require distinct mechanical properties to facilitate control over their deposition with viscosity and gelation mechanisms being of critical importance. These and other properties of polymers for bioprinting are discussed in detail in section 3. Briefly, cell-loadable hydrogels require shear thinning properties to allow for extrusion through a print head and nozzle.[46] Ideally, the hydrogel ink solution would be viscous enough to allow for storage/loading in a print cartridge without leaking and preventing cell sedimentation. Exact figures vary, but it is generally accepted that a bioink should display viscosity values in the range of 30 mPa·s (lower limit) to 25×10^3 mPa·s (upper limit) to be considered suitable for printing.[44] The application of pressure and, consequently, shear force to bioinks in a print head should then trigger shear thinning and a reduction in viscosity allowing for direct dispensing onto the building platform. As the material is extruded, viscosity should increase as the shear force is removed, allowing for control over flow of the material and maximizing resolution.[19,23,46−48] Traditionally, gelation would be subsequently triggered, allowing for preservation of the printed structure. This is, however, often difficult to achieve when using hydrogel precursor solutions of low viscosity. The high water content determines their propensity to flow immediately after printing, thus inhibiting the generation of complex, high-resolution structures.[49] To overcome this issue, hydrogels used for extrusion are often developed to exhibit high viscosity or have self-assembling properties that allow for structuring independent of external factors.[19,48,50] This can improve resolution but often limits the system to biomaterials
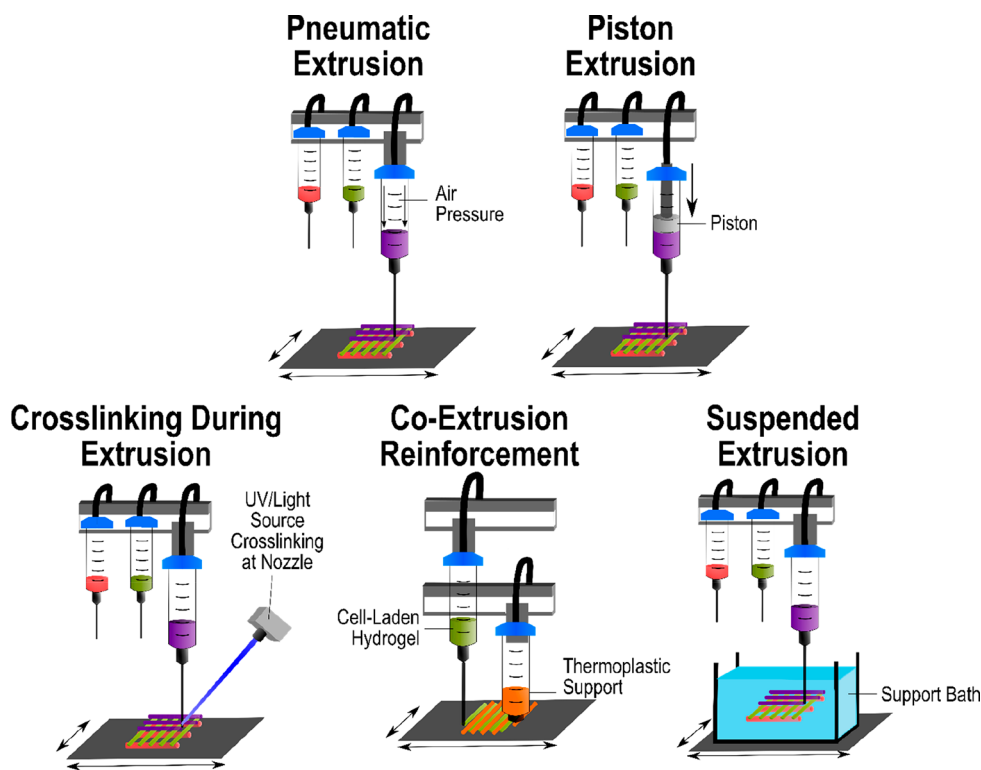
Figure 1. Schematic drawing demonstrating extrusion-based platforms commonly applied in bioprinting. Pneumatic vs piston-assisted extrusion mechanisms (top) and strategies for retaining the shape of structures printed with easily deformable hydrogels (bottom).

for stiff mechanical environments. While useful for tissues such as bone and cartilage, this does not usually allow for printing of materials for soft tissue applications such as the brain.[51,52] In these cases, there is often a trade-off between using a biomaterial that is optimal for cell phenotype and one that provides the desired printing resolution. To avoid such compromise and yet improve resolution and construct complexity in extrusion bioprinting, different new strategies have been developed. Herein we report on three of those strategies and how they can be employed in bioprinting of cell-loadable materials.

2.1.2. Cross-linking During Extrusion. Controlled gelation during extrusion is one strategy that has been applied successfully to improve the complexity and shape fidelity of bioprinted constructs. This process involves modifying a printing system to allow for bioink gelation before, during, or shortly after extrusion in order to prevent flow of the deposited bioink and the subsequent loss of structural resolution (Figure 1).[53−56] The rheological properties of low-viscosity inks can be manipulated prior to extrusion to improve printability by promoting low degrees of covalent cross-linking.[57] Another common approach is to chemically modify bioinks into photopolymerizable polymers with the addition of photoactive functional groups, such as methacrylates, prior to extrusion to allow for UV curing during printing. For this purpose, the printing system can then be designed to include a light source that can irradiate the bioink through a transparent nozzle using either UV or visible light. This method, also known as in situ cross-linking improves material flow, filament stability and allows for the use of a wide range of polymeric materials including norbornene-modified hyaluronic acid (NorHA), gelatin methacrylate (gelMA), and poly(ethylene glycol) diacrylate (PEGDA).[58−60] Alternatively, bioinks can be extruded directly into a bath of cross-linker to trigger physical or chemical cross-linking immediately after deposition or printed with cross-linker solutions simultaneously in a coaxial system to trigger gelation during extrusion.[61,62] These mechanisms can dramatically improve printing resolution but can also limit layer integration, particularly for materials that undergo rapid gelation with one layer undergoing full gelation before the next layer can be added. The resulting structures are often weaker at the interface between layers, bringing their use for modeling of tissue gradients into question.

2.1.3. Co-extrusion Reinforcement. Another technique that has been explored to improve printing resolution and facilitate the creation of layered structures is co-extrusion or thermoplastic reinforcement. Originally used for the printing of macroporous 3D acellular scaffolds, thermoplastic extrusion has recently been explored as a tool to generate hybrid constructs containing low-viscosity hydrogels. This technique requires the use of two or more print heads for the simultaneous or alternated deposition of structural and cell-loadable materials and the capacity to manipulate the processing parameters of each material independently.[63,64] Utilized materials vary, but generally, one of two approaches can be used. The first involves the combination of a hydrogel bioink (often cell-loadable) with a more rigid, cell-free, thermoplastic material such as poly(ε-caprolactone) (PCL).[63] Commonly, a layer of thermoplastic is extruded via a screw- or piston-driven printing head and allowed to cool before subsequent addition of a layer of hydrogel into the same Z-plane via either pneumatic or piston-driven extrusion. This creates a hybrid layer with the thermoplastic controlling the flow of the hydrogel and allowing for the generation of constructs with enhanced structural and mechanical performance.[65,66] The use of PCL allows for the printing of well-

defined structural templates at relatively low processing temperatures (e.g., approximately 60 °C) and fast solidification rates, which is beneficial for the viability of encapsulated cells. However, the dimensions of printed filaments (usually hundreds of micrometers) strongly limit the creation of effective interfaces between thermoplastic and hydrogel materials. Therefore, another interesting approach involves the use of either pneumatic or piston driven mechanisms to deposit, in an alternated manner, two cell-loadable bioinks with distinct mechanical properties.[64] This method allows mitigation of some of the issues around the interface between the two materials while improving oxygen/nutrient diffusion in both soft and hard tissue implants. To avoid potential flow of one material into another, this technique can be combined with self-assembling hydrogels, photo-cross-linking, or extrusion into cross-linker solution in order to create defined structures with biological and mechanical gradients.[67,68]

2.1.4. Suspended Extrusion. Multiple research groups have also started to explore the extrusion of bioinks into a secondary structure (i.e., suspension bath) that provides support and flow restriction throughout gelation. This has been shown to improve resolution and accuracy, particularly in the generation of gradient structures.[69−72] In addition, the use of a secondary support to restrict bioink flow during printing has been shown to facilitate generation of bioprinted constructs with controlled heterogeneity in physical and biological properties such as layered osteochondral plugs and cardiac ventricles.[70,71] Previous methods have utilized materials such as soft gels or high viscosity solutions to improve printing resolutions.[69] The use of casting molds comprised of "sacrificial materials" that can be easily removed without compromising cell viability after generation of a 3D structure has also been widely explored.[73,74] More recently, significant promise has been demonstrated in the extrusion of bioinks into a self-healing suspension of hydrogel particles referred to as a fluid gel. This process is commonly referred to as suspended layer additive manufacture (SLAM) or freeform reversible embedding of suspended hydrogels (FRESH) depending upon the nature of the fluid gel used for printing.[70,71,75] In both formats, it is theorized that the fluid gel restricts flow without interacting and mixing with deposited solutions, thus allowing for layering of different materials of varying densities into high resolution constructs. Cross-linkers can then be introduced to promote the gelation of a suspended structure allowing for generation of heterogeneous structures capable of mimicking biological interfaces. 3D bioprinting using suspension baths has raised significant interest among the scientific community, and we direct the reader to a recent review by McCormack et al. for more in-depth information.[76]

2.2. Material Jetting

Material jetting is commonly referred to as "inkjet printing" and involves the dropwise deposition of small volumes of ink to fabricate 3D constructs in a "bottom-up" manner. The concept of inkjet bioprinting was first introduced in 2003, when Boland demonstrated the feasibility of printing living cells without compromising their viability or function.[77] Since then, many other research groups have adopted this technology and showed its potential in TE,[78,79] RM,[80,81] and more general biomedical applications.[82,83] Depending on the ejection mode, material jetting technologies can be classified as continuous streaming (CS), drop-on-demand (DOD), acoustic, or microvalve printing.[84] In CS systems, the bioink is

ejected from the print head and through the nozzle, producing a continuous jet that breaks into a stream of droplets as a result of hydrodynamic instability.[85] The process is spontaneous, providing little control over the bioink stream. To improve on this, research groups have developed DOD printing systems to facilitate better control over bioink deposition.[86] DOD systems work on the same principles as in CS, but droplets are only formed when required. The ink is held in place inside the material chamber until a piezoelectric or thermal actuator generates enough pressure to overcome the surface tension present at the nozzle orifice and forces the ejection of small droplets of bioink (as small as 10 μm).[87] The systems can contain a single or multiple print heads that move to a desired coordinate before droplet formation, and the bioink is only ejected in specific spatial locations.[88] This allows for small volumes of cell-laden bioink to be patterned into high resolution structures not obtainable via CS, albeit at a much slower printing speed. Acoustic and microvalve are two of the most recent developments in material jetting technology, which make use of acoustic waves or solenoid pumps to eject droplets, respectively.

2.2.1. Material Requirements. Material jetting platforms often place fairly stringent rheological boundaries on candidate bioinks, the most significant of which is viscosity.[89] As stated previously, the main mechanism behind bioink ejection is the ability of the material to overcome the surface tension present at the inner wall of the printing nozzle. In material jetting, nozzles are generally small in order to promote the dispensing of droplets of the order of 10 μm.[87] Consequently, bioinks should display low viscosities, normally in the range of 10−100 times the viscosity of water, which helps preventing nozzle clogging[90] but restricts the use of high cellular densities. Although lower and upper limits can vary, it is generally accepted that a low shear viscosity of 30 mPa·s represents the upper boundary of what is printable in a material jetting system without causing cell damage.[91] Microvalve-based systems can potentially open up the possibility to print materials beyond this limit, but the lack of studies on more complex 3D cell-laden constructs generated with this technology prevents further insights into the maximum usable viscosities.[92] A recent development has, however, demonstrated the potential to considerably broaden the printability spectrum in material jetting systems. In a seminal study, Foresti et al. highlighted the possibility of printing materials with viscosities ranging from 0.5−25 × 10^3 mPa·s.[93] The process involves the application of a subwavelength Fabry−Perot resonator to induce an acousto-phoretic force (dominating the gravitational forces) on bioinks that overcomes the opposing capillary forces and allows for droplet ejection. This new development could, therefore, hugely improve the versatility of material jetting systems in biological applications.

2.2.2. Piezoelectric Jetting. Piezoelectric systems eject bioink droplets using a polycrystalline ceramic actuator placed inside the fluid chamber of the print head. A voltage pulse triggers a change in the actuator shape, resulting in the deformation of the fluid chamber with a subsequent variation in the chamber volume. This sudden change sends a pressure wave that allows droplets of bioink within the print head to overcome the surface tension at the nozzle orifice and be ejected. Piezoelectric jetting has, however, been reported to compromise cell viability, with voltage pulses shown to damage cell membrane integrity and trigger cell death.[94] Therefore, and despite some research groups still reporting successful

biological applications,[95] thermal jetting is often preferred over piezoelectric systems.[96−98]

2.2.3. Thermal Jetting. In thermal jetting, a vapor bubble is generated inside the fluid chamber due to the localized heating provided by a thermal actuator. The bubble expands rapidly reducing the volume inside the chamber. When the bubble collapses, the resulting pressure pulse triggers the ejection of bioink droplets through the printing nozzle while simultaneously applying heat to the drops ($\sim$4−10 °C). During this process, the size and volume of the droplets can be precisely controlled by varying the temperature gradient that is applied to the bioink or by increasing the frequency of the pressure pulses.[99] Additionally, the viscosity of the bioink can also be modified to control droplet volume. The successful regulation of all three parameters can directly impact on bubble size, thus resulting in droplet volumes ranging from 10 to 150 pL.[100] Consequently, thermal jetting is a popular tool for cell-based bioprinting, particularly in applications requiring high levels of control over the spatial orientation of cells such as osteochondral, vascular, and oncological models.[101−103]

2.2.4. Microvalve-Based Jetting. Microvalve-based jetting systems are generally composed of one or more print heads attached to a robotic mechanism that can move across the x, y, and z axis.[104] An electromechanical microvalve comprising a solenoid valve and a plunger is present within each print head between the pressurized bioink cartridge and the nozzle. Upon the application of a voltage pulse, the solenoid generates a magnetic field that pushes the plunger up and opens the nozzle, allowing for the ejection of material. By applying and removing the voltage pulse, it is possible to control the opening and closure of the valve at defined intervals, often on the scale of milli- and microseconds, to precisely control the frequency and size of droplet extrusion. This results in a highly controlled bioink deposition and allows for extrusion of layers of material as thin as 1−2 μm. Depending on the pressure applied to the bioink cartridge and the valve opening time, it is possible to operate microvalve jetting systems in either CS or DOD mode. Tuning these two process parameters along with nozzle geometry, cellular density, and bioink rheology allows for higher resolution and has been shown to improve throughput, precision of cellular positioning, and cell viability,[105] leading to many applications including bioprinted structures for bone, cartilage, and ocular models.[106−108]

2.2.5. Acoustic Jetting. Acoustic jetting systems differ from the previously reported platforms due to the absence of a printing nozzle that defines droplet size. Because nozzles are prone to clogging, particularly with high viscosity fluids, the ability to jet bioinks without a nozzle can widen the range of processable materials.[109] To dispense bioinks in acoustic systems, a droplet is ejected from an air−liquid interface via an acoustic force applied by an ultrasound field. Droplets on a scale of picoliters can be ejected when the acoustic pressure exceeds the surface energy of the liquid, and materials with viscosities up to 150 mPa·s can be dispensed via this method.[110] The technology was first reported in 2007, when acoustic waves were applied to eject picoliter-sized droplets from an ejector array, allowing for the encapsulation of single cells with micrometer precision.[111] Acoustic jetting is now applied in a wide variety of settings, but bioprinting applications are still limited. A few research groups have reported positive data regarding cell-based applications,[110,112,113] but the technology is still early in development

with regards to biological systems. A summary of the different material jetting systems is illustrated in Figure 2.
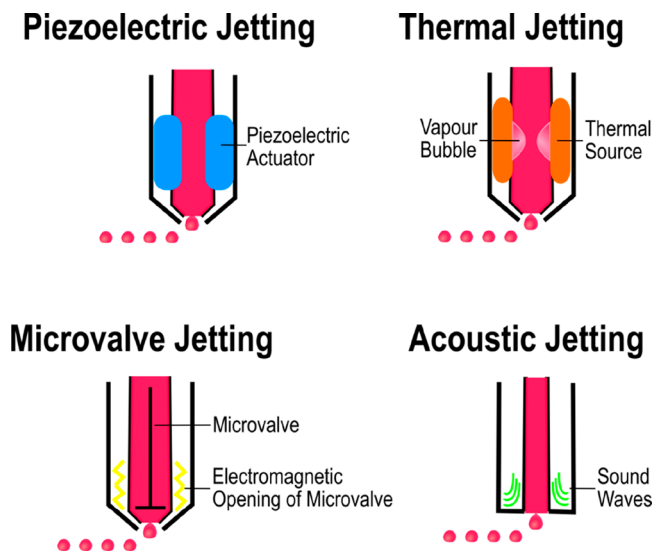

Figure 2. Schematic drawing demonstrating different DOD platforms used in bioprinting. Variations in the volume of the printing chamber are generated via the deformation of a piezoelectric actuator (piezoelectric jetting) or expansion of a vapor bubble (thermal jetting), leading to the formation and ejection of bioink droplets (top). The application of electromagnetic pulses or of an ultrasound field control the ejection of droplets in microvalve and acoustic jetting, respectively (bottom). The latter is the only nozzle-free system currently used in material jetting bioprinting.

2.3. Vat Photopolymerization

Another technique commonly applied to the bioprinting of cell-laden hydrogels is vat photopolymerization, the most common of which is known as stereolithography (SLA).[114] This technology is usually comprised of a building platform, a vat of photopolymer resin, and a light source that irradiates the resin in a layer-by-layer fashion.[115] Since it was initially introduced in the 1980s by Charles Hull,[116] two different patterning methods have been developed, including vectorwise and mask irradiation. In the most traditional apparatus of SLA, also known as vectorwise, scanning galvanometers are used to scan the surface of the resin with a high-resolution UV, infrared (IR), or visible light laser beam. At the scanned regions, the laser will initiate a spatially controlled radical photopolymerization reaction with subsequent solidification of the liquid resin. Once the first layer is built, the building platform descends inside the vat; it is homogeneously recoated with resin and another layer is built on top of the previous one. On the other hand, projection techniques use a dynamic mask to irradiate and solidify the entire surface of the resin in a single step.[117] Digital micromirror devices (DMD), a technique developed and patented by Texas Instruments, is currently the most used dynamic generator of masks in SLA. It consists of a large array of microsized mirrors that can be rotated to either +12 or −12 degrees, thus allowing for a fast and precise spatial modulation of different light patterns.[118] Generally, mask projection facilitates a much more rapid generation of complex bioprinted shapes when compared with standard vectorwise SLA.[119] The flexibility provided by the different patterning systems enables the use of SLA for the precise structuring of a wide array of photopolymers and cell-laden hydrogels, as
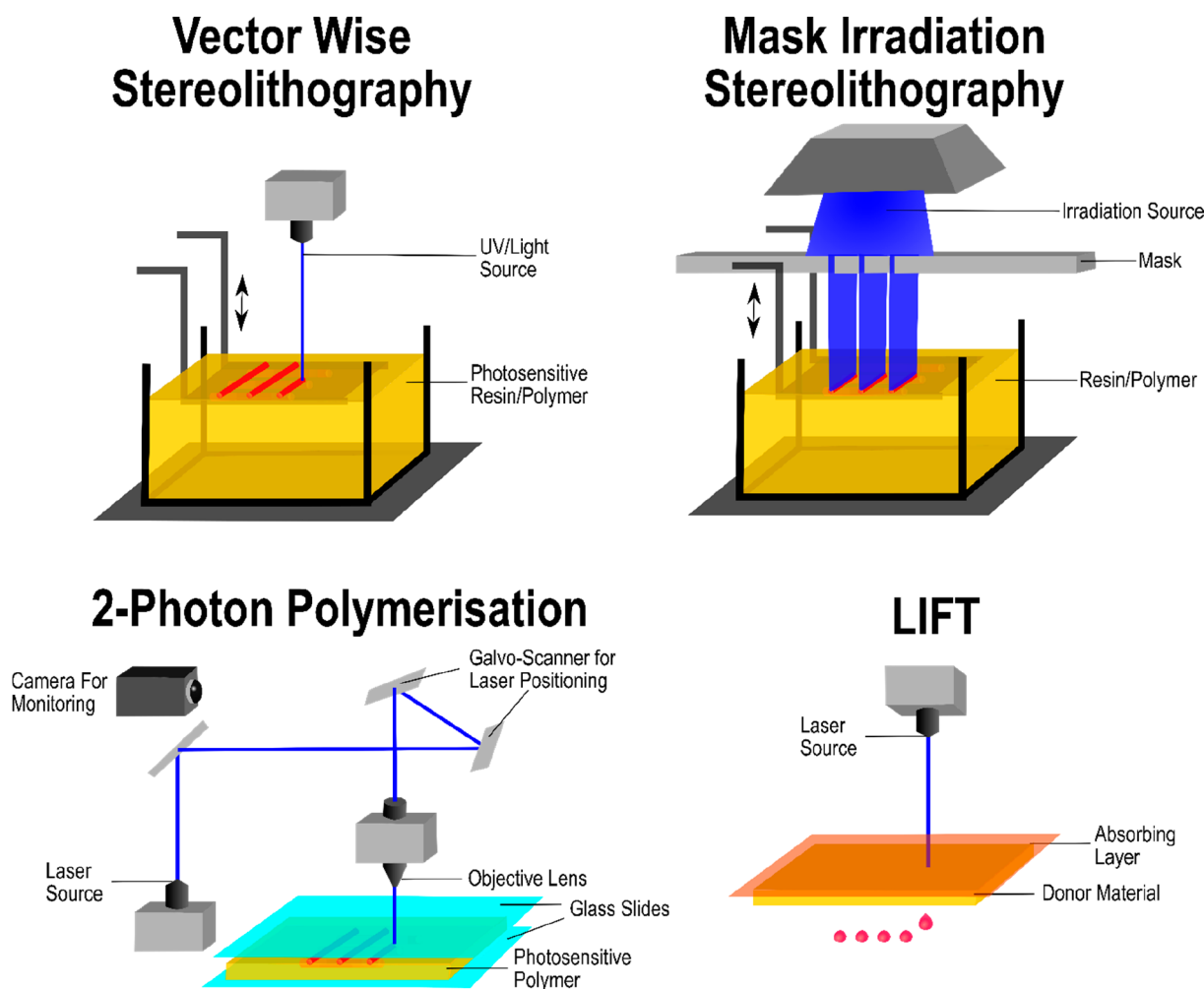
Figure 3. Schematic drawing demonstrating the different irradiation techniques that can be used in vat photopolymerization, two photon polymerization, and laser-assisted bioprinting. Geometrical features can be imprinted in each layer using a point-by-point scanning approach (vectorwise SLA) or in a single step through mask irradiation (top). The combination of optical transparent materials and an ultrafast pulsed laser allows for the direct writing of submicrometer features inside a vat containing photopolymerizable resin (2PP). Transfer of cellular or acellular materials from a metal-coated substrate (donor material) to the building platform (receiver) is triggered by a pulsed laser and allows for the generation of high-resolution constructs in LIFT (bottom).

demonstrated by the growing number of recent publications.[120−123]

2.3.1. Material Requirements. Adaptation of SLA to bioprinting processes does not necessarily place stringent rheological requirements on materials in the same way as extrusion and jetting do, but there are still accommodations to be made. A much wider range of viscosities can be used with a suspension viscosity of 5 Pa·s considered to be the upper limit.[124] There is no generally accepted lower limit for resin viscosity, but it is widely agreed that the material must be sufficiently viscous to prevent cell settling during the curing process. In addition to this, there are key chemical properties that a bioink needs to exhibit in order to be processed via SLA. The process often involves modifying hydrogels to contain chemical groups that can facilitate photoinduced cross-linking such as azides, epoxides, or (meth)acrylates.[115] This cross-linking reaction proceeds through radical or ionic species and is initiated by the cleavage of a labile molecule upon exposure to light: the photoinitiator. The wavelengths of the used light source has to match that of the employed photoinitiator and can range from UV to VIS to IR. The result is the rapid formation of an organized polymer network and transition from a sol to gel state.[125,126] This subsequently allows for the generation of hydrogel structures of higher resolution than those commonly obtained from extrusion printing. Cell viability can, however, be compromised by the gelation mechanisms utilized in SLA. Numerous studies have reported the cytotoxic effects of free radicals and pH changes, both in vitro and in vivo. Additionally, exposure to UV light can cause considerable damage to DNA within bioprinted cells.[127−129] As an alternative, light sources in the visible spectrum can be used to photopolymerize bioinks with negligible impact on the viability of encapsulated cells. The cross-linking chemistry is typically identical to that in UV-initiated cross-linking but using photoinitiators that absorb in the visible part of the spectrum.[53,130,131]

2.3.2. Two-Photon Polymerization (2PP). Two-photon polymerization (2PP) further builds on the process of SLA by adding the capacity to accurately control the spatiotemporal polymerization process of the resins, thus enabling the generation of high-resolution constructs.[132] As with standard SLA, 2PP involves the application of focused light beams to trigger photopolymerization in a resin vat. However, 2PP employs an ultrafast pulsed laser to generate a flux of photons

Table 1. A Comparison of Bioprinting Techniques Based on Resolution, Rheological Requirements, and Key Advantages and Disadvantages

printing platform	maximum resolution	bioink viscosity	key advantage	key limitation	ref
pneumatic/ piston extrusion	∼200 μm	30−600 × 10⁶ mPa·s	printing high viscosity, cell-laden materials with high cell density	high shear forces required to print can compromise cell viability	
cross-linking during extrusion	∼100 μm	30−600 × 10⁶ mPa·s	printing low viscosity polymers with high fidelity	delamination of printed layers due to rapid cross-linking	44
co-extrusion	∼20 μm	12−600 × 10⁶ mPa·s	allows for the generation of structures with mechanical and biological heterogeneity	requires multiple print heads capable of extruding materials under different conditions	64,141
suspended extrusion	∼20 μm	5−800 mPa·s	high-resolution printing of low viscosity polymers with control over flow postprinting	precise mechanisms behind flow prevention still poorly understood	70,71,75
piezoelectric jetting	∼45 μm	3.5−30 mPa·s	high resolution and high printing speed allow for rapid cell patterning	piezoelectric pulses have been shown to negatively affect cell viability	28,91,93
thermal jetting	∼45 μm	3.5−30 mPa·s	thermal ejection process is far more favorable for cell viability than piezoelectric jetting	narrow range of bioink viscosities can be used when compared to extrusion-based systems	28,91,93
microvalve-based jetting	∼220 μm	1−70 mPa·s	increased viscosity range for bioinks	high shear stress can compromise cell viability	104,142,143
acoustic jetting	∼60 μm	1−150 mPa·s	wide range of bioink viscosities can be used due to the system being nozzle-free	disturbancies can easily affect droplet ejection	110,112
vector-wise SLA	∼1 μm	<5 Pa·s	high speed and high-resolution generation of structures	difficult to combine multiple materials	140
mask irradiation	∼1 μm	<5 Pa·s	ability to reticulate multiple areas of a resin in a single laser pulse	difficult to combine multiple materials	130
two-photon polymerization	100 nm	<5 Pa·s	highest resolution form of bioprinting commercially available	optically transparent materials are needed	144
laser-assisted bioprinting	∼20 μm	1−300 mPa·s	high resolution generation of structures from bioinks in solid or liquid phase	laser pulses can impact viability with >15% cell death	44,139

that promotes the simultaneous absorption of two photons by a single molecule, thus producing a higher and more focused energy state within the photopolymer resin.[133] Despite requiring the use of optically transparent materials to operate, the system allows for the generation of constructs with features on a submicrometer level, a resolution not achievable via standard SLA techniques. Such resolution is, however, smaller than a mammalian cell and, thus, 2PP is more commonly applied to the generation of high resolution templates that cells can be seeded into instead of being directly used for bioprinting of cell-laden structures.[134−136] A small number of studies have, however, demonstrated applications in the generation of cell-laden constructs albeit on a larger scale.[137,138]

2.4. Laser-Assisted Bioprinting

Laser-assisted bioprinting, often referred to as laser-induced forward transfer (LIFT) is viewed as one of the technologies developing fastest in the field. LIFT printers have three major components; a pulsed laser source, a ribbon from which a biological material is printed, and a substrate that collects the printed material.[44] Generally, the ribbon is made of a thin absorbing layer of metal (e.g., gold or titanium) coated onto a laser transparent support (e.g., glass).[139] Similarly to acoustic jetting and SLA, LIFT bioprinters provide the operator with a nozzle-free printing platform. Cells are mixed in a hydrogel and deposited at the surface of the metal film. The laser pulse induces vaporization at the metal film, resulting in the production of a jet of liquid, which is deposited onto the facing substrate. Printed materials can range from solids to liquids with solid hydrogels, often preferred for bioprinting applications. Printing cell-laden structures using this technique is, however, often inhibited by issues in cell viability. During the printing process, cell-loaded hydrogels are exposed to high levels of thermal energy. This often occurs on a time scale of nanoseconds, but it is enough to significantly impact cell

viability with studies reporting up to 85% cell death.[139] Modifying the intensity and extent of laser exposure is often employed to try and improve viability, and this has yielded constructs with much greater cell viability,[69] but the technique is still perhaps the least commonly applied form of bioprinting for in vitro tissue models. A summary of all the printing techniques outlined in this section can be found in Figure 3, while information regarding resolution, material requirements, advantages, and limitations can be found in Table 1.

3. POLYMERS AS BIOINKS IN BIOPRINTING

As previously mentioned the materials or "inks" used in bioprinting may contain living cells (the presence of which distinguishes a bioink from a biomaterial ink),[21] bioactive molecules, and/or biomaterials. Here we report exclusively on the different polymers used in bioink formulation, i.e., hydrogels that can be printed with encapsulated cells. Traditionally, they are classed by source, separating naturally derived polymers from synthetic polymers.[8,22,28−30,35,36,145] Many natural polymers possess an inherent bioactivity (although not always toward mammalian cells and enzymes) are often derived from and hence mimetic of an ECM (of either animals or plants), but compared to their synthetic counterparts have less controllable mechanical, chemical, and other properties and typically suffer from batch-to-batch variation. Additional issues related to the immunogenicity of the materials may arise if proteins are used in their formulation. For more information on natural polymers for bioprinting, we direct the reader to a recent review on the topic.[146] Synthetic polymers, in turn, have the possibility of being synthesized with tailored properties (e.g., molecular weight, chemical structure) for a specific application and, although not inherently biomimetic of the ECM, they can be modified to include bioactive motifs (e.g., adhesion promoters).[29] Depending on the gelation mechanism, hydrogels can be further classified

into chemically cross-linked or physically cross-linked.[147] In chemically cross-linked hydrogels, also known as chemical hydrogels, polymer chains are linked by covalent bonds that can be formed using different methods, including free radical cross-linking, enzymatic cross-linking, Michael type-addition, Diels−Alder reaction, or Schiff base reaction. These hydrogels possess better mechanical properties and better physiological stability than their physically cross-linked counterparts. Further details on the different methods of gelation can be found in the excellent reviews by Hospodiuk et al.[22] and by Hu et al.[147] In turn, physically cross-linked hydrogels are formed by intermolecular reversible interactions, like ionic interactions, hydrophobic and hydrogen bonding interactions, crystalliza-tion/stereocomplex formation, and self-assembly. When ionic interactions are used as the gelification method (e.g., alginate in the presence of Ca^{2+} ions), a hydrogel can be obtained within few seconds, contrary to what is commonly observed with the chemical cross-linking methods. The great advantage of these gelation methods lies on the fact that the reactions can occur in the absence of reactive cross-linking agents, thus avoiding any potential cytotoxicity from unreacted cross-linkers.[22,147] The chemically cross-linked hydrogels are often preferred over their physically cross-linked counterparts because of the fine control that could be achieved over the cross-linking density, that rules the porosity, homogeneity of the hydrogel at the microscale, and, consequently, its mechanical properties. However, chemically cross-linked hydrogels usually exhibit an elastic behavior, which is believed to impede the migration and proliferation of the cells. In turn, physically cross-linked hydrogels display a viscoelastic behavior, recapitulating in a better way the microenvironment of tissues and ECM, and allowing better cell spreading, proliferation, and differentiation.[148−150] Many polymeric systems used in bioinks comprise several components, each introducing additional functionality. Rather than reporting on all combinations found in the literature on a case-by-case basis, here we first provide an overview of base polymers with key characteristics, followed by a range of modifications commonly encountered for bioprinting purposes. Finally, some examples of mixed systems are presented, demonstrating that the complexity required for this application often requires a combination of base polymers and modifications, to achieve both processability and the desired biological response.

3.1. Base Polymers

Naturally derived polymers can be divided into the main classes of proteins and polysaccharides. Proteins are often extracted from ECM and therefore come with inherent biofunctionality such as cell-adhesive ligands, cleavable peptide links, and cell-instructive domains that steer cellular differ-entiation, migration, proliferation, and protein expression. Collagen (many subtypes exist) and fibrin are natural ECM and blood clots molecules, respectively, and are suitable materials for encouraging encapsulated cells to proliferate and produce tissue. However, the use of such materials for bioprinting purposes is very challenging. For instance, collagen 1, at neutral pH, self-assembles into fibrillar structures that may cross-link or entangle generating a gel-like structure.[151] This situation is critical in bioprinting because the continuous collagen cross-linking makes the process difficult to control, with repercussion in the properties of the 3D construct that usually exhibits low mechanical stability.[152] To avoid this, collagen solutions have to be kept at temperatures between 4

and 10 °C[153] and combined with supporting materials.[154] Insoluble fibrin is formed through the cross-linking of soluble fibrinogen by action of the enzyme thrombin. This solid-ification is similarly challenging to control in time and space, requiring additional support strategies to harness the tissue healing potential of fibrin, which readily binds to cells and a range of growth factors, while easily allowing the cells to remodel it. The same holds for Matrigel, which is not a single polymer but a mix of proteins including collagens, laminins, and growth factors, secreted by Engelbreth−Holm−Swarm (EHS) mouse sarcoma cells. Its composition is ill-defined and varies from batch-to-batch, but its high bioactivity make it a popular material for 3D cell culture and biofabrication, particularly for organoid culture.[155] Gelatin is obtained from the thermal denaturation of collagen. It has the ability of undergoing a sol−gel transition in water, for temperatures between 20 and 30 °C, forming hydrogels upon cooling. During this transition the gelatin molecules reorganize themselves and are linked together by noncovalent bonds, such as hydrogen bonds, electrostatic, and hydrophobic interactions.[156] However, unlike Matrigel or collagen I, these hydrogels melt at physiological temperatures. In the context of TE and RM, this constitutes a major reason why gelatin is modified prior to the printing process or cross-linked afterward,[22] as will be presented in section 3.2. Polysaccharides are usually derived from plants (e.g., agar, agarose, and alginate from seaweed, and cellulose and pectin from terrestrial plants), or expressed by bacteria (e.g., gellan gum, dextran, xanthan gum) and lack the bioactivity of mammalian cell proteins. Some enzymes, such as alginate lyase and dextran hydrolase, can degrade plant polysaccharides. However, these are normally not expressed by mammalian cells. Polysaccharides do degrade by hydrolysis, a spontaneous process that typically takes weeks to months for these kinds of polymers. Although most polysaccharides do not inherently interact with cells, employing them for 3D cell culture can retain the desired phenotype that would be lost in conventional 2D culture, as is the case for chondrocytes in agarose.[157] Alginate is the most used polysaccharide for bioprinting purposes.[158] It is a linear anionic polysaccharide obtained from the cell walls of brown algae, being composed of two uronic acid units, β-D-mannuronic acid and α-L-glucoronic acid, linked together by β-1,4 glycosidic bonds.[159] Alginate readily gels in contact with solutions containing divalent cations (e.g., Ca^{2+} or Sr^{2+}), through ionic cross-linking, at ambient temperature. These amenable conditions of gelation are very advantageous for cell encapsulation.[160,161] However, this polysaccharide is inad-equate for cell attachment and often has to be modified with moieties that promote cell adhesion (e.g., arginylglycylaspartic acid (RGD) peptide).[22,153] Hyaluronic acid (HA) and chitosan are the other polysaccharides with wide applications in bioprinting. Both polymers (as well as chondroitin sulfate) belong to a specific class of polysaccharides, known as glycosaminoglycans. They are composed of disaccharide repeating units, in which one or both sugar rings in the disaccharide repeating unit has a nitrogen-substitution (e.g., aminosugar). HA is a linear nonsulfated glycosaminoglycan, composed of disaccharide units [D-glucuronic acid and N-acetyl-D-glucosamine] linked by β-1,4 glycosidic bonds, with each unit connected by β-1,3 glycosidic linkages.[162] It is abundant in the extracellular matrix of connective tissues, being also a component of the vitreous humor and synovial fluid.[163] HA establishes strong interactions with water through

Table 2. Overview of Water-Soluble Base Polymers Used in the Formulation of Bioinks in Bioprinting, With Key Characteristics[a]

polymer	bioactivity			cross-link type			gelation trigger				ref
	adhesive	cleavable	instructive	covalent	electrostatic	hydrophobic interaction	temperature	ions	enzymes	mix components	
proteins (Natural)											
collagen	x	x	x			x	irrev				180
elastin (and -like peptides)	x	x	x				LCST		mTG	x	181–183
fibrin	x	x	x	x					thrombin		72
gelatin	x	x	x	x		x	UCST		mTG		156,184
Matrigel	x	x	x			x	irrev				185
silk fibroin	x	x	x	x	x	x			HRP	x	186,187
polysaccharides											
agar(ose)						x	UCST				18,188
alginate		(x)[1]			x			≥divalent			158
cellulose					x						189
dextran											190
gellan gum					x	x	UCST	≥monovalent			191–194
pectin					x			Ca^{2+}			195,196
xanthan gum											197
glycosaminoglycans											
chitosan	x	x	x			x		pH change			165,198
chondroitin sulfate		x	x								199
hyaluronic acid		x	x								200
(Synthetic)											
PHPMA							LCST				201
poloxamer 407							LCST				202–204
poly(ethylene glycol)											57,103
poly(2-oxazoline/oxazine)						x	LCST				205
PNIPAAm							LCST				206
poly(vinyl alcohol)											138,207
synthetic polypeptides	x	x	x		x	x		≥monovalent		x	67,178,208

[a]The references are to reviews on a particular polymer and its use in the field where available, or to key original research articles. PHPMA = poly(hydroxypropyl methacrylamide), PNIPAAm = poly(N-isopropylacrylamide), irrev = irreversible, UCST = upper critical solution temperature, LCST = lower critical solution temperature, mTG = microbial transglutaminase, HRP = horseradish peroxidase.[1] Alginate is cleavable through alginate lyases, which are not normally expressed by mammalian cells.
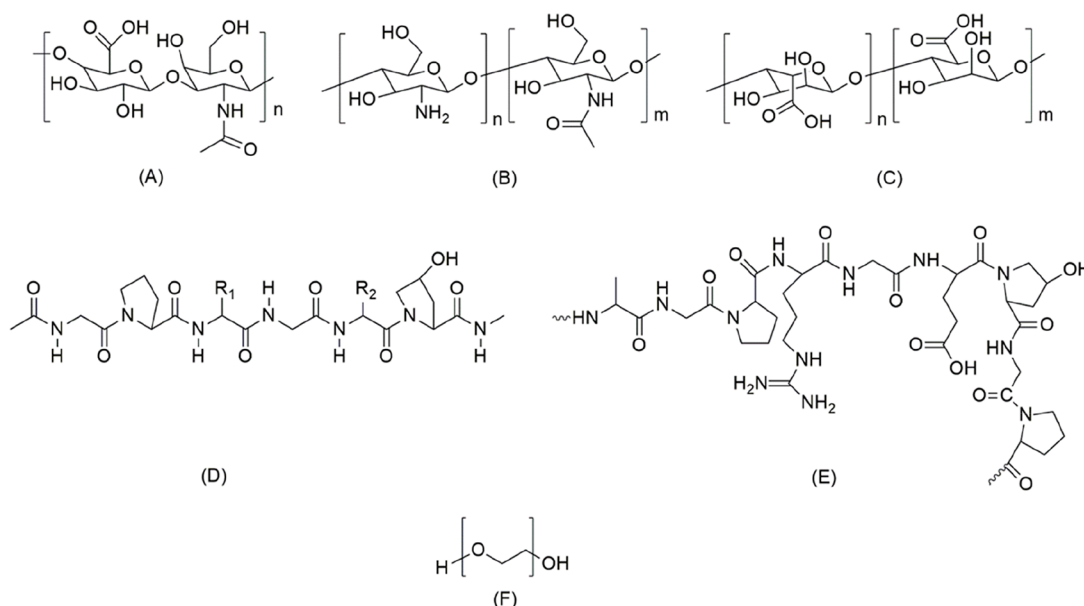
J

Figure 4. Structure of the most used base-polymers in bioprinting: (A) hyaluronic acid, (B) chitosan, (C) alginate, (D) collagen (primary structure), (E) gelatin, (F) PEG.

hydrogen bonds via its hydroxyl, carboxyl, and acetyl groups. Along with its typical high molecular weight, this makes its aqueous solutions highly viscous. HA is also known for its excellent biocompatibility (as a scaffold) and biodegradabil- ity.[163] It is continuously degraded in vivo by hyaluronidase enzymes, as well as being recognized by cells through CD44 cell surface receptors.[164] Because of its low in vivo stability, HA's structure is usually modified with different moieties (e.g., (meth)acrylate, thiols) before being used in bioprinting. By doing such modifications, HA is able to participate in cross- linking reactions, yielding constructs with an increased in vivo stability.[164]

Chitosan, is a linear cationic polysaccharide obtained from the alkaline deacetylation of chitin, an arthropod and fungal polysaccharide also found in some vertebrates like fish. It is composed of β-1,4-linked D-glucosamine groups with randomly located N-acetyl glucosamine residues. The ratio of N-acetyl glucosamine to D-glucosamine residues gives the deacetylation degree, usually between 70% and 90%. This parameter rules chitosan's solubility, hydrophobicity, and its ability to interact with polyanions.[159] This polysaccharide is only soluble under mildly acidic conditions, as protonation of a portion of the amine groups renders the molecule more charged and hence more hydrophilic.[159] This particular feature of chitosan is highly disadvantageous for bioprinting purposes as it exposes encapsulated cells to an acidic environment. To overcome this limitation, Demirtaş et al.[165] recently proposed the cross- linking of chitosan with β-glycerol phosphate, thus allowing the formation of hydrogels at neutral pH and 37 °C.[166] After 21 days of in vitro culture, and when compared to cell-laden alginate gels, chitosan inks showed a much higher ability to promote the proliferation of encapsulated MC3T3-E1 preosteoblasts. Chitosan is characterized by the presence of numerous hydroxyl, carboxylic acid, and amine groups, thus making it attractive for chemical modification or for the attachment of moieties (e.g., epitopes) to enhance bioactivity. This will be discussed further in section 3.2 of this review. Another material that can be used to formulate bioinks is decellularized natural ECM. As the bioink is aimed to take on

the role of the ECM postprinting, the use of native ECM can satisfy many of the requirements, such as the presence of cell adhesion sites and the allowance of cell-mediated degradation to enable tissue remodeling.[167] Typically, tissue from donors or cadavers is subjected to a range of treatments which can include freeze−thaw processes, hydrostatic pressure or exposure to enzymes, surfactants (including sodium dodecyl sulfate (SDS) and Triton X-100), and chelating agents such as ethylenediaminetetraacetic acid (EDTA).[168] These decellular- ized ECMs were first used as scaffolds for tissue or whole organ engineering but are now increasingly being converted into hydrogels. A myocardial-ECM gel (VentriGel) is currently in a phase 1 clinical trial.[169] In recent times, decellularized ECM has been receiving increasing attention as a potential bioink.[170] Pati et al. re-engineered adipose, cartilage, and heart tissue by printing of bioinks, each with their own unique rheological properties, prepared from the respective tissues by decellula- rization.[171] An alternative method to incorporate decellularized ECM into bioprinted structures is to blend the FDA-approved decellularized cartilage product BioCartilage with processing agents, such as gellan gum and alginate. This bioink was used to bioprint large, functional cartilage structures which supported good deposition of cartilage matrix proteins.[172]

Synthetic polymers are the other class of materials with high relevance for bioprinting. The polymers used for this purpose are water-soluble, mostly bioinert, and nonbiodegradable. Because of their nonbiodegradable nature, they are typically synthesized with a molecular weight that is low enough to allow renal clearance. Poly(ethylene glycol) (PEG) is a polyether, soluble in water and in most organic solvents, and it is widely used in biomedical and pharmaceutical applications. It can present a linear or branched structure with variable molecular weights, and its functionalization with other moieties is relatively easy to perform.[173] PEG, in its native form, does not have the capacity to form hydrogels. Typically, its hydroxyl terminal groups are modified with different moieties to allow the formation of a cross-linked structure. More details on the types of modification will be given in section 3.2. Similar to PEG, poly(vinyl alcohol) (PVA) is a bioinert water-soluble

polymer that can be used as a template for a bioink by functionalization with cross-linkable and bioactive moieties, e.g., as a bioresin for digital light processing (DLP) stereolithography printing of cell-laden constructs.[174] A number of synthetic polymers displaying lower critical solution temperature (LCST) behavior, meaning that upon heating a gel is formed, have been employed in bioprinting. These include poly(N-(2-hydroxypropyl)methacrylamide lactate) (PHPMA), poly(N-isopropyl acrylamide) (PNIPAAm), poly-(2-oxazoline)s, and poly(2-oxazines), and above all, poloxamer 407 (also known under trade names Kolliphor P407, Pluronic F127, and Lutrol F127). References of their use in bioprinting are found in Table 2.

Self-assembling peptides are a class of peptides able to undergo hydrogelation via noncovalent interactions such as hydrogen bonds, electrostatic interactions, hydrophobic interactions, and $\pi-\pi$ stacking, forming nanofibrous hydrogels. Typically, the fibers inside the hydrogel have different secondary structures (e.g., β-sheets and α-helices), and these structures are highly dependent on intrinsic factors (e.g., charge of the α-amino acids in the peptide's sequence, number of repeating units of the assembling motif, and peptide concentration) and extrinsic factors (e.g., temperature, pH, and ionic strength of the medium).[175,176] These hydrogels present biodegradability and tunable mechanical stability and, very important, their gelation can occur within physiological conditions. These remarkable features place self-assembling hydrogels as logical candidates to formulate bioinks,[67,177−179] although their exploitation for bioprinting purposes has only recently started. Raphael et al.[19] used a synthetic peptide, with the ability to self-assemble under physiological conditions, to prepare cell-laden constructs via 3D bioprinting. The authors demonstrated the possibility of creating bioinks with tunable stiffness and adequate rheological properties for the printing of 3D matrices with enhanced structural integrity and shape fidelity without jeopardizing the viability and proliferation of encapsulated EpH4 cells. An overview of water-soluble base polymers used in the formulation of bioinks for bioprinting applications is given in Table 2, and the structure of the most commonly used are shown in Figure 4.

3.2. Moieties for Chemical Cross-linking

Cross-linking is indispensable in biofabrication and bioprinting, as it prevents the water-soluble polymers that bioinks are made of from dissolving, and hence fixes printed shapes as well as contributes to the stiffness of the material. Most often the cross-linking is photoinitiated[54] for reasons of high spatiotemporal control and ambient temperatures.[209] Yet, other methods are increasingly being explored. This section examines the chemical modifications available to improve the performance of base polymers in bioprinting.

3.2.1. (Meth)acrylation. Acrylation or methacrylation of polymers allows irreversible cross-linking via chain-growth polymerization of unsaturated end-groups or side groups on polymer chains. Cell encapsulation in hydrogels using this chemistry was pioneered in the early 1990s by Hubbell et al., who used (meth)acryloyl chloride to functionalize PEG.[210] This strategy of (meth)acrylation is also widely used to modify naturally derived polymers. The hydroxyl groups of HA are commonly modified with methacrylic anhydride (MA) or glycidyl methacrylate (GMA). The methacrylated-hyaluronic acid (MeHA or HAMA) can be obtained with different degrees of substitution, leading to hydrogels with a variety of

cross-linking densities, which in turn will dictate their mechanical and biological properties.[211] Gelatin is commonly modified with MA, leading to gelatin derivatives containing both methacrylamide and methacrylate groups. The methacrylamide groups result from the reaction of lysine ($-NH_2$ groups) residues with MA, whereas methacrylate groups are obtained from the reaction of threonine, serine, and tyrosine ($-OH$ groups) with MA.[212] GelMA can be used in material extrusion,[184] material jetting,[213] and vat photopolymerization bioprinting processes.[174] The chemical modification of base polymers can sometimes introduce some changes in the behavior of the material. For example, the self-assembly of collagen and gelatin are frequently weakened by methacrylation; gelMA forms weaker physical gels than its corresponding gelatin, whereas in collagen the otherwise irreversible thermal gelation becomes completely reversible.[214]

3.2.2. Ene or Thiol Moieties. As an alternative to chain-growth cross-linking through (meth)acrylate groups, thiol−ene step-growth cross-linking has been developed with a number of potential advantages, including higher reaction rates, lower oxygen sensitivity, more homogeneous network topology, and the absence of nondegradable chains that are formed in the chain-growth of (meth)acrylate cross-linking.[215] In thiol−ene chemistry, a radical abstracts a hydrogen atom from a thiol (sulfhydryl or SH) group, after which the sulfur-centered radical reacts with a carbon−carbon double bond (ene). The newly formed carbon radical can homopolymerize with another -ene but is often more likely to terminate by abstracting a hydrogen from another thiol group, after which the process can start again. To obtain the "ene" moiety in the base polymers, those can be modified with allyl, norbornene, maleimide, or acrylate groups. Gelatin, for instance, can be modified with allyl glycidyl ether (AGE), at 65 °C in alkaline solutions, to yield allylated gelatin (gelAGE).[216] The norbornene group, in turn, can be used to modify gelatin,[217] HA,[218] alginate,[219] and PEG.[220,221] Each polymer is modified under specific conditions, depending on the type of norbornene-containing reactant used for the modification. The thiol moiety is usually donated by materials that are commercially available like, for instance, dithiothreitol (DTT)[217] or thiolated-PEG.[219,220] The use of thiolated HA is also reported as a thiol moiety for bioinks.[152,222] The thiolation of this polysaccharide can be obtained by different routes as described in a recent review by Griesser et al.[164] For example, Yan et al.[223] used the thiol-maleimide reaction to promote the reaction of thiolated gelatin with PEG functionalized with two maleimide groups, forming a covalent network with thioether bonds. The bioink was supplemented with laminin-derived amphiphilic fibril-forming peptides that supported the formation of a noncovalent network at 4 °C and improved cellular adhesion.

3.2.3. Enzyme-Mediated Cross-linking Moieties. Enzyme-mediated cross-linking is very attractive for bioprinting purposes as it enables a highly specific bio-orthogonal control of the gelation process. Despite its potential, very few studies so far report on the use of enzyme-mediated cross-linking methods to generate bioinks. Perhaps because of this, horseradish peroxidase (HRP) is the only enzyme used and described in the literature as capable of promoting the cross-linking of polymers containing phenols (Ph), phenylamines, indoles, sulfonates, and other similar groups in their structures.[224] When such groups are not present, as in the case of HA,[53] gelatin,[225] and alginate,[225] it becomes necessary
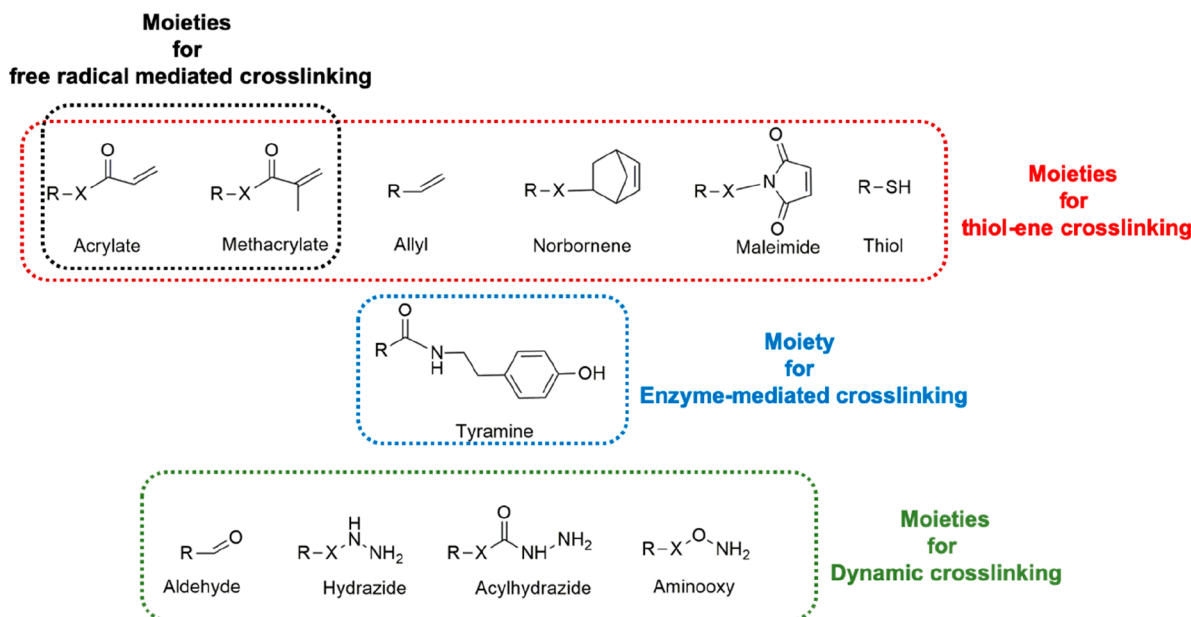
Figure 5. Chemical groups typically used to mediate the chemical cross-linking of bioinks (R corresponds to the polymer, and X corresponds to the chemical bond that is formed between the polymer and the modifying agent containing the group of interest (e.g., ester, amide).

to introduce a tyramine (Tyr) modification for the enzymatic gelation to occur. The cross-linking occurs through the oxidative coupling reaction of Tyr moieties, using hydrogen peroxide (H_2O_2) as the oxidant reactant.[226] This type of cross-linking is characterized by short reaction times, and the cross-linking density of the hydrogel, that dictates its mechanical properties, can be easily tuned by the amount of H_2O_2. This strategy has been used recently to create hybrid HA-Tyr bioinks for the encapsulation and 3D printing of mesenchymal stem cell-laden constructs.[53] Although some polymers have to be modified to introduce the moieties needed to the HRP-mediated cross-linking there are others that already possess such groups in their structure. This is the case for silk fibroin that, due to the presence of the tyrosine residues in its protein, can be cross-linked through the HRP/H_2O_2 route. Despite being intensively studied for TE applications, the bioprinting of silk fibroin is challenging because of the poor gelation kinetics under mild conditions and lack of suitable rheological properties at concentrations relevant to the printing process.[227] This limitation can be circumvented by mixing and printing silk fibroin together with rapidly gelling components that act as support, while the gelation occurs upon addition of HRP/H_2O_2. This approach has been reported by Compaan et al.,[228] in which alginate cross-linked with Ca^{2+} ions acted as the sacrificial support, while the enzymatic cross-linking of silk fibroin took place.

3.2.4. Moieties for Dynamic Cross-linking. The Schiff-base reaction is a type of reaction that involves the formation of a dynamic covalent bond upon the ligation of aldehyde groups with different amine nucleophiles. There are different types of Schiff base linkages, including imines, hydrazones, and oximes. Imines are obtained from the reaction of aldehydes and amines, while the hydrazones and oximes are obtained from the reaction of aldehydes with hydrazides and hydroxylamines.[229] These are dynamic bonds, meaning that they are reversible and in constant equilibrium between the bound and unbound state, while having significant higher strengths than physical bonds. Hydrogels based on such type of cross-linking

are characterized by their good injectability, shear-thinning, and self-healing properties.[118] In the context of bioprinting, the cross-linking mediated by this kind of chemistry is very advantageous as it occurs under physiological conditions. Besides, these hydrogels also display shear-thinning properties, which are extremely beneficial in protecting cells from damaging shear forces during printing.[230] Wang et al.[118] prepared a bioink from HA derivatives bearing both hydrazide and aldehyde groups. The obtained constructs exhibited high shape fidelity, stability to relaxation, and high cytocompatibility with encapsulated fibroblasts (>80% cell viability). In other work, oxidized dextran hydrogels were functionalized with aldehyde groups and gelatin for application in material extrusion bioprinting. The reaction of the aldehyde moieties, present in the dextran, with the amine groups of gelatin took place at physiological pH, yielding imines.[231] Figure 5 gives an overview of the main chemical groups involved in the chemical cross-linking of bioinks.

3.3. Moieties for Physical Cross-linking

The cross-linking of polymeric materials can also be achieved through physical interactions, but similarly to chemical hydrogels, this can be controlled through further modification of base polymers with specific moieties. Some exceptions are alginate, gellan gum, and pectin, which gel in the presence of cations or gelatin, poloxamer, and PNIPAAm, which gel above or below specific temperatures.

3.3.1. Peptide or Oligonucleotide Conjugation. Functionalization of polymers with peptides or oligonucleotides is a method that allows the creation of aqueous-compatible, weakly associated, reversible, and self-assembled networks via molecular recognition. The use of peptides or oligonucleotides presents several advantages, including the abundance of functional groups in their structure (suitable as conjugation sites to base polymers) and the well-established solid-phase chemistry used for their synthesis (often using automated systems) either with short peptides and oligonucleotides or recombinant protein technology for long peptides. The exploitation of protein−protein interactions between
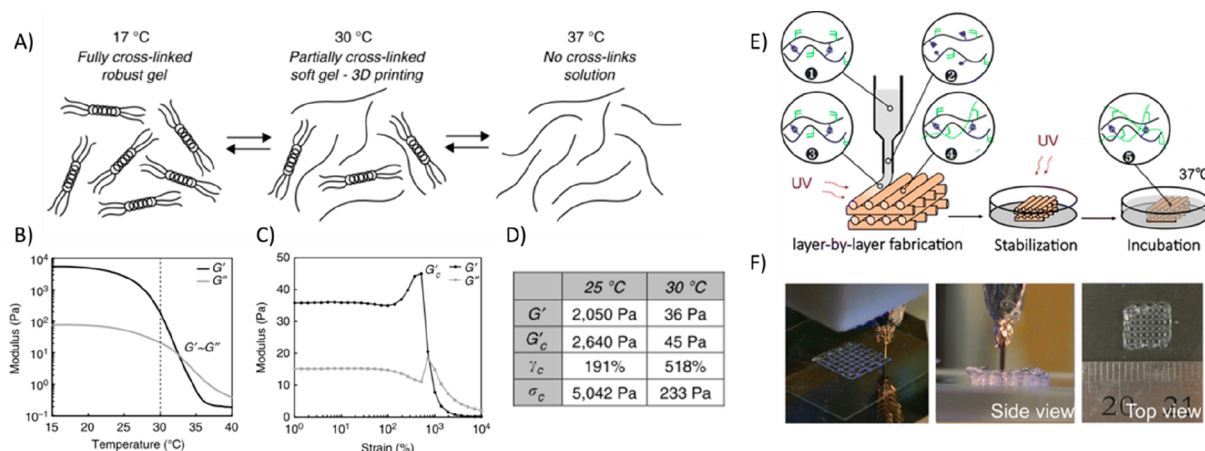
Figure 6. Demonstration of employing transient cross-linking in extrusion 3D bioprinting. (A) Schematic of gelatin chains physically cross-linked through thermal gelation into a robust, solid gel at 17 °C, or a weak, semisolid gel at 30 °C. (B) Temperature sweep of 10% w/v gelatin showing weak gel state at 30 °C. (C) Strain ramp revealing yield point of 10% w/v gelatin gel at 30 °C. (D) Storage modulus, complex modulus, yield strain, and yield stress of 10% w/v gelatin at 25 °C (robust) and 30 °C (weak and printable), respectively. (E) A weak gel of MeHA chains physically cross-linked through guest−host interactions: (1) is broken up through shear in the nozzle (2) and recovers upon exiting the nozzle (3), to be further stabilized by photoinitiated chemical cross-linking (4,5). (F) Photographs of the printing process and a printed multilayer structure of MeHA-based guest−host gels.[260] (A−D) reproduced with permission from ref 309. Copyright 2017 Nature Publishing group under CC BY 4.0. (E) adapted with permission from ref 238. Copyright 2016 American Chemical Society. (F) Adapted with permission from ref 260. Copyright 2009 Royal Society of Chemistry.

specific peptide domains is an interesting approach to be used in bioprinting, as the gelation of the hydrogel occurs at physiological conditions.[232,233] The technology used for the gelation process is called mixing-induced two-component hydrogel (MITCH) and has recently been reported by Dubbin et al.[232] for the preparation of a dual-cross-linked bioink. The authors employed MITCH to formulate a dual-component system based on alginate modified with proline-rich peptide domains and a recombinant engineered protein. The peptide domains were conjugated to alginate through the common (N-hydroxysulfosuccinimide) (NHS) conjugation chemistry. The other cross-linking method was based on the ionotropic gelation of alginate with Ca^{2+} ions. The cell-laden constructs exhibited high shape fidelity and over 90% of cell viability (fibroblasts and human adipose stem cells) one week postprinting. Analogous to peptide molecular recognition, hybridization of DNA is an equally appealing approach to bioink gelation. Combination of a polypeptide−DNA conjugate and a complementary DNA linker forms a gel within seconds of mixing under physiological conditions due to the DNA hybridization. The gel is degradable by proteases and nucleases.[208]

3.4. Moieties for Host−Guest Interactions

Host−guest chemistry is based on the self-recognition and noncovalent interactions between a receptor (host molecule) and a ligand (guest molecule), yielding a supramolecular complex.[234,235] One of the most used host−guest interactions is that between β-cyclodextrin (β-CD) and adamantyl moieties, as the latter tightly fits the β-CD cavity, leading to a host−guest complex association constant of 10^4 M.[236] Highley et al.[237] reported the application of this type of chemistry to create gels for bioprinting through the modification of HA with adamantane or β-CD. Similarly, Ouyang et al.[238] developed a hydrogel based on a dual cross-linking system, one of which was based on the β-CD-Ada host−guest interaction between HA derivatives (Figure 6E,F). The synthetic route used to modify the HA was the same as

previously reported by the authors.[239] Other common host−guest interaction is that between cucurbit[6]uril (CB[6]) and alkylammonium ions, in aqueous solutions. CB[6] tightly binds amines (e.g., 1,6-diaminohexane (DAH)) in their protonated forms to make very stable host−guest complexes with a binding constant up to 10^{10} or 10^{12}.[240,241] Shim et al.[242] used CB[6] modified-HA and DAH modified-HA to prepare multilayered constructs for osteochondral tissue regeneration. Before the preparation of the constructs, HA was modified with CB[6][243] and DAH groups.[244]

3.5. Moieties to Increase Bioactivity

A second class of modifications aims to introduce some of the functionality that is inherent to cell-binding proteins, into other polymers, both natural and synthetic. Typically, they involve the introduction of synthetic oligopeptides that are naturally found in the ECM.

3.5.1. Introduction of Cell Adhesion Motifs. The arginylglycylaspartic acid (RGD) peptide sequence is by far the most commonly incorporated cell-adhesion motif. RGD is the minimal binding domain of fibronectin, and its popularity stems not only from its relatively cheap cost of synthesis (being a short peptide) but also because of its efficiency in targeting integrin receptors, that allow cells to adhere to substrates that would ordinarily not support cell growth very well.[245] Incorporation of RGD onto synthetic polymers is relatively trivial given the abundance of chemical functionalities that are available for conjugation. For instance, an acrylate-PEG-NHS was functionalized with an RGD-serine peptide and was further incorporated into PEGDA hydrogels using a commercial SLA printer. As expected, the peptide improved cell viability, proliferation, and spreading.[246] In another vein, a norbornene moiety was introduced in the RGD peptide, and this was conjugated to PEG-8-arm-thiol hydrogels using the thiol−ene photochemistry.[247] The norbornene group was introduced in the RGD sequence, by the reaction of 5-norbornene-2-carboxylic acid with the N-terminus of the peptide by the HATU technology (i.e., using 1-[bis(dimethylamino)-

methylene]-1*H*-1,2,3-triazolo[4,5-*b*]pyridinium 3-oxid hexa-fluorophosphate). Despite the ease of incorporation of the RGD peptide into hydrogels, there is great potential in using other peptides or proteins and combinations of these to simulate diseased tissue[245] or to drive stem cell differentiation.[248] To the best of our knowledge, these approaches have not yet been applied to bioprinting.

3.5.2. Introduction of Enzyme-Cleavable Linkages. Modifying polymers with enzyme-cleavable links is an elegant method to mimic the natural ECM remodeling found in tissue and was made popular by Hubbell and Lutolf for bulk PEG hydrogels.[249,250] In synthetic polymers, the enzyme-mediated degradation might be achieved by inclusion of selected enzyme substrates in the cross-linking molecules. For example, although not strictly bioprinting, Fairbanks et al. photo-patterned PEG-4-arm-norbornene with dithiolated chymotryp-sin-degradable peptide and cysteine-RGD to control the spreading of human mesenchymal stem cells (hMSCs).[251] Many of the natural polymers used in bioprinting will undergo enzymatic degradation without the need for modification, but for instance alginate,[252−254] one of the most used poly-saccharides in bioprinting, does not present such ability. To endow alginate susceptible to enzyme attack, Fonseca et al.[255] functionalized it with a matrix metalloproteinase (MMP)-sensitive peptide. The functionalized polysaccharide was then successfully used in the preparation hydrogels for the encapsulation and release of hMSCs, being released faster in the MMP-sensitive hydrogels. Although, not strictly related to bioprinting, this work shows the potential of the enzyme-cleavable alginate hydrogels as a cell-delivery material for tissue engineering applications. Hydrogels prepared from gellan gum were also provided with the ability of being degraded by the action of enzymes. For such purpose, gellan gum was first modified with divinyl sulfone moieties and then made to react with a dithiol MMP1-sensitive cross-linker, through a Michael addition reaction. The hydrogels were used to promote the adhesion and proliferation of endothelial cells.[256] The results presented in this work confirm the potential of the developed hydrogel as a bioink material for bioprinting applications. Examples of this approach being used in biofabrication include supramolecular polypeptide−DNA hydrogels[54] and self-assembling peptides,[257] while the wider engineering of proteolytically degradable artificial extracellular matrices was reviewed by Fonseca et al.[258]

3.6. Other Modifications

Besides the main objectives of cross-linking or augmenting bioactivity, other modifications can be performed to make base polymers more suited for a specific application. One type of modification is aimed at influencing nonenzymatic degradation kinetics. For example, partial oxidation of alginate[259] or gellan gum has been employed to speed up their degradation. For the latter, perhaps an even more important result of the partial oxidation is the lowering of the gelation temperature, while native gellan gum[260] gels when cooled below temperatures exceeding 40 °C (depending on concentration), partial oxidation brings this gelation temperature down into the physiological range.[260] Other modifications are aimed at improving processability with a specific technique, such as the acetylation of gelatin to inhibit physical gelation, making it more suitable for material jetting.[213]

Additionally, to mechanically reinforce bioinks and facilitate the generation of scaffolds of high stiffness, polymers can be physically modified via blending of nanocrystalline inorganic compounds. Nanoclays such as laponite, montmorillonite, and sumecton[261] and nanocomposites like hydroxyapatite[262] can be incorporated into hydrogel structures. The resulting interactions between the hydrogel polymer network and nanoceramic phase results in a significant increase in bulk hydrogel stiffness and increase bioink viscosity, thus improving printing resolution.[263]

3.7. Bioink Formulations

Most bioinks are formulated by combining different polymers with a set of different functionalities. Rarely is one type of unadorned polymer used, as most miss one or more key properties. For instance, gelMA has too low viscosity,[264] HA is viscous but does not solidify,[265] agarose solidifies but too slowly.[18] By judicious choice of bioink components, the appropriate rheological properties can be met, greatly broadening the repertoire of printable materials.

3.7.1. Methods for Improved Printability. MeHA has been printed on its own but requires rapid photo-cross-linking after printing.[265] Improvements in printability have been made through functionalization to achieve short-term stability to printed constructs by physical gelation prior to photoinitiated cross-linking[237] or combined with a thermoresponsive PNIPAAm grafted HA to obtain short-term shape stability.[266] As mentioned before, collagen is a highly desirable material for bioprinting, however, its inherent cross-linking ability makes the process very difficult to control, with repercussions in the properties of the 3D construct which usually exhibits low mechanical stability.[152] Although some works in the literature report the use of neat collagen as a biomaterial ink,[267] it is important to mention that, due to the particularities of collagen, some modifications to the printing processes were needed to generate 3D constructs of good quality. In this sense, and as a way to improve the quality of the constructs without changing the printing processes, the use of mixtures of collagen with other polymers, both natural and synthetic, are being used for 3D bioprinting, as reviewed in ref 267. Formulations of alginate and gelatin were optimized by Ouyang et al., who classify the inks into "under-gelation", "proper-gelation", and "over-gelation" to supplement their more quantitative "printability characteristic" parameter based on how close were the shape to squares at the point where two struts overlap (the interconnects).[268] By doing so, they attempt to address the challenge that there is no universally accepted definition for printability, although attempts at standardization have been made.[269−271] The aim of Ouyang et al. was to investigate the effect of the ratio of alginate to gelatin, temperature, and holding time on the rheological properties. This last parameter, holding time, is one often overlooked. For many of the ratios of alginate to gelatin at different temperatures, the holding time had no effect on the printability, but at low temperatures (25 °C) and high gelatin concentration, the printability became worse with holding time. In other words, the bioink was gelling in the syringe. Alginate/gelatin has also been formulated with hydroxyapatite for radiopacity, osteogenicity, and mechanical stiffness.[272] The viscosity was dictated largely by the hydroxyapatite loading (up to 8%) and also increased the gel point from to 25.6 °C (no hydroxyapatite) to 28.2 °C (8%). Combining materials is one way to obtain the desired rheology; functionalizing polymers with reversibly interacting groups to form weak printable gels is another way, which arguably allows tailoring of rheology more

independently from final properties, which will be decisive in its success as a 3D cell culture substrate postprinting.

3.7.2. Photoinitiators in Bioinks. Radical and thiol−ene photopolymerization are the most used methods to promote postprinting cross-linking. This requires the presence of a photoinitiator in the bioink formulation. To date, a limited number of photoinitiators have been reported for bioprinting, mainly due to their cytotoxicity and poor water solubility.[234] The most commonly used photoinitiator for bioprinting is the commercially available Irgacure 2959 (2-hydroxy-4′-(2-hydroxyethoxy)-2-methylpropiophenone), identified as the only viable candidate for the preparation of cell-laden hydrogels by UV photo-cross-linking, in a pioneering comparative study testing several commercial initiators for cell encapsulation.[273] Irgacure 2959 has, however, limited water solubility and low quantum yield,[274] but still remains popular due to the lack of alternatives. The need to use UV light to cross-link polymers in the presence of cells is often met with alarm due to the perceived potential to cause DNA dimerization[275] and other damage due to the high concentration of free radicals present. Of course, any photochemical events will be highly dependent not just on the wavelength used but also the intensity and duration as well as any other competing radical chemistry (e.g., free radical polymerization). Examination of gene expression in hMSCs irradiated with UV in the presence of functional PEG concluded that changes in gene expression were observed not due to the use of UV light but rather due to the polymerization system used.[276] Yet, there is a strong drive toward the application of visible light photoinitiators such as lithium phenyl-2,4,6-trimethylbenzoylphosphinate (LAP),[274] ruthenium (Ru)/sodium persulfate (SPS),[207] and eosin Y.[131,277] The latter can be excited with visible light within the green spectrum (500−565 nm), such that it releases eosin radicals capable of chemically cross-linking hydrogel solutions. This consequently facilitates the generation of bioprinted structures using SLA with a visible light source, replacing the need for UV radiation, and this has been shown to significantly increase cell viability.[119] While the use of visible light may potentially cause less damage to the cells and be cheaper in terms of the light source, presumably much greater care must be taken to avoid undesirable stray-light cross-linking events prior to bioprinting. Even so, the search for more efficient photoinitiators than the commonly used UV active Irgacure 2959 is sure to continue. In a completely different vein, Tromayer et al.[278] conjugated a two-photon initiator onto the hyaluronic acid (HAPI) backbone and used this new conjugate as the photoinitiator in the bioprinting of gelMA. The cytotoxicity tests indicated that the HAPI was less cytotoxic than the conventional water-soluble two-photon initiator from the family of the cyclic benzylidene ketones. Also the cells in the construct presented higher viability after 5 days of printing. This promising novel strategy of conjugating the photoinitiator onto the polymer prevents the cellular uptake of the small photoinitiator molecule that is cytotoxic and could potentially be applied to most photoinitiating systems currently used.

3.8. Bioink Sterilization

An often overlooked, but important, aspect of bioprinting using bioinks is sterilization, especially when the bioprinted product is to be used in vivo. Obviously, like any cell therapy, terminal sterilization of cell bioink constructs is not possible, but fortunately the high level of automation intrinsic to robotic bioprinting means that the process itself should be amenable to

aseptic closed process manufacturing. Sterilization of the bioinks prior to bioprinting, however, creates challenges. This is exacerbated by the sensitivity of the bioprinting process to small changes in physicochemical changes that can occurring during sterilization processing.

Common sterilization methods such as gamma-irradiation and steam treatment (autoclaving) can be detrimental to the physical properties of polymers and result in a change to their rheological properties. Autoclaving of alginate (either in solution or dry form), gelatin, gelMA, HA, and HAMA leads to nonprintable, low-viscosity materials.[279,280] Similarly, and not surprisingly, gamma-radiation treatment of gelMA reduced printability as it is susceptible to modification of the sol−gel transition due to chemical changes in the polymer,[281] as well as presumable radiation-initiated polymerization of the methacrylate groups. Using lower energy photons such as UV radiation does not impact printability of alginate but does not fully sterilize the material.[280] Ethylene oxide sterilization has been recommended for gelatin, gelMA, HA, and HAMA[279] and has also been shown to work with alginate but comes with high safety requirements, high cost,[280] and potential long-term health concerns as a carcinogen.

Filtration through common small pore filters (e.g., 0.2 μm) is a well-established method for sterilization has been used to sterilize alginate solutions prior to encapsulation of pancreatic islets for implantation into macaques.[282] For bioprinting, sterile filtration caused no change in physicochemical properties and printability for alginate,[280] but for gelMA some high molecular weight fraction was removed, thereby affecting the bioprinting.[279]

The important issues of sterilization of bioinks and aseptic bioprinting are not insurmountable challenges, however, it is clear from the recent literature that the sterilization method must be matched to the polymer and the printing method. Beyond alginate, gelatin, gelMA, HA, and HAMA, though, there is little evidence on how sterilization affects the rheological properties of bioinks, hence warranting further investigation. Similarly, novel sterilization methods such as super critical CO_2 may provide a means for gentle sterilization[283,284] of bioinks.

3.9. Commercial Bioinks

Prompted by recent technological developments, bioprinting has found numerous applications in the field of medical research. With an increasing demand for printable materials capable of supporting cell function, many companies have turned their attention to the development and commercialization of bioinks. The Swiss company RegenHU Ltd. commercializes since 2017 the ECM-Bioink, which is a grade of bioinks based on self-assembly peptides.[285] The company offers five different bioink grades that differ in the electrical net charge and stiffness of the obtained scaffold. As stated in the company Web site the ECM-Bioink were successfully used in supporting the growth and differentiation of a wide range of cell types, including fibroblasts, stem cells, neurons, etc. The company also sells OsteoInk, an ink based on calcium phosphate, that is mainly used for hard tissue engineering.[286] All these inks were designed and optimized to work exclusively with the 3D Discovery and BioFactory printers, also commercialized by RegenHU, which can somehow be a limiting factor for a more widespread use of this technology.

Biogelx is a Scottish company founded in 2013 as a spin-off of the University of Strathclyde. It commercializes bioinks

Table 3. Overview of Commercially Available Bionks for 3D Bioprinting

bioink	material	type of cross-linking
	RegenHU Ltd.	
ECM-Bioink	self-assembly peptides	self-assembly
	BiogelX	
Biogelx-INK-S	self-assembly peptides	self-assembly
Biogelx-INK-RGD Biogelx-INK-GFOGER	self-assembly peptides functionalized with biorelevant peptide sequences	self-assembly
	Manchester BIOGEL	
PeptiInk series	alpha 1: self-assembly peptides (neutral charge)	self-assembly
	alpha 2: self-assembly peptides (charged)	self-assembly
	alpha 4: self-assembly peptides (charged)	self-assembly
	Bioink Solutions Inc.	
Gel4Cell	GelMA	UV cross-linking
Gel4Cell-peptide	GelMA functionalized with growth factors mimetic peptides	UV cross-linking
	Cellink Life Sciences	
A Series	alginate (CELLINK A)	ionic gelation
	RGD-functionalized alginate (CELLINK A-RGD)	
CELLINK series	alginate and nanofibrillar cellulose (CELLINK), CELLINK supplemented with fibrinogen (CELLINK FIBRIN and CELLINK SKIN), laminin (CELLINK LAMININ), and CELLINK in which the alginate was functionalized with RGD (CELLINK RGD)	ionic gelation or Ionic gelation/thrombin (in the case of bioinks supplemented with fibrinogen)
collagen series	collagen type 1 (Coll 1) or collagen methacrylate (ColMA)	self-assembly (Coll 1) and self-assembly followed by UV cross-linking (ColMA)
GelMA series	GelMA and carbon nanotubes (Bio Conductink)	photo-cross-linking (LAP photoinitiator)
	GelMA	photo-cross-linking (LAP photoinitiator)
	GelMA and alginate (GelMA A)	photo-cross-linking (LAP photoinitiator), followed by ionic gelation
	GelMA and CELLINK (GelMA C)	photo-cross-linking (LAP photoinitiator), followed by ionic gelation
	GelMA with methacrylated hyaluronic acid (GelMA HA)	photo-cross-linking (LAP photoinitiator)
	solution of GelMA with high concentration (GelMA HIGH)	photo-cross-linking (LAP photoinitiator)
GelX series	GelMA, xanthan gum, and alginate (GelXA)	photo-cross-linking (LAP photoinitiator) and ionic gelation
	GelMA, xanthan gum, alginate, tricalcium phosphate, and hydroxyapatite (GelXA BONE)	photo-cross-linking (LAP photoinitiator) and ionic gelation
	GelMA, xanthan gum, alginate, and fibrinogen (GelXA FIBRIN)	photo-cross-linking (LAP photoinitiator), ionic gelation and thrombin
	GelMA, xanthan gum, alginate, and various laminins (GelXA LAMININ)	photo-cross-linking (LAP photoinitiator) and ionic gelation
	GelMA, xanthan gum, alginate, and fibrinogen (GelXA SKIN)	photo-cross-linking (LAP photoinitiator), ionic gelation and thrombin
	GelMA, xanthan gum (GelXG)	photo-cross-linking (LAP photoinitiator)
	Advanced Biomatrix	
LifeInk series	collagen type 1 (LifeInk 200)	self-assembly
	acidified collagen type 1 (LifeInk240)	self-assembly
PhotoCol series	ColMA (PhotoCol)	photo-cross-linking
	ColMA + Irgacure (PhotoCol-IRG)	UV cross-linking (365 nm)
	ColMA + LAP photoinitiator (PhotoCol-LAP)	blue light mediated cross-linking (405 nm)
	ColMA + ruthenium photoinitiator (PhotoCol-RUT)	visible light mediated cross-linking (400−450 nm)
PhotoGel series	GelMA (PhotoGel)	photo-cross-linking
	GelMA + Irgacure (PhotoGel-IRG)	UV cross-linking (365 nm)
	GelMA + LAP photoinitiator (PhotoGel-LAP)	blue light mediated cross-linking (405 nm)

Table 3. continued

bioink	material	type of cross-linking
	Advanced Biomatrix	
	GelMA + ruthenium photoinitiator (PhotoGel-RUT)	visible light mediated cross-linking (400−450 nm)
PhotoHA series	HAMA (PhotoHA)	photo-cross-linking
	HAMA + Irgacure (PhotoHA-IRG)	UV cross-linking (365 nm)
	HAMA + LAP photoinitiator (PhotoHA-LAP)	blue light mediated cross-linking (405 nm)
	HAMA + ruthenium photoinitiator (PhotoHA-RUT)	visible light mediated cross-linking (400−450 nm)
HyStem series	thiolated HA (HA-SH) and PEGDA (HyStem)	Michael addition
	HA-SH, PEGDA, and thiolated gelatin (HyStem-C)	Michael addition
	HA-SH, PEGDA, thiolated gelatin and thiolated heparin (HyStem-HP)	Michael addition
	HA-SH, thiolated gelatin, PEG-norbornene	Michael addition mediated by UV photo-cross-linking (365 nm)
	UPM Biomedicals	
GrowInk	nanofibrillar cellulose (GrowInk-N)	self-assembly
	anionic nanofibrillar cellulose (GrowInk-T)	self-assembly (with possibility of post-cross-linking)
	nanofibrillar cellulose with alginate (GrowInk-ALG)	self-assembly and ionic cross-linking

based on self-assembly peptides.[287] It has, in its products' portfolio, three grades of bioinks: Biogelx-INK-S, Biogelx-INK-RGD, and Biogelx-INK-GFOGER. The first one is solely based on the self-assembly peptides, whereas in the other two the peptides were functionalized with bioactive molecules, namely RGD and tripeptide sequences present in collagen for enhanced biofunctionality. Manchester BIOGEL, founded in 2014, also produces bioinks based on self-assembly peptides. Its bioinks exhibit shear-thinning properties, being suitable for use in extrusion-based systems. Different grades of bioinks are available, being the main difference between them the charge and type of functionalization that is made with specific biomimetic sequences.[288]

Bioink Solutions Inc. is a Korean company that sells bioinks based on gelMA, the Gel4Cell. The other grade of bioinks, the Gel4Cell-peptide, are functionalized with specific growth factors-mimetic peptides. CellinkLife Sciences, a Swedish company, was founded in 2016 and is one of the most important players regarding commercial bioinks. Interestingly, and despite commercializing also their own 3D bioprinting technology, the company was the first to develop and offer to their clients "'standard'" bioinks that can be used in any extrusion-based printer. The company has in its portfolio[289] a variety of bioinks, for several applications, based on the most common base polymers (e.g., alginate, collagen, gelMA), and mixtures of them (e.g., gelMA and alginate) or in mixtures of such polymers with others less common in bioprinting (e.g., xantham gum, nanocellulose). The main cross-linking methods are the ionic gelation or photopolymerization along with ionic gelation. Advanced Biomatrix is a North American company that, similarly to CellinkLife Sciences, commercializes bioinks based on the main base polymers (e.g., collagen, gelMA, ColMA, and HA-MA).[290] Regarding the cross-linking methods, the most used is photo-cross-linking and for some bioink series (PhotoCol-RUT, PhotoGell-RUT, PhotoHA-RUT), this can be accomplished under visible light. This is highly advantageous because visible light does not have any deleterious effect on cells. In the beginning of 2020, UPM Biomedicals, a Finnish company, launched the GrowInk, which is a series of bioinks based on nanofibrillar cellulose. The

company claims that the viscosity of the bioinks can be easily manipulated in order to achieve the construct with the right mechanical properties for the embedded cell line. The cell laden constructs are made by extrusion bioprinting and the GrowInk is compatible with many of the commercially available bioprinters.[291] Table 3 gives an overview of some of the bioinks available in the market (many more are under development), along with the mechanisms of cross-linking and main producers.

Other companies like Allevi, Brinter, or Sigma-Aldrich also supply bioinks, but these are mainly based on the solutions presented in Table 3. Allevi, for instance, commercializes the bioinks developed by Advanced Biomatrix. Brinter, in turn, presents the general characteristics of different base polymers that can be used to formulate bioinks but does not have available a bioink portfolio.

4. STRUCTURE AND PROPERTIES OF POLYMERS IN BIOPRINTING

4.1. Rheology

Stating that many bioprinting techniques rely on a liquid-to-solid transition would be an oversimplification. Being polymeric systems, for bioinks many states exist between a (purely viscous) liquid and a (purely elastic) solid. Often, a gradual or stepwise progression from liquid-like to solid-like is required to ensure the ink can be processed into a designed shape and have sufficient stability to retain the final shape. Such transient behavior cannot be summarized in a single parameter; hence, it is important to look at several rheological parameters and behaviors together, including viscosity, shear thinning, yield stress, and recovery. A good daily life analogue is the application of tomato ketchup onto a plate with food. It takes a certain amount of squeezing force to start the flow of sauce out of the bottle (yield stress), then to increase the flow takes only little extra force (shear thinning), and once it lands on the plate, it should stay in place and not spread out into a thin layer (recovery). As more and more studies into the rheology of bioinks are published, generic parameters that are associated with "good printability" are becoming apparent.

Naturally, the requirements of rheology strongly depend on the modality used. Material extrusion is the most widely used technology for bioprinting; yet the rheological profiles of well-performing inks are typically complex. Hence, the importance of rheology of polymeric systems technique will be discussed in particular detail for this technique, followed by a short discussion of differences in rheological properties seen in inks used with other bioprinting modalities.

4.1.1. Viscosity. Several leading reviews[28,292,293] report $30-600 \times 10^6$ mPa·s as the viscosity range used for extrusion bioprinting, all referring to a publication that employed poloxamer 407 at 25−40% w/v, corresponding to 20−28.6 wt %.[154] Many bioinks (and polymer solutions in general) show a strong shear rate dependency, therefore viscosities should always be reported alongside the shear rate at which they were measured. A typical range of shear rates for extrusion bioprinting would be $10^{-1}-10^3$ s^{-1}, so it is worthwhile to compare the viscosities of different bioinks at 10^2 s^{-1}. At this shear rate, 28.6 wt % poloxamer 407 shows a viscosity of approximately 6 Pa·s, 5 orders of magnitude lower than the widely reported upper value.[202] Other bioinks show similar viscosities in the range of 1−25 Pa·s around the same shear rate,[294−298] implying this to be a target value for formulating bioinks for this technique. As the main function of viscosity is to counteract the detrimental effects of gravity and surface tension, much lower viscosities could result in widening of a printed filament or its breaking up into droplets and sagging/flow of a printed shape. On the other hand, much higher viscosities would result in increasing fabrication times (as a result of lower flow rates) and/or potential damage to cells by being subjected to high shear stresses. For example, a 10% increase in cell death was observed when MSCs in a 10% alginate ink were deposited through a 210 μm needle at 3 bar pressure, while lower pressures showed no difference from unprinted controls.[299] Nair et al. saw higher cell deaths of 40% at 2.8 bar and 250 μm and still 25% at 1.4 bar and 400 μm using a similar alginate-based bioink, demonstrating that some cell types (endothelial cells in this case) are more sensitive to shear stress than others.[300] Although shear stress is the main parameter in process-induced cell death in most bioprinting cases, for very sensitive cells such as embryonic stem cells, other factors like gel concentration and temperature during the holding time prior to printing can cause significant cell death as well.[268] The effect of shear stress on cell damage was investigated in detail using Schwann cells and 3T3 fibroblasts combined with mathematical modeling, leading to the establishment of a generalized "cell damage law" which accurately predicts the percentage of cell death induced by bioprinting as a function of force and exposure time.[301] In a follow-up study, the same cell damage law was used to predict that straight/cylindrical nozzles would lead to much higher shear stresses and cell death than tapered/conical ones at a similar flow rate, which was confirmed experimentally with high correlation.[302] Additionally, with tapered nozzles higher flow rates can be achieved at much lower pressures, allowing the use of viscous inks at considerable speeds with minimal cell damage. The researchers also found that in contrast to shear stress, hydrostatic pressures have a minimal effect on cell viability, with no significant effect at all up to 500 kPa (5 bar).[302]

4.1.2. Shear Thinning. Many polymer solutions including bioinks show shear thinning. As shear rates are increased, the random coils of polymer chains are unwound, and the chains are stretched in the direction of the flow. This change in conformation reduces entanglements and flow resistance, and hence viscosity. Shear thinning can be expressed as the flow index n in the power law model, which fits many polymer systems: $\tau = K \cdot \gamma^n$, in which τ is shear stress (Pa), K the consistency index (in Pa·s), and γ shear rate (s^{-1}). At $n = 1$, there is no shear thinning, while an increased deviation toward 0 indicates a stronger shear thinning effect. For semidilute polymer systems n depends on molecular weight and concentration and is typically in the range of 0.5−0.9. Much stronger shear thinning often indicates additional interactions contributing to increased viscosity at low shear rates, such as ionic interactions in partially precross-linked alginate[303] or entangled micellar coronas in poloxamer 407 (explaining the strong shear thinning despite the low molecular weight). Shear thinning can facilitate bioprinting by reducing the viscosity at high shear rates within the nozzle, followed by a sharp increase in viscosity after the material is deposited and only the smaller forces of gravity and surface tension remain. A good example is that of MeHA functionalized with either adamantane or β-cyclodextrin groups.[238] These groups bind reversibly via guest−host interaction, creating a supramolecular assembly upon mixing that increases viscosity, particularly at low shear rates (Figure 6E). As a result, flow of printed filaments is slowed down considerably, allowing time for photoinduced cross-linking through the pendant methacrylate groups and making hyaluronic acid into a printable bioink (Figure 6F).[238] It should be noted that shear thinning alone is by no means a guarantee for printability. For example, gelMA solutions of 10% at 37 °C show considerable shear thinning, yet drip out of a nozzle rather than forming filaments.[264,304] A gelMA solution requires partial thermal gelation[305] or addition of other components increasing its viscosity[264] or inducing a yield stress.[304] For example, addition of 1% gellan gum at a tailored cation concentration greatly improved printability of 10% gelMA by inducing yield behavior, without changing the magnitude of shear thinning.[191,304] Besides facilitating printability, shear thinning can have a protective effect on encapsulated cells. For a Newtonian liquid flowing through a nozzle, the shear rate profile increases linearly from the center to the needle wall. For shear-thinning fluids, this profile becomes more parabolic, meaning a smaller part of the printed cell population will be transported closely along the wall, where shear stresses are high. Additionally, the residence time of an equal fraction of the cell population traveling near the wall will be shorter with increased shear-thinning, with shorter exposure likely leading to less damage. This was demonstrated by Paxton et al., who modeled shear profiles through the nozzle and calculated residence time distributions.[23] By simulating longer term (60 s) exposure to shear stress in a rheometer, they showed a reduction of cell viability at higher shear rates that was not noticeable in bioprinted samples, in which only a small part of the cell population is exposed to shear forces for a long time. The combined importance of residence time and shear stress was also demonstrated by Snyder et al., who performed similar modeling and corroborated the results experimentally using MSCs.[306] These reports demonstrate how shear-thinning protects the majority of the cells against excessive shear forces. Furthermore, shear-thinning gels can protect cells from damage particularly at the entrance of a needle when dispensed from a syringe, as has been studied in detail for stem cell delivery via injection.[230,307]

4.1.3. Yield Stress. Yield stress is emerging as an important quantitative parameter determining printability. It refers to the threshold stress required to initiate flow, implying that below this threshold the material behaves like a solid. Advantages of this behavior are the elimination of cell settling in the print cartridge as well as the retainment of shape directly after printing. Yield behavior in bioinks is typically the result of the presence of a polymer network with weak and reversible interactions that can be broken up by moderate flow and re-form when the flow-induced stress is removed. Interactions employed in bioprinting to induce yield behavior include partial chemical cross-linking,[308] partial physical cross-linking,[309] or weak ionic cross-linking such as for gellan gum with tailored ionic strength.[304] Some studies have quantified yield stress through rheometry, which potentially serves as a potent design parameter for bioink development. For example, Laronda et al. employed partial physical cross-linking of 10% w/v gelatin at 30 °C to obtain a yield stress of 233 Pa, which was deemed optimal for printing gelatin constructs (Figure 6A−D).[309] Well-defined structures were printed at 30 °C, whereas at 37 °C the same 10% gelatin solution is a low-viscous liquid that drips from a nozzle when extruded. At 25 °C, however, the gelatin (now exhibiting a yield stress of 5,042 Pa) becomes too robust to be extruded. Where yield stress is the stress required to initiate flow, yield strain is the deformation of the gel at that point. In the example here described, yield strain was 518% for the weak gel at 30 °C and 119% for the rigid gel at 25 °C. As gels are mostly elastic up to the yield point, the ratio of yield stress over yield strain corresponds closely to the gel's apparent modulus, which was 45 Pa and 2640 Pa for the weak and rigid gels, respectively. Interestingly, a study into poloxamer 407 and its methacrylated form for use as reinforcing inks for bioprinting found very similar values for yield stress (in the 200−400 Pa range) of printable formulations (all 28.6 w/w at 20 °C).[202] A systematic study into the influence of yield stress in nonbiological extrusion-based 3D printing corroborated these numbers, relating the yield stress to the maximum achievable curvature. For example, a particle-loaded ink with surface tension of approximately 0.02 N/m required a counteracting yield stress in the order of 100 Pa to prevent shape distortion of single filaments and overhangs of 0.2 mm radius of curvature.[310] Besides the above examples on printing of cell-free inks, evaluation of yield stress has also been performed for cell-laden bioinks. For example, Mouser et al.[191] identified yield stress as an important parameter governing the printability of bioinks for cartilage bioprinting, composed of gelMA and gellan gum. At the optimal conditions (10% gelMA + 0.5% gellan gum in 0.09% saline at 28 °C), a yield stress of 48.2 Pa was measured.[191] As an essential feature for cell printing, this study also related yield stress to the ability to obtain a homogeneously mixed, air bubble-free cell-laden ink. GelMA/gellan composite gels with a yield stress of 35 Pa and higher were too solid to enable the mixing in of cells. Notably, the optimal composition mentioned above that was best printable at 28 °C with a yield stress of 48.2 Pa, could be mixed with cells at 37 °C when its yield stress was approximately 6 Pa. It is therefore important to formulate bioinks that allow mixing in of cells in a state of low yield stress, which would subsequently be increased to higher levels for accurate printing. Others have reported yield stresses for printable gels that are higher than the values above, for example, combining gelatin with a PEG-disuccinimidyl valerate

cross-linker (PEGX).[57] Gelatin was used at 2−3% with a PEGX:gelatin ratio of 0.2, or 5% gelatin at 0.1 PEGX:gelatin at 37 °C, resulting in yield stress values of 144−2,130 Pa. Combinations of higher gelatin concentration or/and higher PEGX:gelatin ratio resulted in robust gels of yield stress around 3 kPa and were either unable to be extruded, or required significant pressure, producing inconsistent strands at very slow mass flow rates.[57] The strategy of employing thermal gelation to improve the printability of cell-free gelatin described above was later extended to cell-laden gelMA, where cooling enabled the extrusion of lower concentrations of gelMA through partial solidification, at increased viscosity and storage/loss moduli (yield stress was not assessed here).[305] The bioink herein is referred as "gel-phase bioink", as in the absence of flow these gels have a solid-like appearance. In conclusion, yield behavior is important in determining printability of a bioink, with the suitable range of yield stress values being approximately between 2 Pa and 2 kPa for printing, while at the time of mixing in cells, yield stress should be below 35 Pa, or absent.

4.1.4. Recovery. Recovery of bioinks refers to the rate at which a cohesive mechanism is restored after being broken up by shear. Recovery is often measured on a rheometer by exposing the ink to a low and a high shear rate alternately (e.g., 0.01 and 100 s^{-1}), and assessing how viscosity (in continuous flow mode) or storage and loss moduli (in oscillatory mode) are restored over time. For highly printable formulations such as 25% poloxamer 407, the recovery is too fast to be followed in a rheometer; after a plateau of 1.5 Pa·s viscosity at 895 s^{-1} shear rate, the first data point when decreasing shear rate to 0.01 s^{-1} is already at 5×10^3 Pa·s, at which flow is negligible.[23] For slower recovering inks, the increase in mechanical properties over time gives an indication of the deformation that can be expected after deposition of a filament, or of the swiftness required to provide additional stability through cross-linking. For example, the solidification of gelatin (or gelMA) through thermal gelation is too slow to rely on a recovery mechanism,[311] therefore, in order to print it, recovery has been improved by partial gelation prior to printing,[312] very tight temperature control throughout the cartridge and nozzle, or by supplementing with faster recovering alginate[313] or gellan gum.[304] Recovery rates are also strongly dependent on concentrations of polymer and cross-linker molecules.[314]

In summary, the ideal bioink for extrusion printing with high shape fidelity shows a number of rheological characteristics and will progress through several states of liquid-like or solid-like appearance during the process of bioprinting (Figure 6). If one parameter had to be selected to judge printability it may be yield stress, however, it does not tell the whole story. In the earlier example of methacrylated HA functionalized with groups that bind reversibly via guest−host interaction, shear thinning was identified as the main parameter improving printability.[238] In oscillatory strain sweep mode, yielding was observed at a certain strain, which the authors also recognized as essential for hydrogel extrusion. However, a simple vial tilting test showed considerable gravity-induced flow after approximately 10 min. This is 2 orders of magnitude slower than for methacrylated HA without guest−host groups, giving enough time for additional photoinitiated cross-linking, but indicated yield stress alone was not enough to keep the printed structure. It is likely that the magnitude of yield stress will depend on the rate at which it is measured, and fast recovery plus additional shear thinning will aid in printability.

4.1.5. Other Techniques. Material jetting bioprinting relies on low viscosities of 3.5–30 mPa·s (for reference, water has a viscosity of 1 mPa·s),[28] greatly limiting the use of polymers in inks unless at very low concentration and/or molecular weight. These techniques have therefore been seen as more suitable for 2D patterning of cells or proteins, which formed the pioneering work in the bioprinting arena.[77,79,94] To use material jetting for 3D printing, a cross-linking solution can be printed onto a viscous pregel, such as the printing of $CaCl_2$ onto sodium alginate.[315] For nonbiological applications, printing of small unsaturated molecules followed by rapid photocuring into polymer networks has been developed into the PolyJet technology commercialized by Objet (currently Stratasys), which enables the fast 3D printing of smooth and accurate objects with a range of material properties and gradients thereof. This shows that the strict requirement of low viscosity does not exclude material jetting technology from being used for 3D printing, and more development in the area of bioprinting is to be expected. Besides viscosity, other rheological phenomena are of importance as well for this technology. The same principles of cell protective effects due to shear thinning are at play in material jetting processes. Furthermore, the yielding behavior of gellan gum has been exploited in these systems to obviate the persisting problem of cells settling in the cartridge.[316] Because of its orifice-free nature, laser-induced forward transfer (LIFT) can handle bioinks of a somewhat greater viscosity range of 1–300 mPa·s.[316] Inks used for LIFT-based bioprinting include cells suspended or protein dissolved in culture media,[317] nano-hydroxyapatite suspensions,[318] and (cell-laden) sodium alginate at 1% w/v,[319] all used for patterning on a 2D substrate. The fabrication of 3D tissues via this technique has been proposed through the alternating deposition of a layer of substrate (here Matrigel) and a cell pattern printed onto it.[320] In stereolithography, viscosities up to 5 Pa·s (similar to extrusion bioprinting) have been reported,[321] which is limited by the layer recoating process. Yet a reasonably high viscosity slows down diffusion of propagating radicals out of the exposed area and of monomers and photoinitiator into the exposed area, thus improving the print resolution. The subsection above focused on the viscosities of inks used in several 3D printing techniques. Regardless of the printing technology employed, a small yield stress or high zero-shear viscosity might aid in preventing cell settling in the ink reservoir[194] and shear-thinning may facilitate processes and reduce cell damage from shear stresses.

4.2. Stiffness and Network Topology

Structural features of a 3D network determine its stiffness and make a major contribution to controlling cell behavior. So, it is critical to consider the properties and influence of the natural matrices surrounding cells of interest when seeking to create the tissue engineered environment. It has become firmly established in the literature, originating from the work of Engler et al.,[322] that stiffness is a fundamental driver of cell differentiation trajectory. A major contributor to the stiffness of tissue is the ECM, in particular collagen. Using mesenchymal stem cells, the original paper indicated that a soft matrix around 1 kPa, akin to brain, was conducive to formation of cells with neuronal attributes while an intermediate stiffness (10 kPa) matrix facilitated differentiation toward muscle-like and rigid (100 kPa) matrices toward bone-like cells. Consequently, differentiation of a whole range of cell types

including muscle,[323] cartilage,[324] cardiomyocytes,[325−327] endothelial cells[328] as well as bone[329] have been investigated further, showing a preference for a particular range of matrix stiffnesses for stable differentiation and function, loosely related to that of their in vivo niche. Since then, we have also learnt that there is a complex mechanotransduction pathway, including cell surface molecules like integrins and channel proteins like TRPV and piezo receptors connected through numerous cytoplasmic transducer molecules and the cytoskeleton to gene activation and cell behavior. These together with nuclear lamina proteins and nuclear shape comprise the machinery which senses external matrix stiffness. Hippo pathway components Yes-associated protein (YAP) and transcriptional activator with PDZ binding motif (TAZ) as transcriptional coactivators are central to nuclear mediation of substrate mechanosensing: phosphorylation of Yap holds it in the cytoplasm, but activation of the stretch response and actin cable formation leads to its dephosphorylation and translocation to the nucleus. These pathways respond to the nature of the ECM, regulating how matrix stiffness together with nanotopography, which mimics it in many ways, dictate gene expression, cell proliferation, cell function, and differentiation. Changes in substrate stiffness can alter the size, composition, and density of focal adhesions which transfer cues from the ECM to the cytoskeleton. Moreover, cell elongation and associated cytoskeletal polymerization, influenced by stiffness and ligand type and density, can dramatically influence cell differentiation[330,331] also shown to be dependent on the stiffness of the cells themselves.[332] The mechanotransduction mechanism can in turn drive matrix stiffness and in one example (TRPV4 and epidermal keratinocytes) drove epithelial−mesenchymal cell type transition.[333] Further, physical cues from the matrix can change the effect of growth factors and other biochemical ligands. For example, PSCs' stiffness related Yap localization and spreading is reliant on stiffness but in conjunction with biochemical ligand cues and regulated by both the nature but also the density of the biochemical ligands.[334]

Cells can migrate through 3D matrices in two distinct ways: either through proteolytic (mesenchymal) or nonproteolytic (amoeboid) strategies.[335] The latter occurs particularly in softer gels through physically pushing the gel aside, thereby taking advantage of pre-existing microcracks and/or forming new ones. The former can occur in gels of any stiffness as long as cleavable links are present, either naturally or engineered.[335] As cross-link density controls stiffness (the importance of which is iterated above), cross-link density is probably one of the most important factors influencing encapsulated cells.[336] However, other topological features of polymer networks also influence cell behavior. Within hydrogels, topology originates from nano-/microstructures relating to network heterogeneity based on the underlying architecture of the polymers, porogens, defects, and cross-linking chemistry. Heterogeneity may also include nanofibrils in peptide-based self-assembled hydrogels. The influence of hydrogel network topography has been illustrated by Sridhar et al., who show that in PEG hydrogels neo-tissue growth by chondrocytes is linked to weakly cross-linked regions around cells and dense cell clusters.[337] In their case, the heterogeneity originated from possible interference of the radical cross-linking locally to the chondrocytes and the hydrolysis of the networks without the need of using more sophisticated cell-mediated degradable networks, for example, those developed by Lutolf and

Hubbell.[249] Heterogeneous networks do not always lead to more favorable conditions for cells. While chain-growth polymerization of the methacrylate groups in gelMA is a convenient method for cross-linking, there have been suggestions that radical-mediated damage to cells and heterogeneous network formation may negate any advantage. Munoz et al. compared gelMA cross-linked via chain-growth polymerization with norbornene-functionalized gelatin (gelNB) cross-linked by thiol−ene step-growth polymerization with small molecular multithiols and found that both systems cured equally quickly but that the gelNB system had lower shear modulus. When hMSCs were encapsulated in each type of gel, higher intercellular connectivity, and faster cell spreading were observed in the gelNB system compared with the gelMA gels for two different percentages of gelatin (4 and 8 wt %), highlighting the influence of network topology. Interestingly, the synthesis of gelNB was less efficient than gelMA due to differences in reactivity of methacrylic anhydride (for gelMA) and carbic anhydride (for gelNB).[217] As discussed above, the synergy between network topology and consequent mechanical properties is a determinant to guide cellular response and generate functional tissues. However, if the final goal is to mimic the native ECM, then careful consideration should to be taken to integrate its time-dependent mechanical properties in the rational design of dynamic bioinks. This is an area of growing interest where many strategies based on supramolecular and dynamic covalent chemistry are becoming available to introduce dynamic reversible interactions in printable hydrogels and hence controlling tissue maturation. To complement the information provided in section 3.2.4, we direct the reader to another comprehensive review on the topic of dynamic bioinks.[338]

4.3. Gradients

Biochemical and physical gradients are commonly found at the interface between natural tissues (e.g., tendon-to-bone, bone-to-cartilage, muscle-to-tendon, etc.). These gradients govern cell migration and differentiation, yet despite their importance, creating gradients within bioprinted structures is not trivial. Incorporation of chemical and physical gradients addressing a range of cell movement "taxis" include chemo- and hepto-taxis for soluble and immobilized chemical signals, respectively, durotaxis for substrate rigidity, galvo-, photo-, geo-, and tenso-taxis for electrostatic potential, light, gravity, and extracellular tension, respectively. These have all been achieved within hydrogels and nonhydrogel materials using a range of methods.[339] While gradients have been reported in 2D and 3D cell culture, microenvironments using lithography of engineered proteins,[340] coprinting of cells in gradient materials is relatively unexplored. Possible reasons are the additional hardware and bioink demands. An elegant approach to simplify the bioink requirements for gradient printing was reported by Forget et al., who used a common agarose base material modified with various degrees of oxidation of hydroxyl groups (to carboxylic acid groups). This allowed the synthesis of a range of chemically very similar materials but with different elastic moduli (5−230 Pa) at almost constant shear viscosity (10−17 mPa·s at the extrusion temperature of 37 °C).[188] The origin of the tailored elastic moduli is due to the shift in ratio of α-helical to β-sheet upon carboxylation. This allowed them to bioprint hMSCs in soft carboxylated agarose surrounded by stiffer carboxylated agarose using a droplet-generating micro-

valve system with four print heads on a three-axis robotic system.

Multimaterials have also been printed using a single print head to improve continuity of the printing process. Liu et al. demonstrated a system with seven small-volume capillaries connected to a single head to allow near delay-free, continuously ejection of bioinks filled with different dyes or cells.[64] Initial fine-tuning experiments used shear thinning nanosilicates at an optimal concentration of 5% (no polymer), with different dyes to demonstrate the continuous switching from one ink to another. They then used a bioink made up in fetal calf serum consisting of 5% gelMA/1% alginate with 0.5% photoinitiator to formulate five inks, each with its own cell type−human dermal fibroblasts, HepG2 human hepatocellular cells, hMSCs, and human umbilical vein endothelial cells (HUVECs). This bioink is shear thinning and has a viscosity at the lower end of the range, typically ca. 1 Pa·s at 10 s^{-1} rate (or 10 Pa·s at 0.1 s^{-1}). Cells were added to the ink immediately prior to printing, and a miniature heart-like structure and microfluidic devices were printed, each undergoing secondary UV curing of the gelMA. No mixing of the bioinks was attempted, meaning the range of structures printed still had distinct layers rather than continuous gradients. GelMA semigradient constructs have also been exploited to mimic the vasculogenic and osteoblastic niches in bone. Byambaa et al. printed bundles of gel rods with a soft central rod printed from rapidly degradable gelMA with low methacryloyl group substitution to create perfusable blood vessels. The outer bundles consisted of composite rods made from silicate nanoplatelets/gelMA (with high methacryloyl group substitution) to induce osteogenesis.[341] The complex bone-like design required printing of the individual gel rods by drawing up the gelMA and cells (HUVECs and hMSCs) into a capillary, followed by UV cross-linking in the capillary, similar to the approach of Burdick and co-workers,[58] and then extrusion of the gel into bundles. Gradients were introduced by printing gel rods arranged in a predefined order with different concentrations of vascular endothelial growth factor (VEGF). After several days of perfusion with media, there was evidence of both blood vessel formation and differentiated osteoblasts.

4.4. Degradability

The degradation of polymer biomaterials is a continuous "cradle-to-grave" process that takes place gradually or stepwise, desired or undesired, controlled or uncontrolled. It starts from the sourcing or synthesis of the base material and continues throughout chemical modification, storage, sterilization, tissue fabrication, in vitro culture and, eventually, in vivo after implantation. Throughout this process, chemical, mechanical, and biological properties of the material change repeatedly, altering how cells interact with the material.

The deliberate degradation of polymers to modify their rheological properties has been discussed in section 3.5.2, but degradation of matrices postprinting either by random hydrolysis or on-demand enzymatic degradation is also important to the long-term performance of printed tissue. If the bioprinted tissue is matured in vitro prior to implantation in vivo, degradation can be controlled through culture conditions, including culture medium composition. In one example, the degradation rate of bioprinted alginate/gelatin/collagen constructs was controlled through the addition of sodium citrate to the culture medium. As citrate removes calcium from the alginate gel, the latter softens (reversion of
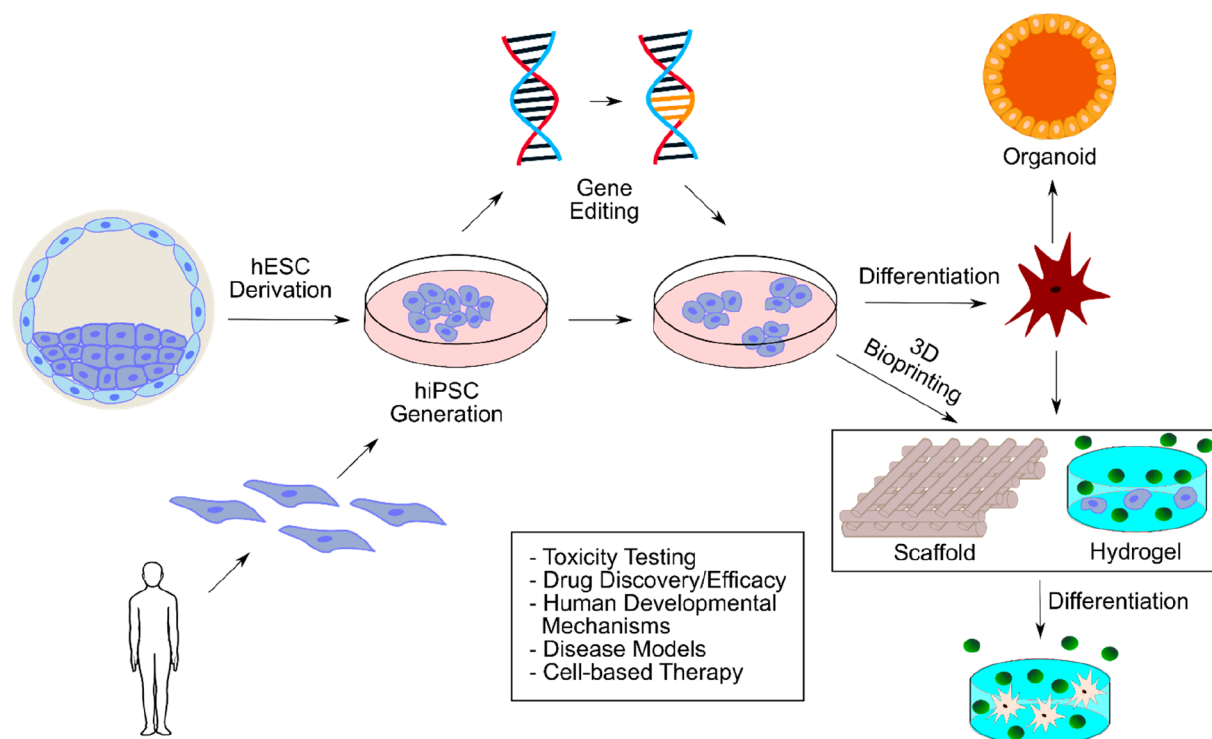
Figure 7. Diagram showing the work flow for generation of tissue engineered constructs or organoids from pluripotent stem cells. Human PSCs derived either for embryos (hESCs) or somatic cells are expanded (blue cells) in 2D adherent culture and, with or without gene-editing, differentiated toward the tissue of interest. As well as methods for differentiation in 2D on tissue culture plastic, cells may be aggregated at different stages to generate organoids (orange), allowing more maturity of differentiation. Alternatively, they may be encapsulated in hydrogels (light blue) as aggregates or single cells and deposited or printed into scaffolds to induce differentiation. Differentiation can be enhanced by use of soluble or scaffold/hydrogel-bound molecules (green) such as ligands or growth factors.

cross-linking), which was found to have a profound influence on cell proliferation and differentiation marker expression.[342] Alternatively, addition of alginate lyase to gelMA/alginate prior to microfluidic based printing allowed double network printing of constructs with good cell viability followed by degradation of the alginate within the first 24 h of culture, leading to a more open network for cell proliferation.[343] Instead of reversion of cross-linking or addition of enzymes, modification of the initial alginate to make it more degradable is a strategy that promotes the loss of low molecular weight degradation products more likely to be cleared by the body. Jia et al. utilized oxidized alginate to extrude encapsulated human adipose-derived stem cells and found that the level of oxidation greatly influenced the cell proliferation and spreading, assumed to be due to an increase in porosity with degradation.[344] The process to create oxidized alginate was originally reported by Bouhadir et al. and uses sodium periodate to cleave the C−C bond of the cis-diol group in the urinate residues, resulting in an open-chain adduct. The hypothesis is that this introduces rotation at the β-glycosidic groups, giving it acetal-like hydrolysis characteristics such that the polymer degrades to low molecular weight oligomers after 5 days in vitro or ca. 7 weeks in vivo.[345]

5. PLURIPOTENT STEM CELLS AND BIOPRINTING

Adult human stem cells and human pluripotent stem cells (PSCs) are ideal source materials for different targeted biological applications involving 3D bioprinting. Mesenchymal stem cells (MSCs) will not be considered further in this section, and we refer the reader to a very comprehensive review by Cidonio et al.[346] Rather, we will focus in this section

on PSCs. Human embryonic stem cells (hESC) are stem cells derived directly from the inner cell mass of preimplantation embryo,[347] which in humans comprises less than a dozen cells found at day 5−6 of development. HESCs are widely used in medical research and clinical grade hESCs, suitable for therapeutic applications, are readily available.[348−350] Induced pluripotent stem cells (iPSCs) have similar properties of continuous replication without differentiation (i.e., self-renewal) and have shown the ability to generate virtually any cell type in the body (i.e., they are pluripotent) if given the correct induction cues. They can be generated by genetic reprogramming of somatic cells, i.e., nonreproductive body cells.[351] HESCs and iPSCs have already been used extensively to generate developmental tissue and organ models or for models of disease.[352] They are also becoming favored by the biopharma industry for toxicity testing and drug efficacy studies.[353−355] The work flow for the generation of tissue engineered constructs and organoids from pluripotent stem cells is illustrated in Figure 7.

IPSCs have the advantage that they can be reprogrammed from cells of patients with known genetic mutations and patient etiology, meaning in vitro differentiation can be measured against authentic human disease states in vivo. Moreover, with the advent of CRISPR related technologies for gene editing,[356] it is possible to create isogenic pairs of the same cell lines with and without a particular genetic change. Additionally, choosing the optimal cells for a biological question is easier due to the vast array of hESC and iPSC lines available, combined with careful sourcing for genetic composition, histocompatibility status, and prior protocol

optimization. Until recently, the majority of differentiation models had concentrated on culturing cells on coated or uncoated 2D tissue culture plastic with the addition of selective growth factors. However, organs are three-dimensional entities often containing multiple cell types, and although these 2D models give good access to added reagents, it is difficult to generate physiological tissues and organs using such systems. The advent of organoid culture has partly solved this difficulty: here cells are cultured as large aggregates encompassing several cell types which mature together often over an extended period of months.[357−360] All the same, there is a clear opportunity to use bioprinting systems to mimic the native distribution of cells occurring in vivo and facilitate generation of the correct microenvironment for cells to proliferate or differentiate as appropriate. The first step has to be to encapsulate PSCs, most commonly in a natural or synthetic hydrogel.[346,361] This hydrogel needs to both provide biochemical signals and the right level of physical support. As previously mentioned, natural hydrogels have the advantage that they can consist of decellularized organ-specific ECM components[362,363] bearing epitopes which interact with the PSC receptor system (e.g., integrins and their associated transduction machinery) and they generally support PSC maintenance or differentiation.[364−367] Synthetic hydrogels may provide more reproducible bioinks but they need to be cell compatible, and these can be altered to allow stem cell-interaction as reported in section 4. Notably, routine fibroblast-compatible hydrogels do not necessarily equate to substrates compatible with undifferentiated PSCs or their committed progenitors. If we need to grow the PSCs themselves in a bioprinted format, we have to be aware that routinely they grow most stably as substrate-attached cells and also that they are poised for differentiation. Retaining appropriate conditions during printing and thereafter to allow essential stem cell maintenance signaling[368] will be critical. Many of the challenges experienced by those attempting to print stem cells are similar to those affecting other cell types. However, for PSCs we have the added disadvantage that the cells may be expected to differentiate in the printed construct. This process is tightly regulated by intracellular and extracellular signals and is highly vulnerable to shear stress related cell damage during printing. One further consideration is the physical properties of hydrogels which tend to be weak and poorly supportive. These properties mean printing into a more rigid scaffold may be necessary to produce constructs which can be handled, but the properties of the scaffold directly influence the PSCs or progenitors. For instance, stiffness or large fiber diameters (of the order of 50 μm) will present to cells (of the order of 10−30 μm) as 2D surfaces, and further, their stiffness will influence signaling within the cell and may alter cell fate.[328] Thus, for use with differentiating PSCs design of the entire construct needs very careful thought.

5.1. Human Disease and Development Modeling

In the context of bioprinting the first question must be: will use of bioprinting answer a question or provide a model that substrate-based culture or organoid differentiation cannot? This is a really important consideration for all bioprinting goals but even more so when trying to mimic human developmental pathways from PSCs. Most of our understanding of human development comes from murine models, and we exploit this knowledge to employ growth factors, cytokines, small molecule agonists/antagonists, and ECM substrates in a temporal sequence, guided by developmental principles. For modeling developmental human disease, we have the benefit of applying these protocols to patient-derived iPSCs carrying mutations or those in which patient-relevant mutations have been engineered and comparing to the nonmutant cells. However, there will be numerous necessary optimizations to produce a highly efficient, reproducible, and authentic human development model, even in a plastic tissue culture dish. Further, some cell selection may be needed because differentiation protocols never produce 100% of a specific single cell type.[369−371] This is generally through antibody-based fluorescence activated cell sorting (FACS) or magnetic bead antibody separation (MACS). If the aim is to use bioprinted 3D systems for modeling human cell and tissue development, it is often advantageous to generate PSC-progenitors in 2D and then continue differentiation of the PSC progenitors within the 3D structure. This is preferred to incorporation of previously differentiated PSCs into 3D constructs, as these tend to have very precise microenvironment requirements and are intolerant of manipulations. The strategy will require not only a printing regimen that supports cell viability and retains phenotype but also the need to use bioinks and processing/culturing conditions that suit both early and later differentiated states. Moreover, we may now need to deal with a percentage of off-target differentiation by, e.g., developing conditions where the unwanted cells senesce or die. Penetration of inducing factors, oxygen, and nutrients will need to be considered. Indeed, using tethered bioactive inducers within the bioink itself may help to ensure uniform differentiation. Additionally, if more complex tissue models are needed, the use of PSC-progenitors differentiated to more than one cell type will be the goal. For instance, for generation of vascular tissue, minimally we require differentiation to endothelial cells and smooth muscle cells/pericytes. PSC-smooth muscle cells and PSC-endothelial cells will associate to approximate vascular tubes when cultured[370,372−374] much as HUVECs and natural smooth muscle cells. So, it may be most efficient to print the progenitors together and allow them to associate once printed in the appropriate hydrogel. Printing regimens will be needed which are compatible with both cell types as well as maximizing cell association. Of course, the human gestation period is over 20 times as long as that of a mouse and even allowing for the fact that much of human embryonic/fetal differentiation and organogenesis occurs during the first 4−6 months, we still have an order of magnitude difference in time required to develop human functional tissues compared to those of rodents. We can speed things up to some extent.[375] However, this means that bioprinting must deliver sustainable systems which will allow a longer time course for human differentiation and so generate stable tissues. Complex models such as the vascularized alveolar system recently developed[376] will require more sophisticated methods in which cells are added to previously bioprinted templates and coincorporation of a means of oxygenation or simulated blood flow. Some other systems such as articular cartilage (AC) may be simpler, but even here capturing the regionalization seen in native cartilage will be challenging although likely achievable. In theory, both bone and cartilage cells can be derived from a PSC derived skeletal progenitor which would differentiate according to the local microenvironment after printing. To generate an osteochondral construct mimicking the mineralized subchondral bone together with overlying nonmineralized AC may thus be achievable with the appropriate bioinks and scaffolds.

5.2. Tissue Engineering Using Bioprinted PSC Derivatives for Cell-Based Therapy

A plethora of stem cell-based therapies are currently reported to be in clinical trials.[377] However, in most cases, these are phase 1 safety trials and so we have little idea yet of efficacy. For MSCs, it is clear that their most important attribute relates to the factors they release, particularly for immunomodulation, rather than as agents of cell replacement. For PSCs, a notable success has been the use of hESCs in retinal pigment epithelium (RPE) repair for wet age-related macular degeneration.[378] One frequently mentioned fear for PSC-derived therapies is the development of teratomas from residual PSCs. These were not found in this or other hESC-RPE or iPSC-RPE trials, nor were other construct-induced adverse effects reported.[378−381] In fact, in some of these studies, the implanted PS-RPE gave functional visual improvement. However, it is important to mention that genetic changes were reported in cells from one patient in a trial using autologous reprogrammed iPSC-RPE,[382] and the trial was stopped. Here, a single layer of differentiated retinal pigment epithelial cells is required to repair the macula. Although this is a most promising proof of principle for human PSC-based therapy, this single-cell-layer-type repair is not what is necessary for most tissues. Therefore, bioprinting will have an important role, as for disease modeling, in generating multilayer native-like arrangements of cells for tissue reconstruction. A major consideration is the best stage of differentiation at which to implant the cells for in vivo application. The answer is, unsurprisingly, cell type specific. Interestingly, early day 12 progenitors survived and differentiated better than a later stage of PSC-kidney progenitors after subcutaneous implantation in mice,[383] while day 25 differentiated dopaminergic neurons did better than PSC-derived cells after day 16 and day 35 of differentiation in generating functional recovery when implanted in a rodent Parkinson brain model.[384] One of the challenges for bioprinting PSC-derived cell constructs will be the survival of the printed progenitors once in vivo. This will generally require rapid connection of pre-existing vessels to the host vasculature or host angiogenesis, although the latter may be too slow in larger constructs. Existing printed vascular templates distributed through the construct could be the answer, around which PSC endothelial cells would congregate and which would then be remodeled or chemically removed to give patent vessels. Another consideration is the cell density at which cells should be delivered and which will be crucial for both cell survival and function. Many groups in the past used very large numbers of cells in an attempt to ensure sufficient living functional cells in the repair site. This reflects the fact that many cells do not survive implantation into a defect site which may be an inflammatory or otherwise hostile environment. However, for MSCs, higher (doubling) the cell density was shown to promote cell communication and hence bone differentiation in a rat model.[385] A good strategy may be to use moderate cell densities but deposit the cells as aggregates exploiting the signaling triggered through cell−cell interactions which promote cell survival. However, printing cell aggregates may be challenging because of their dimensions (possible occlusion of the nozzles), and aggregates may also be more difficult to distribute evenly through the bioink. Moreover, using aggregates will change the properties of the bioink. There are many examples of preclinical PSC-based therapies in development, some within section 6 of this review. TE vascular

grafts would be useful for repair of diseased or damaged blood vessels after trauma or following stroke or thrombosis. PSC-cardiac patches incorporating blood vessels could be printed for repair after myocardial infarcts. Osteochondral constructs may do better than just autologous cartilage for joint repair in osteoarthritis because both the cartilage and subchondral bone is frequently affected. PSC derived midbrain dopaminergic neurons are being brought to the clinic for Parkinson disease through clinical trials.[386−388] Using conventional grafting, results in preclinical assessments have been good.[388] However, performance and survival of implanted dopaminergic neurons might be even better with midbrain organoids which include interaction with supporting cell types, or these same cells organized in multicellular bioprinted scaffolds. Overall, it will depend on the application, together with the adoption of appropriate bioinks and careful attention to cell microenvironment requirements whether bioprinting will be suitable for use of PSC−progenitor constructs as cellular treatments.

6. BIOPRINTED TISSUE MODELS

6.1. Cardiac

The human heart has a complex anatomy comprising four different chambers and heart valves enclosed by a thick wall. The latter displays a multilayered structure (i.e., endocardium, myocardium, and pericardium), with a multicellular arrangement where cardiomyocytes (CMs) and endothelial cells (ECs) play a pivotal role in regulating heart function. Owing to its specific fiber arrangement and cellular composition, the myocardium is responsible for the contraction and relaxation of the organ. CMs rhythmically generate contractile forces in the myocardium so that blood can be pumped into the circulatory system and supply cells with oxygen and essential nutrients. These structural and functional features are extremely challenging to replicate using traditional 2D or 3D cardiac cell models considering the entire anatomy of the heart is required for in vivo function. 3D Bioprinting offers the possibility to manufacture anatomically relevant cardiac models where the whole-organ architecture can be replicated with high shape fidelity by direct extrusion of cell-laden hydrogels into a fluid bath (Figure 8A).[72] Recently, different cell types, particularly iPSC-derived ECs and CMs, have been incorporated, and cardiac models with increased resolution and complexity have been developed (Figure 8B) using hydrogel formulations composed of different materials such as decellularized ECM or collagen.[71,389] Despite it being possible to produce constructs with high shape fidelity, most research has been focused on less architecturally complex models, which are still valuable to study phenomena related to tissue organization and organ functionality. An example employed a scaffold-free coculture model composed of multicellular spheroids containing iPSC-derived CMs, fibroblasts, and ECs. By using an array of needles as the delivery system, the ability of cells to self-organize after printing was demonstrated, with iPSC-derived CMs arranged around the periphery of the spheroid or tubular-shaped constructs.[390] A three-step process with enhanced control over spatial organization of cells was also proposed by Zhang et al. for cardiac applications. First, an endothelial cell-laden gelMA bioink was extruded into a lattice structure. Then, ECs were allowed to self-organize around the printed filaments into vascular-like structures. Finally, CMs were seeded on top of the printed construct, resulting in the formation of an endothelialized myocardium model.[391]
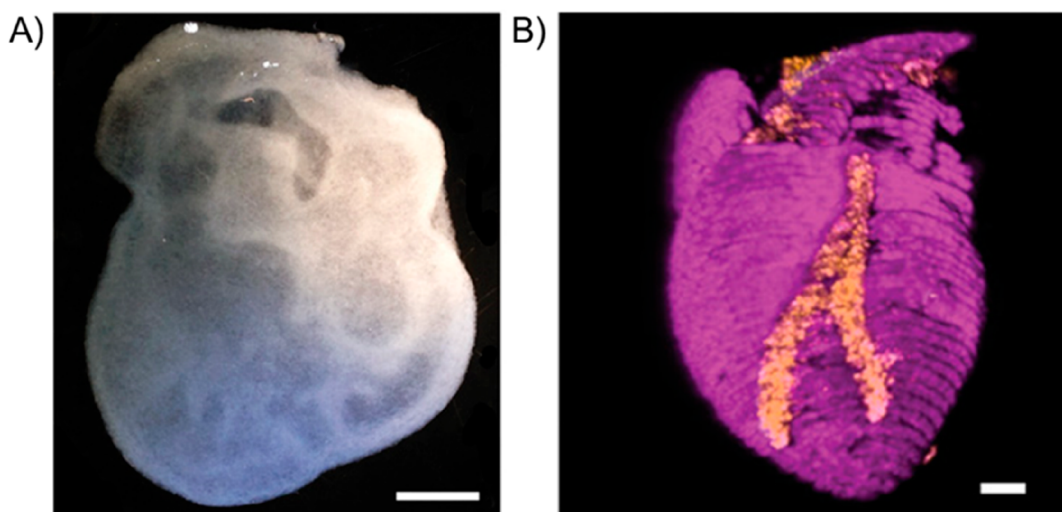
Figure 8. 3D bioprinted cardiac models produced by extrusion of cellularized hydrogels into a fluid bath. (A) Heart model printed using an alginate-based bioink, displaying the main components of the organ. Reproduced with permission from ref 72. Copyright 2015 AAAS. (B) Cellularized heart model containing human iPSC-derived cardiomyocytes (pink) and endothelial cells (orange). Reproduced with permission from ref 389. Copyright 2019 Wiley. Scale bars: (A) = 10 mm; (B) = 5 mm.

To pump blood in an efficient manner, the heart requires synchronous beating of the myocardial tissue. Bioprinted models displaying contractile properties have been developed using cell-laden bioinks containing CMs derived from murine models,[61,391,392] hESCs,[71,393] or hiPSCs.[390,394] Bioinks have been prepared using materials such as gelatin or fibrin[61,395] and processed using different techniques including material extrusion[392] or mask irradiation.[394] Mimicking the native organization of cardiac ECM, where the parallel arrangement of collagen fibers contributes to the alignment of CMs, is of great importance to promote the anisotropic muscular contraction. This feature has been replicated in vitro using mask irradiation with a DMD and a bioink composed of iPSC-derived CMs embedded in gelMA blended with decellularized cardiac ECM. By patterning the bioink as parallel lines, it was possible to generate synchronous contraction along the printed structures.[394] The replication of these features in bioprinted cardiac models opens the possibility to study the effects of biochemical compounds in tissue-specific aspects such as changes in heart beating rate, force, and calcium gradients.[392,393] However, to create more realistic models, it becomes necessary to find a balance between architectural complexity and functionality, as demonstrated by the diminished functional outputs obtained when more structurally complex constructs were produced.[72,389] Progress in bioprinting techniques coupled with ex vivo perfusion systems are expected to advance cardiac research toward the generation of physiologically relevant tissue models where engineered structures support biological function.

6.2. Musculoskeletal

The skeletal system is composed of bone, cartilage, tendons, and ligaments. These have distinct load-bearing properties and are subjected to different physiological stresses such as compression, tension, and shear. Articular cartilage has a multilayered structure, displaying gradients of composition, mechanical, and biochemical properties, thus making it extremely hard to replicate in vitro.[396,397] Working in a layer-by-layer fashion, bioprinting techniques stand out as ideal candidates to mimic the zonal organization of AC through the deposition of multiple materials and cells with controlled 3D spatial positioning. One of the earliest bioprinted AC models was focused on the development of a decellularized tissue specific ECM bioink processed by piston-assisted extrusion. When combined with human inferior turbinate-tissue derived mesenchymal stromal cells (hTMSCs), it revealed high cell viability and increased expression of key chondrogenic markers when compared to cells cultured in collagen.[171] Despite physicochemical properties playing important roles in regulating the phenotype of encapsulated cells,[398,399] this can also be modulated by controlling cell density and printing process parameters. As reported in section 3, printing nozzles with large internal diameters and tapered geometries have been suggested as ideal systems for the printing of 3D constructs with enhanced cell viability and chondrogenic expression. In contrast, the reduction in diameter and the use of straight geometries can lead to cell damage due to higher shear stresses generated during the printing process.[106]

Hydrogel bioinks have also been used to mimic features of bone such as tissue mineralization. This has been reproduced in vitro using bioprinting of polysaccharide-based hydrogels containing osteosarcoma[400] or human bone-marrow derived MSCs.[401,402] However, the use of hydrogels alone for bone TE has the downside of mechanical mismatch between printed constructs and the native tissue. Therefore, strategies such as the use of microcarriers[20] and multimaterial 3D printing[403] have been used to reinforce hydrogels for skeletal tissue applications. Co-extrusion reinforcement has been employed by direct deposition of bioinks into the lacunae of porous thermoplastic scaffolds[404] (Figure 9A) or by extrusion on top of or next to thermoplastic filaments[69,171,405] (Figure 9B). Strategies to increase complexity have also been developed by combining melt extrusion and solution electrospinning with extrusion of a cell-laden hydrogels to fabricate constructs with multiscale physical features[400] (Figure 9C).

Besides the ability to allow for structural reinforcement, bioprinting also offers the possibility to create heterogeneous tissue constructs which can be used for interfacial TE in order to replicate continuous or discrete gradients of mechanical and biological properties present in biological tissues. One example
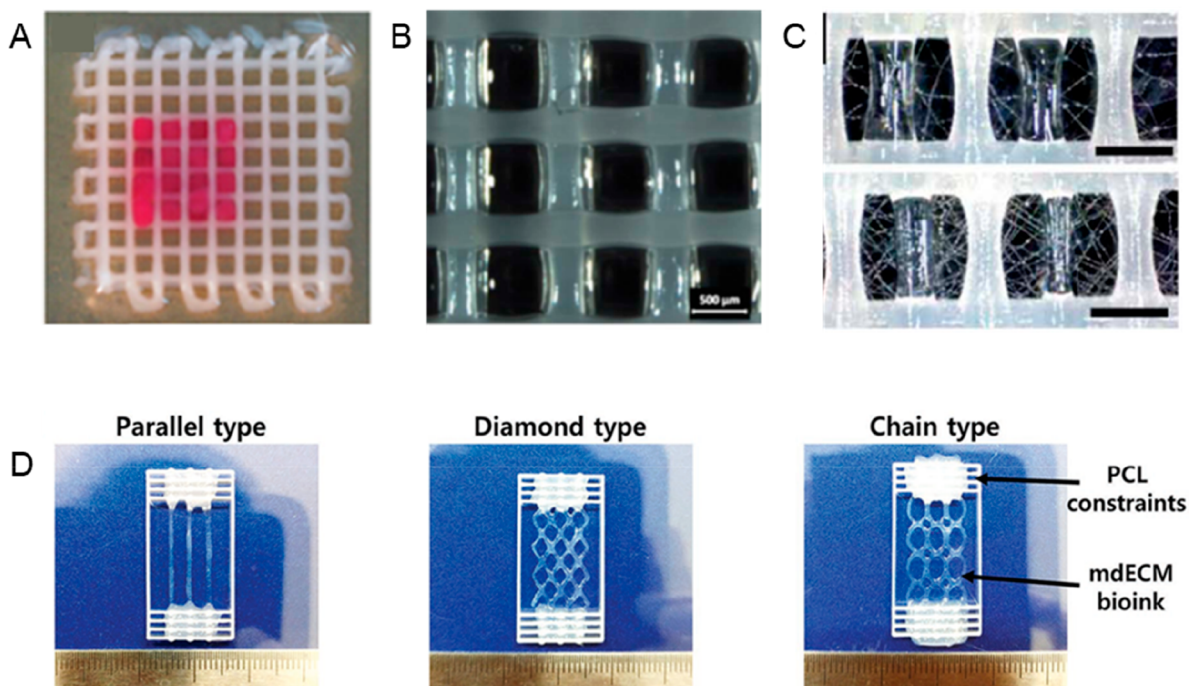
Figure 9. Hybrid strategies for skeletal tissue engineering. (A) Injection of cellularised material into scaffold lacunae. Reproduced with permission from ref 404. Copyright 2018 IOP. (B) Extrusion of a thermoplastic structure followed by printing of cell laden bioink. Adapted with permission from ref 405. Copyright 2017 IOP. (C) Hierarchical constructs fabricated by melt extrusion, solution electrospinning, and cell-laden hydrogel printing. Adapted with permission from ref 400. Copyright 2013 Royal Society Of Chemistry. (D) 3D bioprinted skeletal muscle models with distinct architectures using a myoblast-laden bioink and varying the deposition pattern. Adapted with permission from ref 408. Copyright 2016 Wiley.

of such interface is the osteochondral (OC) tissue. This is comprised of a layer of AC interlocked with a layer of subchondral bone with the AC, providing a low-friction, shock absorbing surface that protects the bone from damage during joint movement.[406] Understanding how this function can be compromised and restored is extremely important for the treatment of joint disorders such as osteoarthritis (OA). For that purpose, OC tissue models displaying functional and structural gradients have been developed using 3D bioprinting. Using techniques such as material extrusion,[407] or SLAM-based bioprinting,[70] it has been possible to coculture chondrocytes and osteoblasts in a precise spatial relationship. This can result in the development of a hydrogel-based OC plug with defined mechanical and biological gradients and signs of OC tissue formation in vitro.[70] Extrusion bioprinting has also been used to fabricate skeletal muscle models with complex architectures (Figure 9D) by varying extruded patterns and filament thickness, which resulted in distinct levels of cell orientation.[408] In fact, myotube formation has been observed with cell fusion and aligned along the printing direction.[62] Using extrusion of cell-laden hydrogels into dumbbell-shaped constructs attached to two postholders, it was possible to create an array of tissue models with an anisotropic microstructure displaying aligned myofibrils and the ability to contract.[409] The application of mechanical stimuli to musculoskeletal tissue engineered constructs has been explored as a way to promote cell differentiation and tissue formation using cyclic compression,[410,411] tension,[412] or shear.[413] Besides providing a unique environment mimicking physiological forces in vitro, the use of dynamic cell culture systems has been employed as an alternative to medium supplementation with growth factors. One study evaluated the

effects of cyclic compression in chondrocyte-laden GelMA hydrogels reinforced with PCL fibers produced by melt electrowriting. The application of mechanical stimulation resulted in a similar GAG production to the addition of exogenous TGF-β1 to culture medium after 28 days of culture.[410] Despite their advantages, the use of specialized bioreactors to apply mechanical stimuli is often a complex and low-throughput process, which has limited their widespread adoption. Bioprinting allows the fabrication of cell-laden constructs in an automated and high-throughput manner, which is helping to overcome the barriers of conventional bioreactor systems. Recently, material jetting has been used to fabricate an array of cell-laden GelMA microgels on top of a stretchable PDMS platform. The application of a mechanical stimulus led to cell alignment along the stretching direction, which was dependent on hydrogel concentration and stiffness.[412]

6.3. Dermal

The main components of the skin are the epidermis, dermis, and hypodermis. The epidermis is an epithelial layer with keratinocytes as the main cell type covered by the stratum corneum, a protective layer of dead cells on its surface. Underneath it lies the dermis, a layer rich in collagen, elastin, and GAGs in which fibroblasts are the key cellular component.[414] The hypodermis in turn is the deepest adipose-rich layer. Bioprinting offers the possibility to create multilayered constructs mimicking the native skin organization.[415] Using technologies such as DOD material jetting[416] and material extrusion,[415,417] different in vitro dermal[418] or full-thickness skin models have been developed.[415−417,419] Whereas the DOD method only included fibroblasts, extrusion
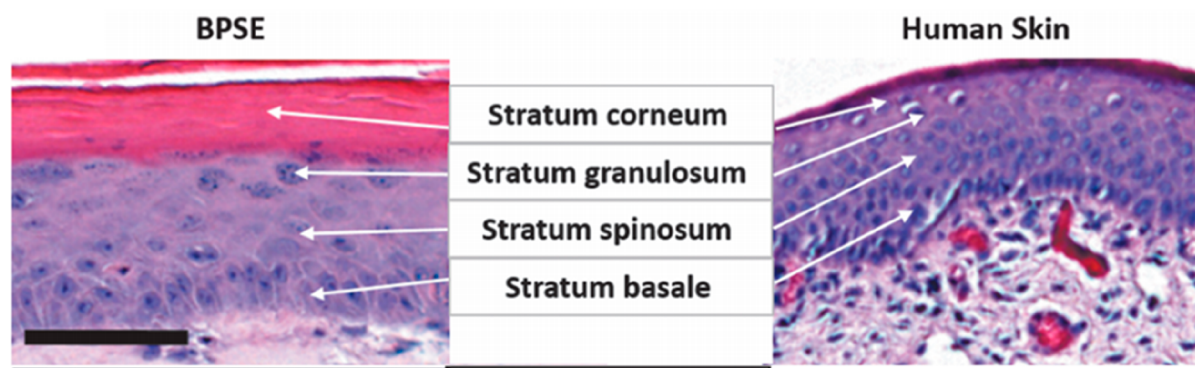
Figure 10. Histological comparison of a bioprinted full-thickness skin equivalent (BPSE) and human skin. All layers of the native skin are represented in the skin equivalent, albeit with different relative thicknesses. Scale bar: 100 μm. Adapted with permission from from 415. Copyright 2019 Mary Ann Liebert Inc.
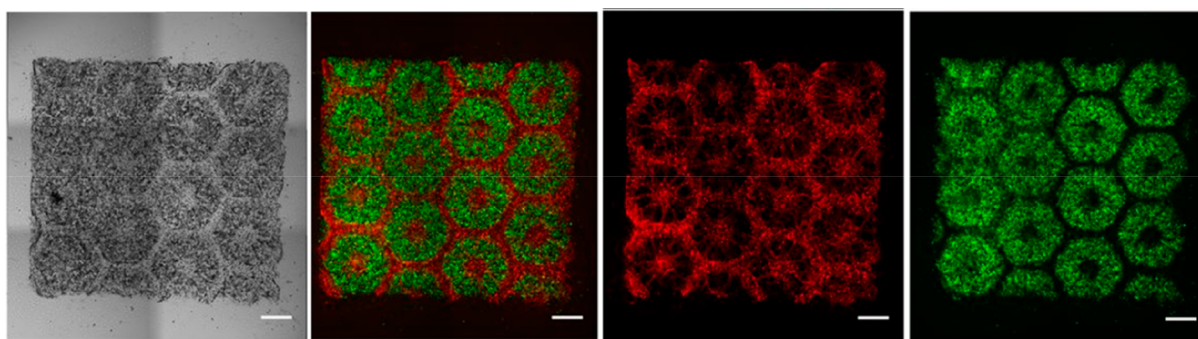

Figure 11. 3D bioprinted model with biomimetic hexagonal organization of liver lobules fabricated using mask irradiation. IPSC-derived hepatic progenitor cells are labeled green and supporting cells are labeled red. Scale bar: 500 μm. Adapted with permission from from 423. Copyright 2016 PNAS.

printing has used both fibroblasts and keratinocytes which can be sequentially deposited in precise locations[415−417,419] to generate full-thickness skin equivalents (Figure 10). To replicate skin composition, natural materials such as type-I collagen[415,416,419] have been employed as bioink components. However, using a combination of gelatin, alginate, and fibrinogen, a bioprinted skin model was developed, resulting in a similar morphology, histological features, and composition to human skin, with production of key ECM proteins such as collagen I and V, elastin and fibrillin. Interestingly, when dermal and epidermal layers are cultured together, laminin presence is detected at the interface, suggesting the formation of dermal−epidermal junctions.[417]

The development of skin models with barrier functionality similar to native tissue is important for applications such as drug delivery and toxicity studies. The stratum corneum is the top epidermal layer responsible for this feature in vivo. It can be generated in vitro by culturing tissue constructs at the air−liquid interface,[415,417] and its barrier efficiency can be evaluated using electric conductivity measurements.[415] Recently, efforts toward increasing the complexity of skin models have been taken, with the inclusion of structures such as vascular channels,[419] the hypodermis,[419] sweat glands,[420,421] and hair follicles.[422]

6.4. Hepatic

The liver is composed of hexagonal-shaped lobules surrounding vascular channels. The microarchitecture of this organ has been replicated in vitro using 3D bioprinting of cells organized in hexagonal patterns. Using mask irradiation of a gelMA/ MeHA bioink, it was possible to distribute hiPSC-derived hepatocytes and supporting cells in a complex arrangement resulting in an improved phenotype compared to 2D or 3D monoculture[423] (Figure 11). Besides the use of this technology, the majority of bioprinted liver models have been fabricated using extrusion-based bioprinting,[424−429] employing bioink components such as alginate,[81,427,430] gelMA,[426,428] or collagen.[431]

One of the main functions of the liver is the production of albumin. This feature has been replicated in vitro using bioprinted models containing various cell types including mouse,[430,431] human PSC-derived,[81] or human hepatocytes.[432] Albumin secretion by hepatocytes has also been shown to increase using coculture systems with endothelial cells[429] or fibroblasts.[431] When the three cell types are cultured together, a synergistic effect in albumin secretion has been detected, highlighting the need to develop complex models.[431] Interestingly, coculture has also been shown to increase urea production, showing the importance of creating in vitro models with multiple cell types.[429,431] To provide more physiologically relevant conditions, tissue constructs can be cultured within tailor-made bioreactors. The ability to use a range of materials during the bioprinting process can facilitate this process by 3D printing the bioreactor and the tissue construct simultaneously. This strategy was pursued by enclosing an in vitro bioprinted liver model inside a 3D printed microfluidic device, which was then perfused with cell culture medium under dynamic conditions resulting in increased cell viability and albumin secretion.[429]
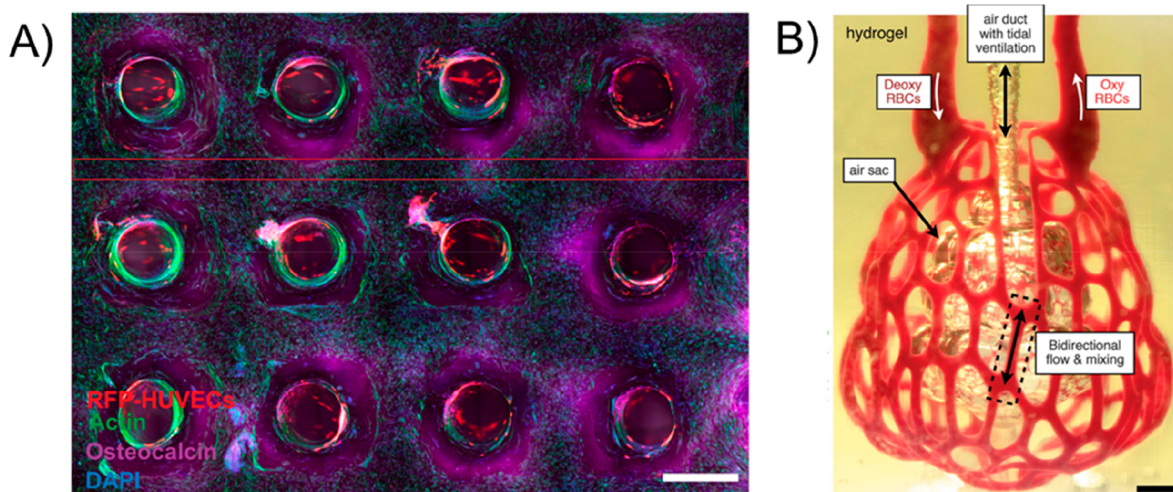
Figure 12. Perfusable hollow channels fabricated using different bioprinting technologies to create in vitro vascularized models. (A) Cross-section view of a thick (>1 cm) vascularized tissue model used to investigate the osteogenic differentiation of bioprinted MSCs. Through the combination of material extrusion with sacrificial inks, hollow channels can be generated and perfused with growth media to support cell proliferation and differentiation. Adapted with permission from ref 204. Copyright 2016 PNAS. (B) Vascularized distal lung model (subunit) generated by vat photopolymerization and displaying the ventilated air sac enclosed by a red blood cell (RBC) perfused network. Reprinted with permission from ref 376. Copyright 2019 AAAS.

The liver plays a prominent role in drug metabolism and detoxification, which makes it the focus of a large number of in vitro models for drug screening. Its important role in first pass metabolism, for which cytochrome P450 enzymes are crucial,[433] led to the development of models that assessed the activity of these enzymes in vitro. This has been achieved under static or dynamic culture conditions, using cell-only[434] or cell-laden hydrogel[423,432] bioinks, with printed constructs retaining the ability to metabolize known compounds such as midazolam, a well-established cytochrome P450 3A4 substrate.[432] Another use of bioprinted hepatic tissues is to model liver damage, which can be caused by radiation or biochemical compounds. The effects of radiation on the liver have been evaluated using a coculture system of hepatocytes with epithelial cells, with the bioprinted model being used to evaluate the potential of amifostine, a cytoprotective drug to avoid DNA damage. Interestingly, whereas treatment with the drug resulted in lower levels of DNA damage after exposure to radiation, the effects of this drug were enhanced in the coculture system.[185] Recently, a model using cell spheroids embedded in a GelMA bioink was developed, by direct printing onto a microfluidic system. This approach allowed study of the response of a human hepatocarcinoma cell line to acute exposure to acetaminophen, a known hepatotoxic compound. This resulted in reduced levels of metabolic activity and lower secretion of key hepatic biomarkers such as albumin, transferrin, and ceruloplasmin.[426] Similarly, exposure to TGF-β1, methotrexate, or thioacetamide has resulted in the accumulation of fibrillary collagen in a bioprinted liver model fabricated by material extrusion, which has allowed the establishment of a disease model of liver fibrosis.[435]

6.5. Vascular

Macro- and microvasculature are present in most human tissues and organs, being essential for the adequate supply of nutrients and oxygen to the cells. Therefore, the ability to replicate these features in vitro becomes of great importance for TE and RM applications. Prevascularized tissue models provide a unique opportunity to interrogate different biological

mechanisms underpinning both organ development (e.g., the role of angiogenesis) and disease progression (e.g., kidney failure) under relevant physiological conditions. From another perspective, vascular networks of relevant physiological dimensions are also a key aspect in TE grafts. Without these diffusion limits, they can result in hypoxic environments that seriously compromise cell function and ultimately lead to implant failure.[204,376,425] In this regard, 3D bioprinting has proven to be extremely useful in the fabrication of vascularized tissues, particularly through the combination of extrusion-based processes and sacrificial biomaterial inks (Figure 12A). These strategies harness the ability of materials with thermally reversible gelation to be dissolved using high[59] or low temperatures,[17] resulting in the formation of hollow vessel-like channels for perfusion purposes. An important feature of vascular networks is the presence of an endothelial cell layer lining the lumen. The most common strategy to achieve this is by a three-stage process: (1) a filament of sacrificial ink is deposited and surrounded by a cell-laden hydrogel, (2) the sacrificial ink is then liquefied using high or low temperature and removed by aspiration forming hollow channels, and (3) channels are endothelialized by direct cell seeding through the channels.[17,59,436] More recently, using an extrusion-based process and exploring the self-assembling capacity of endothelial cells encapsulated in a sacrificial gelatin ink, an alternative method was proposed to overcome the need to perfuse the channels with a cell suspension.[389] A similar strategy was employed using DOD bioprinting, allowing replication of the stratified nature of native blood vessels (i.e., tunica intima, media, and adventitia) by 3D patterning different cell types.[437] The use of sacrificial biomaterial inks is a versatile approach that has also been used to vascularize tissue constructs of high cell densities (10^8 cells/mL) through a process of sacrificial writing into functional tissue (SWIFT). This technique harnesses principles of suspended extrusion by using a slurry composed of cell aggregates within an ECM solution as a self-healing suspension. By extruding the sacrificial ink into this supporting structure, it was possible
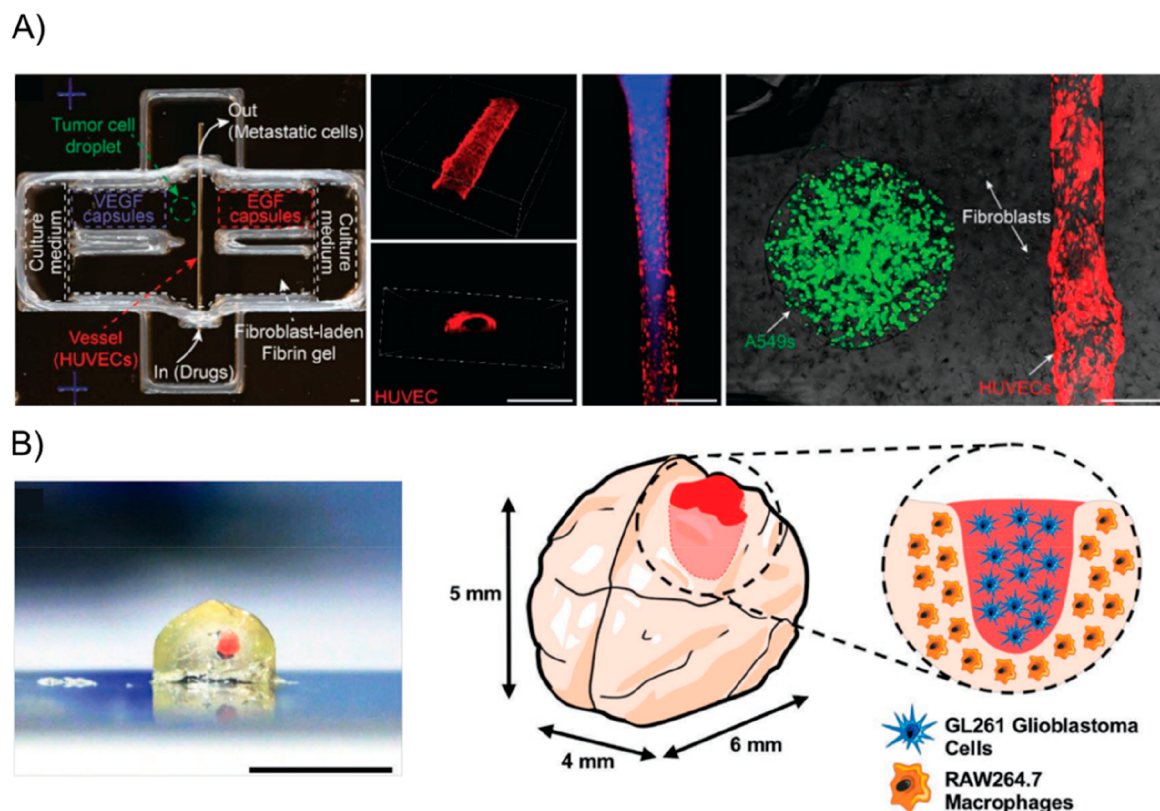
Figure 13. In vitro models used to emulate key aspects of tumor development. (A) 3D printed culture chamber containing endothelialized vascular channels for the evaluation of growth factor gradients and anticancer drugs on guided tumor metastasis. Endothelial and lung cancer cells are labeled in red and green, respectively. Adapted with permission from ref 447. Copyright 2019 Wiley. (B) Bioprinted mini-brain (left) and a schematic representation (right) of a glyobastoma model established to investigate the interaction between macrophages and glioblastoma cells (red area) during tumor progression. Adapted with permission from ref 442. Copyright 2019 Wiley.

to create perfusable channels within the cellularized suspension. This technology has found applications in the development of vascularized cardiac or cerebral models, depending on the cellular composition of the aggregates.[438] Vascular networks with increased complexity have been recently obtained using vat photopolymerization processes in combination with a PEGDA resin and nontoxic light blockers (Figure 12B). These constructs were then used to create an alveolar model to evaluate the transport and oxygenation of red blood cells. By creating distinct channels for ventilation and perfusion with red blood cells, it was possible to study the influence of complex geometries on gaseous exchange, allowing the in vitro modeling of phenomena such as bidirectional flow and mixing of red blood cells as a result of ventilation.[376] Vascularized constructs containing hollow channels can be used to study biological processes such as the formation of capillary networks and blood vessel sprouting.[436,439] Importantly, by supplying relevant compounds through the channels, it is possible to induce differentiation of the surrounding cells[204] or evaluate molecular diffusion through the endothelial barrier.[439] The presence of engineered vasculature also influences other phenomena such as the propagation of calcium gradients in myocardial models.[389] The principles underpinning engineered vasculature have been employed to create channels in various types of tissue models including kidney. In this case, an in vitro proximal tubule model fabricated using extrusion printing of a sacrificial ink followed by seeding with epithelial cells was developed to model crucial features such as albumin uptake.[425]

The use of bioprinting to generate vascularized channels has also been applied for disease modeling and drug screening purposes. A model of vascular thrombosis has been developed by perfusion of hollow channels with blood supplemented with $CaCl_2$. This model was then further used to evaluate the effect of thrombolytic drugs and investigate fibroblast invasion in formation of fibrotic clots.[440] Vascular channels fabricated using 3D printing have also been used to evaluate the role of an endothelial barrier in drug diffusion and metabolism. In a model system, the presence of this endothelium resulted in increased levels of viability of hepatocellular carcinoma cells embedded in a gelMA hydrogel after perfusion with a toxic compound.[439]

6.6. Cancer

The native tumor microenvironment (TME) is a complex system with heterogeneous composition of cellular and ECM elements regulated by specific biophysical and chemical cues. The interaction between the TME and tumor cells is responsible for coordinating intracellular signaling and triggering downstream biological responses which regulate cell survival, invasiveness, and metastatic dissemination. These key aspects of tumor development and progression have been the focus of many recent studies where the TME of pancreatic,[376] brain,[441−443] ovarian,[444] cervical,[445] and breast[446] tissues was reproduced using 3D bioprinting and used to evaluate increased cell proliferation levels,[441,445] formation of metastasis (Figure 13A),[447] and tissue invasion (Figure 13B).[442] Tumors are often heterogeneous, and the study of the influence of neighboring cell types and their

microenvironment can be difficult to replicate with conventional fabrication technologies. Bioprinting can be used to address this challenge by allowing the combination of multiple cell types with a controlled architecture to generate complex constructs.[442,446,448] By using piston-assisted extrusion to deposit breast cancer cells and fibroblasts in precise locations separated by an acellular region, it was possible to investigate the formation of multicellular tumor spheroids and to evaluate fibroblast migration toward the tumor cells within alginate/gelatin hydrogels.[448] A different model used vat photopolymerization to fabricate a breast cancer model in coculture with bone stromal cells embedded within a gelMA matrix. When the two cell types were cultured together, increased proliferation and secretion of VEGF by breast cancer cells was observed[449] Similarly, the extrusion of a gelMA-based bioink containing glioblastoma cells and macrophages in distinct locations made it possible to identify possible paracrine and juxtacrine interactions between these cell types during tumor development[442] (Figure 13B). Bioprinted tumor models have also been used for screening of chemotherapeutic drugs such as paclitaxel, Temozolomide, or novel compounds for potential antitumor applications.[441,443,445−447,450] Even though the majority of these studies were focused on evaluating the effects of these compounds on cell viability,[441,445,447,450] molecules with the capacity to influence cell proliferation and migration have also been assessed. These were able to demonstrate the ability of bioprinted models to recapitulate important features of disease progression as the response to biochemical stimuli.[446]

7. CONCLUSIONS AND OUTLOOK

The introduction of bioprinting technologies in the fields of TE and RM has enabled mimicking human tissue complexity through the 3D spatially controlled deposition of multiple materials and cells, for the creation of tissue models for organogenesis, disease modeling, and drug screening. Here we have reviewed the latest evolutions in terms of printing techniques for cell-laden hydrogels with a particular focus on extrusion, vat photopolymerization, and material jetting systems. Clearly, each system presents its own advantages and limitations in terms of resolution, scanning speed, and building volume, but ultimately, it will be the targeted cell composition of the tissue/organ and the bioink's properties that dictate the choice of the manufacturing technique. Having said this, and despite the limited resolution (compared to vat polymerization and material jetting), it is plausible that in the short term (2−5 years) extrusion-based systems will retain their status as the preferred bioprinting technique for the generation of clinically relevant constructs. The building volume, ease of operation, and compatibility with cells are key advantages supporting the widespread use of extrusion-based systems. Other, more recently introduced printing systems (e.g., volumetric printing and LIFT) are expected to greatly impact the field of bioprinting, driven mainly by advances in scalability and printing speed. As briefly outlined in section 2, the printing process of high shape fidelity constructs capable of supporting adequate cellular function both in vitro and in vivo, places very stringent requirements on the formulation of bioinks. Modulating the rheological properties of ink-materials does often imply a trade-off between the requirements for optimal printability and intended biological response. As reported in section 3, this can be achieved through the combination of different base polymers with additional modifications to achieve the desired functionality, with particular emphasis on cell adhesion motifs and enzyme cleavable linkages. In section 4, we discuss on the effect of viscosity, shear-thinning, yield stress, and recovery on the flow and state transition (i.e., from viscous to purely elastic) of non-Newtonian fluids in bioprinting, particularly in material extrusion systems. While viscosity remains the first property to consider for "'good printability'" of bioinks, it is important to bear in mind that small yield stresses and shear-thinning are desirable to prevent cell settling in the cartridge and shield the cells from damaging shear stresses, respectively. After introducing the concepts underlying the rheological behavior of polymeric materials, we conclude section 4 by discussing some structural features (e.g., topology and gradients) of bioinks that can impact the migration, differentiation, and ECM deposition of encapsulated cells. As presented in section 5, the use of hPSCs as cellular components in bioinks is still in its infancy. If the full potential of these cell sources is to be exploited, then much of the future research will need to encompass the design of polymeric materials specifically tailored to match the unique functional requirements of hPSCs and importantly hPSC-derived progenitors. Because of their higher sensitivity compared to other cell lines, the rheological properties and cross-linking densities (i.e., stiffness) of selected materials will need to be carefully tuned to support postprinting phenotype maintenance and long-term tissue maturation. This sets the stage for the final section of this review, where we report on the latest efforts to create 3D bioprinted models of healthy and diseased human tissues and organs. From cardiac to hepatic tissues, for therapy development or drug testing, the number and diversity of studies reported in the literature is vast. On the one hand, this reflects the revolutionary benefits that bioprinting has brought to the modeling of complex tissue microenvironments. On the other hand, it also raises important challenges that need to be addressed if a new generation of bioprinted models with clinical relevance are to progress from the bench to the bedside.[44] From a manufacturing viewpoint, we expect significant advances in the hardware of 3D printing systems to enable the expansion of processable ink materials at higher printing speeds and increased spatial resolution. New technologies will likely continue to emerge that allow for greater control over both the complexity and resolution of bioprinted structures. Recent developments have already shown promise with technologies like acoustophoretic DOD jetting, which expands the viscosity range for inkjet bioinks by several orders of magnitude[93] or volumetric bioprinting, allowing for the generation of full-scale structures from a wide variety of materials in seconds.[451] Moreover, developments in the application of magnetic fields to organize cells into precise spatial locations represent a major step forward in high resolution printing although a current lack of scalability is an issue.[119,338,452] Additionally, the development of SLAM and FRESH systems facilitate the extrusion of low-viscosity materials that would otherwise be very difficult to print. This has already been explored in the fabrication of soft tissue constructs,[70,71,75] but other related fields like neurovascular engineering are expected to greatly benefit from suspended manufacturing methods.[51,453] The number of cell-based studies involving SLAM and FRESH are few in number, but these are expected to increase in the future with more attempts to build large, complex, multimaterial, and multicellular constructs being reported. While isolated advances in the hardware of

manufacturing technologies can improve the resolution, speed, and size of printed constructs, the fabrication of complex, multiscale structures recapitulating biological tissue will ultimately require the convergence of several technologies in one device. For example, extrusion bioprinting can be used to fabricate the bulk of a large and relatively coarse tissue construct in a limited time, while employing material jetting or LIFT where exact placement of certain cell types is required.[454] Similarly, the coprinting of fibers using melt electrowriting and bioprinting of bioinks allows control over spatial placement of cells using the fibers to compartmentalize the cells.[455]

Besides mimicking the ECM, polymeric materials can be designed with additional functions to enhance the performance of bioprinted constructs. These functions can relate to the sensing or actuation but can also be connected with different stages of tissue maturation (e.g., preprinting and postprinting). 3D printing of living or nonliving constructs can be followed by changes occurring over time after the printing process, often referred to as 4D bioprinting. Arguably nearly all printed tissue is 4D as it changes upon maturation, but in this case the printed material, also referred to as shape memory polymer (SMP), is designed to change shape over time, often as a result of a specific stimulus. Actuation can be brought about through a large array of stimuli, including thermal, electric, magnetic, or immersion in water. One application of SMPs is the DLP SLA printing of scaffolds from epoxidized and acrylated soybean oil, which supported the attachment and growth of human bone marrow-derived MSCs.[456] The same group has further exploited the potential of this bioprinting technique to generate 4D cell-laden cardiac patches with physiological adaptability. By tuning the cross-linking density of GelMA-PEGDA bioinks, the authors demonstrate the ability of the patch to undergo stress-induced morphing changes in response to the dynamic heart beating of a murine model.[457] One other study looked at the influence of shape recovery of a scaffold on seeded cells, and it was concluded that the mechanical stimulus imparted by shape recovery was able to influence the shape of cells and nuclei.[458] Yet, the influence imparted by a one-way shape changing SMP on cells may remain limited. Complex SMPs with adequate rheological properties that show reversible shape memory behavior may one day be utilized to direct cellular behavior over a longer term in more sophisticated ways. The translation of well-established cellular protocols and assays from 2D to 3D creates challenges but also introduces new opportunities to add function and create in situ monitoring techniques using sensors. Molecular force sensors, relying on the self-assembly of molecules which can then be pulled apart by application of a force, have recently proven useful for investigating cellular mechanotransduction. Although early studies have been conducted on gold or glass surfaces, the technique is highly amendable for use in hydrogels as eluded to in a recent article from the group of Blank.[459] One of the major questions pertaining to the evolving field of bioprinting that remains, is to what extent spatial organization should be engineered and what should be left to the cells to self-organize? There is no doubt that most tissues require a strict organization to function but that functioning also depends on the interaction of the different cell types and tissue structures. Hence, some degree of maturation is usually required to obtain the desired responses. In this sense, polymeric materials must be formulated to play an active role in tissue maturation (pre and post printing), e.g., through transducing mechanical forces, presenting or releasing signaling

molecules, thereby maintaining or restoring phenotype, inducing differentiation, or initiating certain signaling cascades. In this context, it is important to realize that materials not only directly influence the behavior of encapsulated cells but perhaps even more so indirectly by influencing the ability of cells to deposit pericellular proteins. Nascent proteins are deposited at the cell–matrix interface within the first day of encapsulation, their quantity and distribution being dependent on the hydrogel's cross-link density, viscoelasticity, and degradability.[460] In turn, this structure of pericellular proteins influences cell spreading, differentiation, and other behaviors.[461] Besides this emerging field of research looking at cell self-assembly within hydrogels, other researchers have focused on self-assembly of cells in the form of organoids. Organoids are self-organized multicellular structures typically originated from a single stem cell, which recapitulate some of the structural features and functions of an organ, or its primary building blocks.[462] As such, they are highly suited for modeling tissue development and disease as well as for drug testing. Combining organoid culture with bioprinting technology presents a promising but largely unexplored opportunity to engineer larger functional tissues and organs of more sophisticated architecture and complexity.[463] In particular, the ability to engineer vascularization in 3D organoid cultures may provide critical cues required for large-scale and more reproducible tissue organization, as complex networks of vasculature do not only allow for oxygen, nutrient, and waste exchange but also provide a structural template for growth and spatially controlled gradients of growth factors.[464] While the lofty goal of creating whole organs using 3D bioprinting may still be some way off, many other applications using biofabrication are in the here and now. Microfluidics, in the form of "organs-on-a-chip", is one more example of this with clear near-term commercial benefits in drug screening to this technology. If, for example, multiple chips are connected, it is possible to test the toxicity of secondary metabolites on organs as it is these interorgan toxic effects that often lead to a drug failing in the clinical stage. With this goal in mind, the group of Atala have used PDMS molds as microreactors with liver, heart, and lung organoids serially connected with PTFE tubing in different pairs to test various metabolites.[465] A prerequisite for integrated multiorgan fabrication is the development of better multimaterial printing. Toward this aim, Khademhosseini and co-workers have demonstrated a digital micromirror device enabled DLP printing to rapidly switch between different gelMA and PEGDA bioinks in microfluidic channels.[466] Using this technique, they were able to make multimaterial cell-laden structures with 10 μm resolution. As discussed throughout this review, the benefits brought by 3D bioprinting to the field of TE and RM are undeniable, making this group of technologies the most essential and cutting-edge tool for the development of 3D models with a high degree of human tissue mimicry. Despite the challenges that still need to be addressed to improve the quality of bioprinted analogues, particularly in terms of manufacturing hardware and performance of bioinks, the future looks auspicious. Driven mainly by the recent advances in manufacturing technologies and biomaterials, the bioprinting market is projected to reach USD$ 1647.4 million by 2024.[467] Companies providing 3D printing technology are expected to retain the biggest share of this market but not without significant changes to their business model. With technology prices in a downward trend (essentially due to increased competition) and facing an

increase demand for standardization, many of these companies are likely to make of the development and selling of inks their core business, in a very similar process to that of inkjet printers.[468] With pharmaceutical and cosmetic companies leading the way, the demand for bioprinted tissue models to replace animal testing is likely to increase in the coming years. Companies like Organovo already offer such products (e.g., ExVive) for research purposes, and many more players are expected to enter this market where regulatory compliance can be simpler to meet than for other clinical products (e.g implants). While research and commercialization continue to advance rapidly, the translational pathway of bioprinted products to clinical practice remains unclear and challenging. If it is true that technical requirements for individual constituents of 3D bioprinting technology such as material compatibility, cell source, hardware (bioprinter), and software are being met and, in some cases, regulated (e.g., materials for in vivo application), the assessment of these same constituents as a whole (e.g., tissue or organ model) is still lacking. Fragmented guidelines provided by international regulatory agencies, including Food and Drug Administration (FDA) and European Medicines Agency (EMA) have proven insufficient to regulate TE products. Therefore, the establishment of an international agency supported by regulatory panels at the national level becomes urgent to address all ethical, legal, and social aspects of bioprinting and regulate its successful translation to clinical practice.[469] If we manage to overcome these roadblocks and progress continues at the same pace as in the past decade, then it is very likely that we will soon see the effective integration of bioprinting with stem cell reprogramming and gene editing technologies, thus definitely opening the door to a new era of tissue models for personalized medicine.

AUTHOR INFORMATION

Corresponding Author

Marco Domingos — *Department of Mechanical, Aerospace and Civil Engineering, School of Engineering, Faculty of Science and Engineering, The University of Manchester, Manchester M13 9PL, U.K.;* ⊙ orcid.org/0000-0002-6693-790X; Email: marco.domingos@manchester.ac.uk

Authors

Ana Clotilde Fonseca — *Centre for Mechanical Engineering, Materials and Processes, Department of Chemical Engineering, University of Coimbra, 3030-790 Coimbra, Portugal;* ⊙ orcid.org/0000-0002-7145-2472

Ferry P. W. Melchels — *Institute of Biological Chemistry, Biophysics and Bioengineering, School of Engineering and Physical Sciences, Heriot-Watt University, Edinburgh EH14 4AS, U.K.;* ⊙ orcid.org/0000-0002-5881-837X

Miguel J. S. Ferreira — *Department of Mechanical, Aerospace and Civil Engineering, School of Engineering, Faculty of Science and Engineering, The University of Manchester, Manchester M13 9PL, U.K.;* ⊙ orcid.org/0000-0001-7529-6553

Samuel R. Moxon — *Division of Neuroscience and Experimental Psychology, School of Biological Sciences, Faculty of Biology Medicine and Health, University of Manchester, Manchester M13 9PT, U.K.;* ⊙ orcid.org/0000-0002-9819-9622

Geoffrey Potjewyd — *Division of Neuroscience and Experimental Psychology, School of Biological Sciences, Faculty of Biology Medicine and Health, University of Manchester, Manchester M13 9PT, U.K.;* ⊙ orcid.org/0000-0002-1970-9429

Tim R. Dargaville — *Institute of Health and Biomedical Innovation, Science and Engineering Faculty, Queensland University of Technology, Queensland 4001, Australia;* ⊙ orcid.org/0000-0003-4665-9508

Susan J. Kimber — *Division of Cell Matrix Biology and Regenerative Medicine, School of Biological Sciences, Faculty of Biology Medicine and Health, University of Manchester, Manchester M13 9PT, U.K.;* ⊙ orcid.org/0000-0002-0568-6342

Complete contact information is available at:
https://pubs.acs.org/10.1021/acs.chemrev.0c00342

Author Contributions

∇A.C.F. and F.P.W.M. contributed equally to this work

Notes

The authors declare no competing financial interest.

Biographies

Ana Clotilde Fonseca graduated in Chemical Engineering from the University of Coimbra in 2007. She obtained her Ph.D. from the same University, working on the development of α-amino acids based poly(ester amide)s, in 2013. Currently, she is an Assistant Professor at the Department of Chemical Engineering of the University of Coimbra and her research interests are focused on the development of biodegradable and biocompatible polymers for biomedical application, namely additive manufacturing.

Ferry P. W. Melchels is associate professor in the Institute of Biological Chemistry, Biophysic,s and Bioengineering at Heriot—Watt University, Edinburgh (UK). He holds an M.Sc. (2005) in chemical engineering and a Ph.D. (2010) in biomaterials from the University of Twente (The Netherlands). He was a Marie Curie postdoctoral fellow between Queensland University of Technology (Brisbane, Australia) and University Medical Center Utrecht (The Netherlands) before taking up his position in Edinburgh in 2015.

Miguel J. S. Ferreira is a CDT in Regenerative Medicine Ph.D. researcher funded by the EPSRC and MRC at The University of Manchester (UK). Under the supervision of Dr. Marco Domingos, he is combining 3D bioprinting and pluripotent stem cells to develop new strategies for osteochondral regeneration. He holds a Master's in Bioengineering from the University of Porto (Portugal) and is currently serving as Science Coordinator of the New Organ Alliance and Management Committee member of the Student European Low Gravity Research Association.

Samuel R. Moxon is a biomaterials researcher at the University of Manchester. He received his Ph.D. in Tissue Engineering in 2017 and is currently developing 3D iPSC culture models for studying dementia-causing diseases. He works in Prof. Nigel Hooper's research group and collaborates with Dr. Marco Domingos on advanced manufacturing techniques for generating in vitro tissue models. He has particular expertise in biopolymers and rheological analyses.

Geoffrey Potjewyd is a CDT in Regenerative Medicine Ph.D. researcher funded by the EPSRC and MRC at The University of Manchester (UK). He holds an MRes in Translational Medicine from The University of Manchester (2015) and currently works under the supervision of Prof. Nigel Hooper and Dr. Marco Domingos on developing 3D models of the brain for dementia research, using 3D biomaterials, bioprinting, and human iPS cells.

Tim R. Dargaville completed his Ph.D. in Polymer Chemistry in 2003 at the University of Queensland and then worked at Sandia National Laboratories in Albuquerque, New Mexico, investigating polymer

degradation. In 2006, he returned to Australia to take up a position at the Queensland University of Technology. He is now an Associate Professor and Australian Research Council Future Fellow, with research interests in synthetic hydrogels and polymer processing for biomaterial applications.

Susan J. Kimber is Professor of Stem Cells and Development at the University of Manchester (UK). She obtained her B.A. (Natural Sciences) and Ph.D. from the University of Cambridge UK, where she went on to take up a postdoctoral position in early mammalian development. She set up the North West Embryonic Stem Cell Centre (NWESCC) with Professor Daniel Brison, aimed at deriving embryonic stem cell (hESC) lines suitable for therapy and generated 17 lines, 7 at clinical grade. Her lab has developed advanced protocols for targeting pluripotent stem cell differentiation, particularly along mesodermal lineages such as to chondrocytes, nephric progenitors, and vascular cells in 2D and 3D constructs. They also use patient derived induced pluripotent stem cells for modelling genetic diseases, especially of cartilage and kidney, with a view to their application for drug-target discovery.

Marco Domingos is a senior lecturer in the Department of Mechanical, Aerospace, and Civil Engineering at the University of Manchester (UK). He graduated in Mechanical Engineering (2006) from the Polytechnic Institute of Leiria (Portugal) and holds a Ph.D. (2013) cum laude in Mechanical Engineering from the University of Girona (Spain). Before joining the University of Manchester (2014), he worked for two years (2010−2012) as an assistant researcher in additive manufacturing at the Centre for Rapid and Sustainable Product Development (Portugal) and for one year (2013) at Dias de Sousa, SA (Portugal) in the field of medical imaging. Since 2019, he is a principal investigator at the Henry Royce Institute (Manchester) with research interests in advanced biomaterials and biofabrication for regenerative medicine.

REFERENCES

(1) Rimann, M.; Graf-Hausner, U. Synthetic 3D Multicellular Systems for Drug Development. *Curr. Opin. Biotechnol.* 2012, 23, 803.
(2) Yamada, K. M.; Cukierman, E. Modeling Tissue Morphogenesis and Cancer in 3D. *Cell* 2007, 130, 601−610.
(3) Jackson, S. J.; Thomas, G. J. Human Tissue Models in Cancer Research: Looking beyond the Mouse. *Dis. Models & Mech.* 2017, 10, 939−942.
(4) Groll, J.; Boland, T.; Blunk, T.; Burdick, J. A.; Cho, D.-W.; Dalton, P. D.; Derby, B.; Forgacs, G.; Li, Q.; Mironov, V. A.; Moroni, L.; Nakamura, M.; Shu, W.; Takeuchi, S.; Vozzi, G.; Woodfield, T. B. F.; Xu, T.; Yoo, J. J.; Malda, J. Biofabrication: Reappraising the Definition of an Evolving Field. *Biofabrication* 2016, 8, 013001.
(5) Nie, M.; Takeuchi, S. Bottom-up Biofabrication Using Microfluidic Techniques. *Biofabrication* 2018, 10, 044103.

(6) Moroni, L.; Burdick, J. A.; Highley, C.; Lee, S. J.; Morimoto, Y.; Takeuchi, S.; Yoo, J. J. Biofabrication Strategies for 3D in Vitro Models and Regenerative Medicine. *Nat. Rev. Mater.* 2018, 3, 21−37.
(7) Mironov, V.; Trusk, T.; Kasyanov, V.; Little, S.; Swaja, R.; Markwald, R. Biofabrication: A 21st Century Manufacturing Paradigm. *Biofabrication* 2009, 1, 022001.
(8) Melchels, F. P. W.; Domingos, M. A. N.; Klein, T. J.; Malda, J.; Bartolo, P. J.; Hutmacher, D. W. Additive Manufacturing of Tissues and Organs. *Prog. Polym. Sci.* 2012, 37, 1079−1104.
(9) Bourell, D. L. Perspectives on Additive Manufacturing. *Annu. Rev. Mater. Res.* 2016, 46, 1−18.
(10) Domingos, M.; Intranuovo, F.; Gloria, A.; Gristina, R.; Ambrosio, L.; Bártolo, P. J.; Favia, P. Improved Osteoblast Cell Affinity on Plasma-Modified 3-D Extruded PCL Scaffolds. *Acta Biomater.* 2013, 9, 5997.
(11) Malda, J.; Woodfield, T. B. F.; Van Der Vloodt, F.; Kooy, F. K.; Martens, D. E.; Tramper, J.; Van Blitterswijk, C. A.; Riesle, J. The Effect of PEGT/PBT Scaffold Architecture on Oxygen Gradients in Tissue Engineered Cartilaginous Constructs. *Biomaterials* 2004, 25, 5773−5780.
(12) D'Amora, U.; Ronca, A.; Raucci, M. G.; Lin, H.; Soriente, A.; Fan, Y.; Zhang, X.; Ambrosio, L. Bioactive Composites Based on Double Network Approach with Tailored Mechanical, Physico-Chemical, and Biological Features. *J. Biomed. Mater. Res., Part A* 2018, 106, 3079−3089.
(13) Cipitria, A.; Reichert, J. C.; Epari, D. R.; Saifzadeh, S.; Berner, A.; Schell, H.; Mehta, M.; Schuetz, M. A.; Duda, G. N.; Hutmacher, D. W. Polycaprolactone Scaffold and Reduced RhBMP-7 Dose for the Regeneration of Critical-Sized Defects in Sheep Tibiae. *Biomaterials* 2013, 34, 9960−9968.
(14) Meng, D.; Erol, M.; Boccaccini, A. R. Processing Technologies for 3D Nanostructured Tissue Engineering Scaffolds. *Adv. Eng. Mater.* 2010, 12, B467−B487.
(15) Amani, H.; Arzaghi, H.; Bayandori, M.; Dezfuli, A. S.; Pazoki-Toroudi, H.; Shafiee, A.; Moradi, L. Controlling Cell Behavior through the Design of Biomaterial Surfaces: A Focus on Surface Modification Techniques. *Adv. Mater. Interfaces* 2019, 6, 1900572.
(16) Jeon, H.; Simon, C. G.; Kim, G. A Mini-Review: Cell Response to Microscale, Nanoscale, and Hierarchical Patterning of Surface Structure. *J. Biomed. Mater. Res., Part B* 2014, 102, 1580.
(17) Kolesky, D. B.; Truby, R. L.; Gladman, A. S.; Busbee, T. A.; Homan, K. A.; Lewis, J. A. 3D Bioprinting of Vascularized, Heterogeneous Cell-Laden Tissue Constructs. *Adv. Mater.* 2014, 26, 3124−3130.
(18) Fedorovich, N. E.; De Wijn, J. R.; Verbout, A. J.; Alblas, J.; Dhert, W. J. A. Three-Dimensional Fiber Deposition of Cell-Laden, Viable, Patterned Constructs for Bone Tissue Printing. *Tissue Eng., Part A* 2008, 14, 127−133.
(19) Raphael, B.; Khalil, T.; Workman, V. L.; Smith, A.; Brown, C. P.; Streuli, C.; Saiani, A.; Domingos, M. 3D Cell Bioprinting of Self-Assembling Peptide-Based Hydrogels. *Mater. Lett.* 2017, 190, 103−106.
(20) Levato, R.; Visser, J.; Planell, J. A.; Engel, E.; Malda, J.; Mateos-Timoneda, M. A. Biofabrication of Tissue Constructs by 3D Bioprinting of Cell-Laden Microcarriers. *Biofabrication* 2014, 6, 035020.
(21) Groll, J.; Burdick, J. A.; Cho, D.-W.; Derby, B.; Gelinsky, M.; Heilshorn, S. C.; Jüngst, T.; Malda, J.; Mironov, V. A.; Nakayama, K.; Ovsianikov, A.; Sun, W.; Takeuchi, S.; Yoo, J. J.; Woodfield, T. B. F. A Definition of Bioinks and Their Distinction from Biomaterial Inks. *Biofabrication* 2019, 11, 013001.
(22) Hospodiuk, M.; Dey, M.; Sosnoski, D.; Ozbolat, I. T. The Bioink: A Comprehensive Review on Bioprintable Materials. *Biotechnol. Adv.* 2017, 35, 217−239.
(23) Paxton, N.; Smolan, W.; Bock, T.; Melchels, F.; Groll, J.; Jungst, T. Proposal to Assess Printability of Bioinks for Extrusion-Based Bioprinting and Evaluation of Rheological Properties Governing Bioprintability. *Biofabrication* 2017, 9, 044107.

(24) Freeman, F. E.; Kelly, D. J. Tuning Alginate Bioink Stiffness and Composition for Controlled Growth Factor Delivery and to Spatially Direct MSC Fate within Bioprinted Tissues. *Sci. Rep.* **2017**, *7*, 17042.

(25) Skardal, A.; Devarasetty, M.; Kang, H. W.; Mead, I.; Bishop, C.; Shupe, T.; Lee, S. J.; Jackson, J.; Yoo, J.; Soker, S.; Atala, A. A Hydrogel Bioink Toolkit for Mimicking Native Tissue Biochemical and Mechanical Properties in Bioprinted Tissue Constructs. *Acta Biomater.* **2015**, *25*, 24.

(26) Yao, B.; Hu, T.; Cui, X.; Song, W.; Fu, X.; Huang, S. Enzymatically Degradable Alginate/Gelatin Bioink Promotes Cellular Behavior and Degradation in Vitro and in Vivo. *Biofabrication* **2019**, *11*, 045020.

(27) Peak, C. W.; Singh, K. A.; Adlouni, M.; Chen, J.; Gaharwar, A. K. Printing Therapeutic Proteins in 3D Using Nanoengineered Bioink to Control and Direct Cell Migration. *Adv. Healthcare Mater.* **2019**, *8*, 1−10.

(28) Jungst, T.; Smolan, W.; Schacht, K.; Scheibel, T.; Groll, J. Strategies and Molecular Design Criteria for 3D Printable Hydrogels. *Chem. Rev.* **2016**, *116*, 1496−1539.

(29) Jose, R. R.; Rodriguez, M. J.; Dixon, T. A.; Omenetto, F.; Kaplan, D. L. Evolution of Bioinks and Additive Manufacturing Technologies for 3D Bioprinting. *ACS Biomater. Sci. Eng.* **2016**, *2*, 1662−1678.

(30) Chimene, D.; Lennox, K. K.; Kaunas, R. R.; Gaharwar, A. K. Advanced Bioinks for 3D Printing: A Materials Science Perspective. *Ann. Biomed. Eng.* **2016**, *44*, 2090−2102.

(31) Gu, Q.; Tomaskovic-Crook, E.; Wallace, G. G.; Crook, J. M. 3D Bioprinting Human Induced Pluripotent Stem Cell Constructs for In Situ Cell Proliferation and Successive Multilineage Differentiation. *Adv. Healthcare Mater.* **2017**, *6*, 1700175.

(32) Li, Y.; Jiang, X.; Li, L.; Chen, Z. N.; Gao, G.; Yao, R.; Sun, W. 3D Printing Human Induced Pluripotent Stem Cells with Novel Hydroxypropyl Chitin Bioink: Scalable Expansion and Uniform Aggregation. *Biofabrication* **2018**, *10*, 044101.

(33) Murphy, S. V.; De Coppi, P.; Atala, A. Opportunities and Challenges of Translational 3D Bioprinting. *Nat. Biomed. Eng.* **2020**, *4*, 370.

(34) Guvendiren, M.; Molde, J.; Soares, R. M. D.; Kohn, J. Designing Biomaterials for 3D Printing. *ACS Biomater. Sci. Eng.* **2016**, *2*, 1679−1693.

(35) Zhu, W.; Ma, X.; Gou, M.; Mei, D.; Zhang, K.; Chen, S. 3D Printing of Functional Biomaterials for Tissue Engineering. *Curr. Opin. Biotechnol.* **2016**, *40*, 103−112.

(36) Hölzl, K.; Lin, S.; Tytgat, L.; Van Vlierberghe, S.; Gu, L.; Ovsianikov, A. Bioink Properties before, during and after 3D Bioprinting. *Biofabrication* **2016**, *8*, 032002.

(37) Feinberg, A. W.; Miller, J. S. Progress in Three-Dimensional Bioprinting. *MRS Bull.* **2017**, *42*, 557−562.

(38) Chimene, D.; Kaunas, R.; Gaharwar, A. K. Hydrogel Bioink Reinforcement for Additive Manufacturing: A Focused Review of Emerging Strategies. *Adv. Mater.* **2020**, *32*, 1902026.

(39) Peng, W.; Datta, P.; Ayan, B.; Ozbolat, V.; Sosnoski, D.; Ozbolat, I. T. 3D Bioprinting for Drug Discovery and Development in Pharmaceutics. *Acta Biomater.* **2017**, *57*, 26−46.

(40) Pati, F.; Jang, J.; Lee, J. W.; Cho, D.-W. *Essentials of 3D Biofabrication and Translation*; Academic Press: Boston, 2015; p 123.

(41) Jiang, T.; Munguia-Lopez, J. G.; Flores-Torres, S.; Kort-Mascort, J.; Kinsella, J. M. Extrusion Bioprinting of Soft Materials: An Emerging Technique for Biological Model Fabrication. *Appl. Phys. Rev.* **2019**, *6*, 011310.

(42) Ning, L.; Chen, X. A Brief Review of Extrusion-Based Tissue Scaffold Bio-Printing. *Biotechnol. J.* **2017**, *12*, 1600671.

(43) Liu, F.; Vyas, C.; Poologasundarampillai, G.; Pape, I.; Hinduja, S.; Mirihanage, W.; Bartolo, P. J. Process-Driven Microstructure Control in Melt-Extrusion-Based 3D Printing for Tailorable Mechanical Properties in a Polycaprolactone Filament. *Macromol. Mater. Eng.* **2018**, *303*, 1800173.

(44) Derakhshanfar, S.; Mbeleck, R.; Xu, K.; Zhang, X.; Zhong, W.; Xing, M. 3D Bioprinting for Biomedical Devices and Tissue Engineering: A Review of Recent Trends and Advances. *Bioact. Mater.* **2018**, *3*, 144−156.

(45) Ozbolat, I. T.; Hospodiuk, M. Current Advances and Future Perspectives in Extrusion-Based Bioprinting. *Biomaterials* **2016**, *76*, 321−343.

(46) Kim, M. H.; Lee, Y. W.; Jung, W.-K.; Oh, J.; Nam, S. Y. Enhanced Rheological Behaviors of Alginate Hydrogels with Carrageenan for Extrusion-Based Bioprinting. *J. Mech. Behav. Biomed. Mater.* **2019**, *98*, 187−194.

(47) Gao, T.; Gillispie, G. J.; Copus, J. S.; Pr, A. K.; Seol, Y.-J.; Atala, A.; Yoo, J. J.; Lee, S. J. Optimization of Gelatin-Alginate Composite Bioink Printability Using Rheological Parameters: A Systematic Approach. *Biofabrication* **2018**, *10*, 034106.

(48) Yu, Y.; Moncal, K. K.; Li, J.; Peng, W.; Rivero, I.; Martin, J. A.; Ozbolat, I. T. Three-Dimensional Bioprinting Using Self-Assembling Scalable Scaffold-Free "Tissue Strands" as a New Bioink. *Sci. Rep.* **2016**, *6*, 28714.

(49) Picout, D. R.; Ross-Murphy, S. B. Rheology of Biopolymer Solutions and Gels. *Sci. World J.* **2003**, *3*, 105−121.

(50) Cofiño, C.; Perez-Amodio, S.; Semino, C. E.; Engel, E.; Mateos-Timoneda, M. A. Development of a Self-Assembled Peptide/Methylcellulose-Based Bioink for 3D Bioprinting. *Macromol. Mater. Eng.* **2019**, *304*, 1900353.

(51) Potjewyd, G.; Moxon, S.; Wang, T.; Domingos, M.; Hooper, N. M. N. M. Tissue Engineering 3D Neurovascular Units: A Biomaterials and Bioprinting Perspective. *Trends Biotechnol.* **2018**, *36*, 457−472.

(52) Cox, T. R.; Erler, J. T. Remodeling and Homeostasis of the Extracellular Matrix: Implications for Fibrotic Diseases and Cancer. *Dis. Models & Mech.* **2011**, *4*, 165−178.

(53) Petta, D.; Armiento, A. R.; Grijpma, D.; Alini, M.; Eglin, D.; D'Este, M. 3D Bioprinting of a Hyaluronan Bioink through Enzymatic-and Visible Light-Crosslinking. *Biofabrication* **2018**, *10*, 044104.

(54) Knowlton, S.; Yenilmez, B.; Anand, S.; Tasoglu, S. Photo-crosslinking-Based Bioprinting: Examining Crosslinking Schemes. *Bioprinting* **2017**, *5*, 10−18.

(55) Bendtsen, S. T.; Quinnell, S. P.; Wei, M. Development of a Novel Alginate-Polyvinyl Alcohol-Hydroxyapatite Hydrogel for 3D Bioprinting Bone Tissue Engineered Scaffolds. *J. Biomed. Mater. Res., Part A* **2017**, *105*, 1457−1468.

(56) Tabriz, A. G.; Hermida, M. A.; Leslie, N. R.; Shu, W. Three-Dimensional Bioprinting of Complex Cell Laden Alginate Hydrogel Structures. *Biofabrication* **2015**, *7*, 045012.

(57) Rutz, A. L.; Hyland, K. E.; Jakus, A. E.; Burghardt, W. R.; Shah, R. N. A Multimaterial Bioink Method for 3D Printing Tunable, Cell-Compatible Hydrogels. *Adv. Mater.* **2015**, *27*, 1607−1614.

(58) Ouyang, L.; Highley, C. B.; Sun, W.; Burdick, J. A. A Generalizable Strategy for the 3D Bioprinting of Hydrogels from Nonviscous Photo-Crosslinkable Inks. *Adv. Mater.* **2017**, *29*, 1604983.

(59) Bertassoni, L. E.; Cecconi, M.; Manoharan, V.; Nikkhah, M.; Hjortnaes, J.; Cristino, A. L.; Barabaschi, G.; Demarchi, D.; Dokmeci, M. R.; Yang, Y.; Khademhosseini, A. Hydrogel Bioprinted Micro-channel Networks for Vascularization of Tissue Engineering Constructs. *Lab Chip* **2014**, *14*, 2202−2211.

(60) Hockaday, L. A.; Kang, K. H.; Colangelo, N. W.; Cheung, P. Y. C.; Duan, B.; Malone, E.; Wu, J.; Girardi, L. N.; Bonassar, L. J.; Lipson, H.; Chu, C. C.; Butcher, J. T. Rapid 3D Printing of Anatomically Accurate and Mechanically Heterogeneous Aortic Valve Hydrogel Scaffolds. *Biofabrication* **2012**, *4*, 035005.

(61) Colosi, C.; Shin, S. R.; Manoharan, V.; Massa, S.; Costantini, M.; Barbetta, A.; Dokmeci, M. R.; Dentini, M.; Khademhosseini, A. Microfluidic Bioprinting of Heterogeneous 3D Tissue Constructs Using Low-Viscosity Bioink. *Adv. Mater.* **2016**, *28*, 677−684.

(62) Costantini, M.; Testa, S.; Mozetic, P.; Barbetta, A.; Fuoco, C.; Fornetti, E.; Tamiro, F.; Bernardini, S.; Jaroszewicz, J.; Święszkowski, W.; Trombetta, M.; Castagnoli, L.; Seliktar, D.; Garstecki, P.; Cesareni, G.; Cannata, S.; Rainer, A.; Gargioli, C. Microfluidic-

Enhanced 3D Bioprinting of Aligned Myoblast-Laden Hydrogels Leads to Functionally Organized Myofibers in Vitro and in Vivo. *Biomaterials* **2017**, *131*, 98−110.

(63) Shim, J.-H.; Lee, J.-S.; Kim, J. Y.; Cho, D.-W. Bioprinting of a Mechanically Enhanced Three-Dimensional Dual Cell-Laden Construct for Osteochondral Tissue Engineering Using a Multi-Head Tissue/Organ Building System. *J. Micromech. Microeng.* **2012**, *22*, 085014.

(64) Liu, W.; Zhang, Y. S.; Heinrich, M. A.; De Ferrari, F.; Jang, H. L.; Bakht, S. M.; Alvarez, M. M.; Yang, J.; Li, Y.-C.; Trujillo-De Santiago, G.; Miri, A. K.; Zhu, K.; Khoshakhlagh, P.; Prakash, G.; Cheng, H.; Guan, X.; Zhong, Z.; Ju, J.; Zhu, G. H.; Jin, X.; Shin, S. R.; Dokmeci, M. R.; Khademhosseini, A. Rapid Continuous Multimaterial Extrusion Bioprinting. *Adv. Mater.* **2017**, *29*, 1604630.

(65) Kundu, J.; Shim, J.; Jang, J.; Kim, S.; Cho, D. An Additive Manufacturing-based PCL−Alginate−Chondrocyte Bioprinted Scaffold for Cartilage Tissue Engineering. *J. Tissue Eng. Regener. Med.* **2015**, *9*, 1286−1297.

(66) You, F.; Eames, B. F.; Chen, X. Application of Extrusion-Based Hydrogel Bioprinting for Cartilage Tissue Engineering. *Int. J. Mol. Sci.* **2017**, *18*, 1597.

(67) Loo, Y.; Hauser, C. A. E. Bioprinting Synthetic Self-Assembling Peptide Hydrogels for Biomedical Applications. *Biomed. Mater.* **2016**, *11*, 014103.

(68) Hirst, A. R.; Escuder, B.; Miravet, J. F.; Smith, D. K. High-Tech Applications of Self-Assembling Supramolecular Nanostructured Gel-Phase Materials: From Regenerative Medicine to Electronic Devices. *Angew. Chem., Int. Ed.* **2008**, *47*, 8002−8018.

(69) Kang, H.-W.; Lee, S. J.; Ko, I. K.; Kengla, C.; Yoo, J. J.; Atala, A. A 3D Bioprinting System to Produce Human-Scale Tissue Constructs with Structural Integrity. *Nat. Biotechnol.* **2016**, *34*, 312−319.

(70) Moxon, S. R.; Cooke, M. E.; Cox, S. C.; Snow, M.; Jeys, L.; Jones, S. W.; Smith, A. M.; Grover, L. M. Suspended Manufacture of Biological Structures. *Adv. Mater.* **2017**, *29*, 1605594.

(71) Lee, A.; Hudson, A. R.; Shiwarski, D. J.; Tashman, J. W.; Hinton, T. J.; Yerneni, S.; Bliley, J. M.; Campbell, P. G.; Feinberg, A. W. 3D Bioprinting of Collagen to Rebuild Components of the Human Heart. *Science* **2019**, *365*, 482−487.

(72) Hinton, T. J.; Jallerat, Q.; Palchesko, R. N.; Park, J. H.; Grodzicki, M. S.; Shue, H. J.; Ramadan, M. H.; Hudson, A. R.; Feinberg, A. W. Three-Dimensional Printing of Complex Biological Structures by Freeform Reversible Embedding of Suspended Hydrogels. *Sci. Adv.* **2015**, *1*, e1500758.

(73) Mohanty, S.; Larsen, L. B.; Trifol, J.; Szabo, P.; Burri, H. V. R.; Canali, C.; Dufva, M.; Emnéus, J.; Wolff, A. Fabrication of Scalable and Structured Tissue Engineering Scaffolds Using Water Dissolvable Sacrificial 3D Printed Moulds. *Mater. Sci. Eng., C* **2015**, *55*, 569−578.

(74) Sachlos, E.; Czernuszka, J. T. Making Tissue Engineering Scaffolds Work. Review: The Application of Solid Freeform Fabrication Technology to the Production of Tissue Engineering Scaffolds. *Eur. Cell. Mater.* **2003**, *5*, 29−40.

(75) Senior, J. J.; Cooke, M. E.; Grover, L. M.; Smith, A. M. Fabrication of Complex Hydrogel Structures Using Suspended Layer Additive Manufacturing (SLAM). *Adv. Funct. Mater.* **2019**, *29*, 1904845.

(76) McCormack, A.; Highley, C. B.; Leslie, N. R.; Melchels, F. P. W. 3D Printing in Suspension Baths: Keeping the Promises of Bioprinting Afloat. *Trends Biotechnol.* **2020**, *38*, 584.

(77) Roth, E. A.; Xu, T.; Das, M.; Gregory, C.; Hickman, J. J.; Boland, T. Inkjet Printing for High-Throughput Cell Patterning. *Biomaterials* **2004**, *25*, 3707−3715.

(78) Xu, T.; Zhao, W.; Zhu, J. M.; Albanna, M. Z.; Yoo, J. J.; Atala, A. Complex Heterogeneous Tissue Constructs Containing Multiple Cell Types Prepared by Inkjet Printing Technology. *Biomaterials* **2013**, *34*, 130−139.

(79) Nakamura, M.; Kobayashi, A.; Takagi, F.; Watanabe, A.; Hiruma, Y.; Ohuchi, K.; Iwasaki, Y.; Horie, M.; Morita, I.; Takatani, S. Biocompatible Inkjet Printing Technique for Designed Seeding of Individual Living Cells. *Tissue Eng.* **2005**, *11*, 1658−1666.

(80) Ilkhanizadeh, S.; Teixeira, A. I.; Hermanson, O. Inkjet Printing of Macromolecules on Hydrogels to Steer Neural Stem Cell Differentiation. *Biomaterials* **2007**, *28*, 3936−3943.

(81) Faulkner-Jones, A.; Fyfe, C.; Cornelissen, D.; Gardner, J.; King, J.; Courtney, A.; Shu, W. Bioprinting of Human Pluripotent Stem Cells and Their Directed Differentiation into Hepatocyte-like Cells for the Generation of Mini- Livers in 3D. *Biofabrication* **2015**, *7*, 44102.

(82) Rodríguez-Dévora, J. I.; Zhang, B.; Reyna, D.; Shi, Z. D.; Xu, T. High Throughput Miniature Drug-Screening Platform Using Bio-printing Technology. *Biofabrication* **2012**, *4*, 035001.

(83) Matsusaki, M.; Sakaue, K.; Kadowaki, K.; Akashi, M. Three-Dimensional Human Tissue Chips Fabricated by Rapid and Automatic Inkjet Cell Printing. *Adv. Healthcare Mater.* **2013**, *2*, 534−539.

(84) Gudapati, H.; Dey, M.; Ozbolat, I. A Comprehensive Review on Droplet-Based Bioprinting: Past, Present and Future. *Biomaterials* **2016**, *102*, 20−42.

(85) Delaney, J. T.; Smith, P. J.; Schubert, U. S. Inkjet Printing of Proteins. *Soft Matter* **2009**, *5*, 4866−4877.

(86) Moon, S.; Kim, Y.-G.; Dong, L.; Lombardi, M.; Haeggstrom, E.; Jensen, R. V.; Hsiao, L.-L.; Demirci, U. Drop-on-Demand Single Cell Isolation and Total RNA Analysis. *PLoS One* **2011**, *6*, No. e17455.

(87) Angelopoulos, I.; Allenby, M. C.; Lim, M.; Zamorano, M. Engineering Inkjet Bioprinting Processes toward Translational Therapies. *Biotechnol. Bioeng.* **2020**, *117*, 272.

(88) Saunders, R. E.; Gough, J. E.; Derby, B. Delivery of Human Fibroblast Cells by Piezoelectric Drop-on-Demand Inkjet Printing. *Biomaterials* **2008**, *29*, 193−203.

(89) Derby, B. Inkjet Printing of Functional and Structural Materials: Fluid Property Requirements, Feature Stability, and Resolution. *Annu. Rev. Mater. Res.* **2010**, *40*, 395−414.

(90) Bishop, E. S.; Mostafa, S.; Pakvasa, M.; Luu, H. H.; Lee, M. J.; Wolf, J. M.; Ameer, G. A.; He, T.-C.; Reid, R. R. 3-D Bioprinting Technologies in Tissue Engineering and Regenerative Medicine: Current and Future Trends. *Genes Dis.* **2017**, *4*, 185−195.

(91) Saunders, R. E.; Derby, B. Inkjet Printing Biomaterials for Tissue Engineering: Bioprinting. *Int. Mater. Rev.* **2014**, *59*, 430−448.

(92) Lee, W.; Lee, V.; Polio, S.; Keegan, P.; Lee, J.-H.; Fischer, K.; Park, J.-K.; Yoo, S.-S. On-Demand Three-Dimensional Freeform Fabrication of Multi-Layered Hydrogel Scaffold with Fluidic Channels. *Biotechnol. Bioeng.* **2010**, *105*, 1178−1186.

(93) Foresti, D.; Kroll, K. T.; Amissah, R.; Sillani, F.; Homan, K. A.; Poulikakos, D.; Lewis, J. A. Acoustophoretic Printing. *Sci. Adv.* **2018**, *4*, No. eaat1659.

(94) Wilson, W. C. J.; Boland, T. Cell and Organ Printing 1: Protein and Cell Printers. *Anat. Rec.* **2003**, *272A*, 491−496.

(95) Cui, X.; Dean, D.; Ruggeri, Z. M.; Boland, T. Cell Damage Evaluation of Thermal Inkjet Printed Chinese Hamster Ovary Cells. *Biotechnol. Bioeng.* **2010**, *106*, 963−969.

(96) Masaeli, E.; Forster, V.; Picaud, S.; Karamali, F.; Nasr-Esfahani, M.-H.; Marquette, C. A. Tissue Engineering of Retina through High Resolution 3-Dimentional Inkjet Bioprinting. *Biofabrication* **2020**, *12*, 025006.

(97) Wu, B.; Li, S.; Shi, J.; Vijayavenkataraman, S.; Lu, W. F.; Trau, D.; Fuh, J. Y. H. Homogeneous Cell Printing on Porous PCL/F127 Tissue Engineering Scaffolds. *Bioprinting* **2018**, *12*, No. e00030.

(98) Tse, C.; Whiteley, R.; Yu, T.; Stringer, J.; MacNeil, S.; Haycock, J. W.; Smith, P. J. Inkjet Printing Schwann Cells and Neuronal Analogue NG108−15 Cells. *Biofabrication* **2016**, *8*, 015017.

(99) Huang, Y.; He, K.; Wang, X. Rapid Prototyping of a Hybrid Hierarchical Polyurethane-Cell/Hydrogel Construct for Regenerative Medicine. *Mater. Sci. Eng., C* **2013**, *33*, 3220−3229.

(100) Cui, X.; Boland, T.; D'Lima, D. D.; Lotz, M. K. Thermal Inkjet Printing in Tissue Engineering and Regenerative Medicine. *Recent Pat. Drug Delivery Formulation* **2012**, *6*, 149−155.

(101) Solis, L. H.; Ayala, Y.; Portillo, S.; Varela-Ramirez, A.; Aguilera, R.; Boland, T. Thermal Inkjet Bioprinting Triggers the

Activation of the VEGF Pathway in Human Microvascular Endothelial Cells in Vitro. *Biofabrication* **2019**, *11*, 045005.

(102) Campbell, A.; Mohl, J. E.; Gutierrez, D. A.; Varela-Ramirez, A.; Boland, T. Thermal Bioprinting Causes Ample Alterations of Expression of LUCAT1, IL6, CCL26, and NRN1L Genes and Massive Phosphorylation of Critical Oncogenic Drug Resistance Pathways in Breast Cancer Cells. *Front. Bioeng. Biotechnol.* **2020**, *8*, 82.

(103) Gao, G.; Hubbell, K.; Schilling, A. F.; Dai, G.; Cui, X. *3D Cell Culture*; Humana Press: New York, 2017; p 391.

(104) Ng, W. L.; Lee, J. M.; Yeong, W. Y.; Win Naing, M. Microvalve-Based Bioprinting - Process, Bio-Inks and Applications. *Biomater. Sci.* **2017**, *5*, 632−647.

(105) Rose, J. C.; De Laporte, L. Hierarchical Design of Tissue Regenerative Constructs. *Adv. Healthcare Mater.* **2018**, *7*, 1701067.

(106) Müller, M.; Öztürk, E.; Arlov, Ø.; Gatenholm, P.; Zenobi-Wong, M. Alginate Sulfate−Nanocellulose Bioinks for Cartilage Bioprinting Applications. *Ann. Biomed. Eng.* **2017**, *45*, 210−223.

(107) Shi, P.; Edgar, T. Y. S.; Yeong, W. Y.; Laude, A. Hybrid Three-Dimensional (3D) Bioprinting of Retina Equivalent for Ocular Research. *International Journal of Bioprinting* **2017**, *3*, 138−146.

(108) da Conceicao Ribeiro, R.; Pal, D.; Ferreira, A. M.; Gentile, P.; Benning, M.; Dalgarno, K. Reactive Jet Impingement Bioprinting of High Cell Density Gels for Bone Microtissue Fabrication. *Biofabrication* **2019**, *11*, 15014.

(109) Rosen, D. W.; Margolin, L.; Vohra, S. Printing High Viscosity Fluids Using Ultrasonic Droplet Generation. In *In International Solid Freeform Fabrication Symposium−An Additive Manufacturing Conference*, 2008; pp 239−253.

(110) Fang, Y.; Frampton, J. P.; Raghavan, S.; Sabahi-Kaviani, R.; Luker, G.; Deng, C. X.; Takayama, S. Rapid Generation of Multiplexed Cell Cocultures Using Acoustic Droplet Ejection Followed by Aqueous Two-Phase Exclusion Patterning. *Tissue Eng., Part C* **2012**, *18*, 647−657.

(111) Demirci, U.; Montesano, G. Single Cell Epitaxy by Acoustic Picolitre Droplets. *Lab Chip* **2007**, *7*, 1139−1145.

(112) Castro, J. O.; Ramesan, S.; Rezk, A. R.; Yeo, L. Y. Continuous Tuneable Droplet Ejection via Pulsed Surface Acoustic Wave Jetting. *Soft Matter* **2018**, *14*, 5721−5727.

(113) Moon, S.; Hasan, S. K.; Song, Y. S.; Xu, F.; Keles, H. O.; Manzur, F.; Mikkilineni, S.; Hong, J. W.; Nagatomi, J.; Haeggstrom, E.; Khademhosseini, A.; Demirci, U. Layer by Layer Three-Dimensional Tissue Epitaxy by Cell-Laden Hydrogel Droplets. *Tissue Eng., Part C* **2010**, *16*, 157−166.

(114) Skoog, S. A.; Goering, P. L.; Narayan, R. J. Stereolithography in Tissue Engineering. *J. Mater. Sci.: Mater. Med.* **2014**, *25*, 845−856.

(115) Bártolo, P. J. *Stereolithography: Materials, Processes and Applications*; Springer Science & Business Media: New York, 2011; 1.

(116) Hull, C. W. Apparatus for production of three-dimensional objects by stereolithography. U.S. Patent 4575330A, 1986, .

(117) Miri, A. K.; Mirzaee, I.; Hassan, S.; Mesbah Oskui, S.; Nieto, D.; Khademhosseini, A.; Zhang, Y. S. Effective Bioprinting Resolution in Tissue Model Fabrication. *Lab Chip* **2019**, *19*, 2019−2037.

(118) Wang, L. L.; Highley, C. B.; Yeh, Y.-C.; Galarraga, J. H.; Uman, S.; Burdick, J. A. Three-Dimensional Extrusion Bioprinting of Single- and Double-Network Hydrogels Containing Dynamic Covalent Crosslinks. *J. Biomed. Mater. Res., Part A* **2018**, *106*, 865−875.

(119) Bowser, D. A.; Moore, M. J. Biofabrication of Neural Microphysiological Systems Using Magnetic Spheroid Bioprinting. *Biofabrication* **2020**, *12*, 015002.

(120) Han, X.; Courseaus, J.; Khamassi, J.; Nottrodt, N.; Engelhardt, S.; Jacobsen, F.; Bierwisch, C.; Meyer, W.; Walter, T.; Weisser, J. Optimized Vascular Network by Stereolithography for Tissue Engineered Ski. *International Journal of Bioprinting* **2018**, *4*, 134.

(121) Shiraishi, I.; Kurosaki, K.; Kanzaki, S.; Ichikawa, H. Development of Suepr Flexible Replica of Congenital Heart Disease with Stereolithography 3D Printing for Simulation Surgery and Medical Education. *J. Card. Failure* **2014**, *20*, S180−S181.

(122) Wadnap, S.; Krishnamoorthy, S.; Zhang, Z.; Xu, C. Biofabrication of 3D Cell-Encapsulated Tubular Constructs Using Dynamic Optical Projection Stereolithography. *J. Mater. Sci.: Mater. Med.* **2019**, *30*, 36.

(123) Chen, P.; Zheng, L.; Wang, Y.; Tao, M.; Xie, Z.; Xia, C.; Gu, C.; Chen, J.; Qiu, P.; Mei, S.; Ning, L.; Shi, Y.; Fang, C.; Fan, S.; Lin, X. Desktop-Stereolithography 3D Printing of a Radially Oriented Extracellular Matrix/Mesenchymal Stem Cell Exosome Bioink for Osteochondral Defect Regeneration. *Theranostics* **2019**, *9*, 2439−2459.

(124) Moritz, T.; Maleksaeedi, S. *Additive Manufacturing of Ceramic Components*; Zhang, J., Jung, Y.-G. B. T.-A. M., Eds.; Butterworth-Heinemann, 2018; Vol. 4, pp 105−161.

(125) Jeon, O.; Bouhadir, K. H.; Mansour, J. M.; Alsberg, E. Photocrosslinked Alginate Hydrogels with Tunable Biodegradation Rates and Mechanical Properties. *Biomaterials* **2009**, *30*, 2724−2734.

(126) Smeds, K. A.; Grinstaff, M. W. Photocrosslinkable Polysaccharides for in Situ Hydrogel Formation. *J. Biomed. Mater. Res.* **2001**, *54*, 115−121.

(127) Ramachandran, S.; Prasad, N. R. Effect of Ursolic Acid, a Triterpenoid Antioxidant, on Ultraviolet-B Radiation-Induced Cytotoxicity, Lipid Peroxidation and DNA Damage in Human Lymphocytes. *Chem.-Biol. Interact.* **2008**, *176*, 99−107.

(128) Trémezaygues, L.; Seifert, M.; Tilgen, W.; Reichrath, J. 1, 25-Dihydroxyvitamin D3 Protects Human Keratinocytes against UV-B-Induced Damage: In Vitro Analysis of Cell Viability/Proliferation, DNA-Damage and Repair. *Derm.-Endocrinol.* **2009**, *1*, 239−245.

(129) Stacey, M.; Stickley, J.; Fox, P.; Statler, V.; Schoenbach, K.; Beebe, S. J.; Buescher, S. Differential Effects in Cells Exposed to Ultra-Short, High Intensity Electric Fields: Cell Survival, DNA Damage, and Cell Cycle Analysis. *Mutat. Res., Genet. Toxicol. Environ. Mutagen.* **2003**, *542*, 65−75.

(130) Lin, H.; Zhang, D.; Alexander, P. G.; Yang, G.; Tan, J.; Cheng, A. W.-M.; Tuan, R. S. Application of Visible Light-Based Projection Stereolithography for Live Cell-Scaffold Fabrication with Designed Architecture. *Biomaterials* **2013**, *34*, 331−339.

(131) Wang, Z.; Abdulla, R.; Parker, B.; Samanipour, R.; Ghosh, S.; Kim, K. A Simple and High-Resolution Stereolithography-Based 3D Bioprinting System Using Visible Light Crosslinkable Bioinks. *Biofabrication* **2015**, *7*, 045009.

(132) Ovsianikov, A.; Chichkov, B.; Mente, P.; Monteiro-Riviere, N. A.; Doraiswamy, A.; Narayan, R. J. Two Photon Polymerization of Polymer−Ceramic Hybrid Materials for Transdermal Drug Delivery. *Int. J. Appl. Ceram. Technol.* **2007**, *4*, 22−29.

(133) Weiß, T.; Hildebrand, G.; Schade, R.; Liefeith, K. Two-Photon Polymerization for Microfabrication of Three-Dimensional Scaffolds for Tissue Engineering Application. *Eng. Life Sci.* **2009**, *9*, 384−390.

(134) Rebollar, E.; Frischauf, I.; Olbrich, M.; Peterbauer, T.; Hering, S.; Preiner, J.; Hinterdorfer, P.; Romanin, C.; Heitz, J. Proliferation of Aligned Mammalian Cells on Laser-Nanostructured Polystyrene. *Biomaterials* **2008**, *29*, 1796−1806.

(135) Teixeira, A. I.; Nealey, P. F.; Murphy, C. J. Responses of Human Keratocytes to Micro- and Nanostructured Substrates. *J. Biomed. Mater. Res.* **2004**, *71A*, 369−376.

(136) Miller, P. R.; Aggarwal, R.; Doraiswamy, A.; Lin, Y. J.; Lee, Y.-S.; Narayan, R. J. Laser Micromachining for Biomedical Applications. *JOM* **2009**, *61*, 35−40.

(137) Ovsianikov, A.; Mühleder, S.; Torgersen, J.; Li, Z.; Qin, X.-H.; Van Vlierberghe, S.; Dubruel, P.; Holnthoner, W.; Redl, H.; Liska, R.; Stampfl, J. Laser Photofabrication of Cell-Containing Hydrogel Constructs. *Langmuir* **2014**, *30*, 3787−3794.

(138) Lim, K. S.; Levato, R.; Costa, P. F.; Castilho, M. D.; Alcala-Orozco, C. R.; van Dorenmalen, K. M. A.; Melchels, F. P. W.; Gawlitta, D.; Hooper, G. J.; Malda, J.; Woodfield, T. B. F. Bio-Resin for High Resolution Lithography-Based Biofabrication of Complex Cell-Laden Constructs. *Biofabrication* **2018**, *10*, 034101.

(139) Antoshin, A. A.; Churbanov, S. N.; Minaev, N. V.; Zhang, D.; Zhang, Y.; Shpichka, A. I.; Timashev, P. S. LIFT-Bioprinting, Is It Worth It? *Bioprinting* **2019**, *15*, No. e00052.

(140) Kyle, S.; Jessop, Z. M.; Al-Sabah, A.; Whitaker, I. S. 'Printability" of Candidate Biomaterials for Extrusion Based 3D Printing: State-of-the-Art'. *Adv. Healthcare Mater.* **2017**, *6*, 1−16.

(141) Sears, N. A.; Seshadri, D. R.; Dhavalikar, P. S.; Cosgriff-Hernandez, E. A Review of Three-Dimensional Printing in Tissue Engineering. *Tissue Eng., Part B* **2016**, *22*, 298−310.

(142) Lee, W.; Debasitis, J. C.; Lee, V. K.; Lee, J.-H.; Fischer, K.; Edminster, K.; Park, J.-K.; Yoo, S.-S. Multi-Layered Culture of Human Skin Fibroblasts and Keratinocytes through Three-Dimensional Freeform Fabrication. *Biomaterials* **2009**, *30*, 1587−1595.

(143) Sun, J.; Ng, J. H.; Fuh, Y. H.; Wong, Y. S.; Loh, H. T.; Xu, Q. Comparison of Micro-Dispensing Performance between Micro-Valve and Piezoelectric Printhead. *Microsyst. Technol.* **2009**, *15*, 1437−1448.

(144) Zhou, X.; Hou, Y.; Lin, J. A Review on the Processing Accuracy of Two-Photon Polymerization. *AIP Adv.* **2015**, *5*, 030701.

(145) Malda, J.; Frondoza, C. G. Microcarriers in the Engineering of Cartilage and Bone. *Trends Biotechnol.* **2006**, *24*, 299−304.

(146) Bedell, M. L.; Navara, A. M.; Du, Y.; Zhang, S.; Mikos, A. G. Polymeric Systems for Bioprinting. *Chem. Rev.* **2020**. DOI: 10.1021/acs.chemrev.9b00834.

(147) Hu, W.; Wang, Z.; Xiao, Y.; Zhang, S.; Wang, J. Advances in Crosslinking Strategies of Biomedical Hydrogels. *Biomater. Sci.* **2019**, *7*, 843−855.

(148) Chaudhuri, O.; Gu, L.; Darnell, M.; Klumpers, D.; Bencherif, S. A.; Weaver, J. C.; Huebsch, N.; Mooney, D. J. Substrate Stress Relaxation Regulates Cell Spreading. *Nat. Commun.* **2015**, *6*, 6365.

(149) Lee, H.; Gu, L.; Mooney, D. J.; Levenston, M. E.; Chaudhuri, O. Mechanical Confinement Regulates Cartilage Matrix Formation by Chondrocytes. *Nat. Mater.* **2017**, *16*, 1243−1251.

(150) Chaudhuri, O.; Gu, L.; Klumpers, D.; Darnell, M.; Bencherif, S. A.; Weaver, J. C.; Huebsch, N.; Lee, H.; Lippens, E.; Duda, G. N.; Mooney, D. J. Hydrogels with Tunable Stress Relaxation Regulate Stem Cell Fate and Activity. *Nat. Mater.* **2016**, *15*, 326−334.

(151) Zhu, J.; Kaufman, L. J. Collagen i Self-Assembly: Revealing the Developing Structures That Generate Turbidity. *Biophys. J.* **2014**, *106*, 1822−1831.

(152) Mazzocchi, A.; Devarasetty, M.; Huntwork, R. C.; Soker, S.; Skardal, A. Optimization of Collagen Type I-Hyaluronan Hybrid Bioink for 3D Bioprinted Liver Microenvironments. *Biofabrication* **2019**, *11*, 015003.

(153) Kim, J. H.; Yoo, J. J.; Lee, S. J. Three-Dimensional Cell-Based Bioprinting for Soft Tissue Regeneration. *Tissue Eng. Regener. Med.* **2016**, *13*, 647−662.

(154) Chang, C. C.; Boland, E. D.; Williams, S. K.; Hoying, J. B. Direct-Write Bioprinting Three-Dimensional Biohybrid Systems for Future Regenerative Therapies. *J. Biomed. Mater. Res., Part B* **2011**, *98B*, 160−170.

(155) Horvath, L.; Umehara, Y.; Jud, C.; Blank, F.; Petri-Fink, A.; Rothen-Rutishauser, B. Engineering an in Vitro Air-Blood Barrier by 3D Bioprinting. *Sci. Rep.* **2015**, *5*, 7974.

(156) Wang, X.; Ao, Q.; Tian, X.; Fan, J.; Tong, H.; Hou, W.; Bai, S. Gelatin-Based Hydrogels for Organ 3D Bioprinting. *Polymers* **2017**, *9*, 401.

(157) Benya, P. D.; Shaffer, J. D. Dedifferentiated Chondrocytes Reexpress the Differentiated Collagen Phenotype When Cultured in Agarose Gels. *Cell* **1982**, *30*, 215−224.

(158) Axpe, E.; Oyen, M. L. Applications of Alginate-Based Bioinks in 3D Bioprinting. *Int. J. Mol. Sci.* **2016**, *17*, 1976.

(159) Fonseca, A. C.; Ferreira, P.; Cordeiro, R. A.; Mendonça, P. V.; Góis, J. R.; Gil, M. H.; Coelho, J. F. J. *New Strategies to Advance Pre/Diabetes Care: Integrative Approach by PPPM*; Springer: Dordrecht, 2013; 399.

(160) Kim, H.; Bae, C.; Kook, Y. M.; Koh, W. G.; Lee, K.; Park, M. H. Mesenchymal Stem Cell 3D Encapsulation Technologies for Biomimetic Microenvironment in Tissue Regeneration. *Stem Cell Res. Ther.* **2019**, *10*, 51.

(161) Choe, G.; Park, J.; Park, H.; Lee, J. Y. Hydrogel Biomaterials for Stem Cell Microencapsulation. *Polymers* **2018**, *10*, 997.

(162) Fallacara, A.; Baldini, E.; Manfredini, S.; Vertuani, S. Hyaluronic Acid in the Third Millennium. *Polymers* **2018**, *10*, 701.

(163) Numata, K.; Kaplan, D. L. *Advanced Wound Repair Therapies*; Woodhead Publishing: Cambridge, 2011; p 524.

(164) Griesser, J.; Hetényi, G.; Bernkop-Schnürch, A. Thiolated Hyaluronic Acid as Versatile Mucoadhesive Polymer: From the Chemistry behind to Product Developments-What Are the Capabilities? *Polymers* **2018**, *10*, 243.

(165) Demirtaş, T. T.; Irmak, G.; Gümüşderelioğlu, M. A Bioprintable Form of Chitosan Hydrogel for Bone Tissue Engineering. *Biofabrication* **2017**, *9*, 035003.

(166) Zhou, H. Y.; Jiang, L. J.; Cao, P. P.; Li, J. B.; Chen, X. G. Glycerophosphate-Based Chitosan Thermosensitive Hydrogels and Their Biomedical Applications. *Carbohydr. Polym.* **2015**, *117*, 524−536.

(167) Kabirian, F.; Mozafari, M. Decellularized ECM-Derived Bioinks: Prospects for the Future. *Methods* **2020**, *171*, 108−118.

(168) Badylak, S. F.; Taylor, D.; Uygun, K. Whole-Organ Tissue Engineering: Decellularization and Recellularization of Three-Dimensional Matrix Scaffolds. *Annu. Rev. Biomed. Eng.* **2011**, *13*, 27−53.

(169) Saldin, L. T.; Cramer, M. C.; Velankar, S. S.; White, L. J.; Badylak, S. F. Extracellular Matrix Hydrogels from Decellularized Tissues: Structure and Function. *Acta Biomater.* **2017**, *49*, 1−15.

(170) Kim, B. S.; Kim, H.; Gao, G.; Jang, J.; Cho, D.-W. Decellularized Extracellular Matrix: A Step towards the next Generation Source for Bioink Manufacturing. *Biofabrication* **2017**, *9*, 034104.

(171) Pati, F.; Jang, J.; Ha, D.; Won Kim, S.; Rhie, J.; Shim, J.; Kim, D.; Cho, D. Printing Three-Dimensional Tissue Analogues with Decellularized Extracellular Matrix Bioink. *Nat. Commun.* **2014**, *5*, 3935.

(172) Kesti, M.; Eberhardt, C.; Pagliccia, G.; Kenkel, D.; Grande, D.; Boss, A.; Zenobi-Wong, M. Bioprinting Complex Cartilaginous Structures with Clinically Compliant Biomaterials. *Adv. Funct. Mater.* **2015**, *25*, 7406−7417.

(173) Harris, J. M. Introduction to Biomedical and Biotechnical Applications of Polyethylene Glycol. *Am. Chem. Soc. Polym. Prepr. Div. Polym. Chem.* **1997**, *38*, 520−521.

(174) Gauvin, R.; Chen, Y. C.; Lee, J. W.; Soman, P.; Zorlutuna, P.; Nichol, J. W.; Bae, H.; Chen, S.; Khademhosseini, A. Microfabrication of Complex Porous Tissue Engineering Scaffolds Using 3D Projection Stereolithography. *Biomaterials* **2012**, *33*, 3824−3834.

(175) Gazit, E. Self-Assembled Peptide Nanostructures: The Design of Molecular Building Blocks and Their Technological Utilization. *Chem. Soc. Rev.* **2007**, *36*, 1263−1269.

(176) Li, J.; Xing, R.; Bai, S.; Yan, X. Recent Advances of Self-Assembling Peptide-Based Hydrogels for Biomedical Applications. *Soft Matter* **2019**, *15*, 1704−1715.

(177) Wu, E. C.; Zhang, S.; Hauser, C. A. E. Self-Assembling Peptides as Cell-Interactive Scaffolds. *Adv. Funct. Mater.* **2012**, *22*, 456−468.

(178) Loo, Y.; Lakshmanan, A.; Ni, M.; Toh, L. L.; Wang, S.; Hauser, C. A. E. Peptide Bioink: Self-Assembling Nanofibrous Scaffolds for Three-Dimensional Organotypic Cultures. *Nano Lett.* **2015**, *15*, 6919−6925.

(179) Hedegaard, C. L.; Collin, E. C.; Redondo-Gómez, C.; Nguyen, L. T. H.; Ng, K. W.; Castrejón-Pita, A. A.; Castrejón-Pita, J. R.; Mata, A. Hydrodynamically Guided Hierarchical Self-Assembly of Peptide-Protein Bioinks. *Adv. Funct. Mater.* **2018**, *28*, 1703716.

(180) Drzewiecki, K. E.; Malavade, J. N.; Ahmed, I.; Lowe, C. J.; Shreiber, D. I. A Thermoreversible, Photocrosslinkable Collagen Bio-Ink for Free-Form Fabrication of Scaffolds for Regenerative Medicine. *TECHNOLOGY* **2017**, *05*, 185−195.

(181) Rodríguez-Cabello, J. C.; Martín, L.; Alonso, M.; Arias, F. J.; Testera, A. M. Recombinamers" as Advanced Materials for the Post-Oil Age. *Polymer* **2009**, *50*, 5159−5169.

(182) Zhu, D.; Wang, H.; Trinh, P.; Heilshorn, S. C.; Yang, F. Elastin-like Protein-Hyaluronic Acid (ELP-HA) Hydrogels with Decoupled Mechanical and Biochemical Cues for Cartilage Regeneration. *Biomaterials* **2017**, *127*, 132−140.

(183) Miranda-Nieves, D.; Chaikof, E. L. Collagen and Elastin Biomaterials for the Fabrication of Engineered Living Tissues. *ACS Biomater. Sci. Eng.* **2017**, *3*, 694−711.

(184) Klotz, B. J.; Gawlitta, D.; Rosenberg, A. J. W. P.; Malda, J.; Melchels, F. P. W. Gelatin-Methacryloyl Hydrogels: Towards Biofabrication-Based Tissue Repair. *Trends Biotechnol.* **2016**, *34*, 394−407.

(185) Snyder, J. E.; Hamid, Q.; Wang, C.; Chang, R.; Emami, K.; Wu, H.; Sun, W. Bioprinting Cell-Laden Matrigel for Radioprotection Study of Liver by pro-Drug Conversion in a Dual-Tissue Microfluidic Chip. *Biofabrication* **2011**, *3*, 034112.

(186) Chawla, S.; Midha, S.; Sharma, A.; Ghosh, S. Silk-Based Bioinks for 3D Bioprinting. *Adv. Healthcare Mater.* **2018**, *7*, 1701204.

(187) Zheng, Z.; Wu, J.; Liu, M.; Wang, H.; Li, C.; Rodriguez, M. J.; Li, G.; Wang, X.; Kaplan, D. L. 3D Bioprinting of Self-Standing Silk-Based Bioink. *Adv. Healthcare Mater.* **2018**, *7*, 1701026.

(188) Forget, A.; Blaeser, A.; Miessmer, F.; Köpf, M.; Campos, D. F. D.; Voelcker, N. H.; Blencowe, A.; Fischer, H.; Shastri, V. P. Mechanically Tunable Bioink for 3D Bioprinting of Human Cells. *Adv. Healthcare Mater.* **2017**, *6*, 1700255.

(189) Sultan, S.; Siqueira, G.; Zimmermann, T.; Mathew, A. P. 3D Printing of Nano-Cellulosic Biomaterials for Medical Applications. *Current Opinion in Biomedical Engineering.* **2017**, *2*, 29−34.

(190) Pescosolido, L.; Schuurman, W.; Malda, J.; Matricardi, P.; Alhaique, F.; Coviello, T.; Van Weeren, P. R.; Dhert, W. J. A.; Hennink, W. E.; Vermonden, T. Hyaluronic Acid and Dextran-Based Semi-IPN Hydrogels as Biomaterials for Bioprinting. *Biomacromolecules* **2011**, *12*, 1831−1838.

(191) Mouser, V. H. M.; Melchels, F. P. W.; Visser, J.; Dhert, W. J. A.; Gawlitta, D.; Malda, J. Yield Stress Determines Bioprintability of Hydrogels Based on Gelatin-Methacryloyl and Gellan Gum for Cartilage Bioprinting. *Biofabrication* **2016**, *8*, 035003.

(192) Wu, D.; Yu, Y.; Tan, J.; Huang, L.; Luo, B.; Lu, L.; Zhou, C. 3D Bioprinting of Gellan Gum and Poly (Ethylene Glycol) Diacrylate Based Hydrogels to Produce Human-Scale Constructs with High-Fidelity. *Mater. Des.* **2018**, *160*, 486−495.

(193) Silva-Correia, J.; Oliveira, J. M.; Reis, R. L. *Biomaterials from Nature for Advanced Devices and Therapies*; John Wiley & Sons, Inc.: Hoboken, NJ, 2016; p 320.

(194) Ferris, C. J.; Gilmore, K. J.; Beirne, S.; McCallum, D.; Wallace, G. G.; In Het Panhuis, M. Bio-Ink for on-Demand Printing of Living Cells. *Biomater. Sci.* **2013**, *1*, 224−230.

(195) Banks, A.; Guo, X.; Chen, J.; Kumpaty, S.; Zhang, W. Novel Bioprinting Method Using a Pectin Based Bioink. *Technol. Heal. Care* **2017**, *25*, 651−655.

(196) Pereira, R. F.; Sousa, A.; Barrias, C. C.; Bártolo, P. J.; Granja, P. L. A Single-Component Hydrogel Bioink for Bioprinting of Bioengineered 3D Constructs for Dermal Tissue Engineering. *Mater. Horiz.* **2018**, *5*, 1100−1111.

(197) Tan, Y. S. E.; Yeong, W. Y. Direct Bioprinting of Alginate-Based Tubular Constructs Using Multi-Nozzle Extrusion-Based Technique. *Proceedings of the 1st International Conference on Progress in Additive Manufacturing*; Research Publishing Services: Singapore, 2014; p 423.

(198) Wu, Q.; Therriault, D.; Heuzey, M. C. Processing and Properties of Chitosan Inks for 3D Printing of Hydrogel Microstructures. *ACS Biomater. Sci. Eng.* **2018**, *4*, 2643−2652.

(199) Abbadessa, A.; Blokzijl, M. M.; Mouser, V. H. M.; Marica, P.; Malda, J.; Hennink, W. E.; Vermonden, T. A Thermo-Responsive and Photo-Polymerizable Chondroitin Sulfate-Based Hydrogel for 3D Printing Applications. *Carbohydr. Polym.* **2016**, *149*, 163−174.

(200) Burdick, J. A.; Prestwich, G. D. Hyaluronic Acid Hydrogels for Biomedical Applications. *Adv. Mater.* **2011**, *23*, H41−H56.

(201) Censi, R.; Schuurman, W.; Malda, J.; di Dato, G.; Burgisser, P. E.; Dhert, W. J. A.; van Nostrum, C. F.; di Martino, P.; Vermonden, T.; Hennink, W. E. A Printable Photopolymerizable Thermosensitive p(HPMAm-Lactate)-PEG Hydrogel for Tissue Engineering. *Adv. Funct. Mater.* **2011**, *21*, 1833−1842.

(202) Melchels, F. P. W.; Blokzijl, M. M.; Levato, R.; Peiffer, Q. C.; Ruijter, M. De; Hennink, W. E.; Vermonden, T.; Malda, J. Hydrogel-Based Reinforcement of 3D Bioprinted Constructs. *Biofabrication* **2016**, *8*, 035004.

(203) Müller, M.; Becher, J.; Schnabelrauch, M.; Zenobi-Wong, M. Nanostructured Pluronic Hydrogels as Bioinks for 3D Bioprinting. *Biofabrication* **2015**, *7*, 035006.

(204) Kolesky, D. B.; Homan, K. A.; Skylar-Scott, M. A.; Lewis, J. A. Three-Dimensional Bioprinting of Thick Vascularized Tissues. *Proc. Natl. Acad. Sci. U. S. A.* **2016**, *113*, 3179−3184.

(205) Lorson, T.; Jaksch, S.; Lübtow, M. M.; Jüngst, T.; Groll, J.; Lühmann, T.; Luxenhofer, R. A Thermogelling Supramolecular Hydrogel with Sponge-Like Morphology as a Cytocompatible Bioink. *Biomacromolecules* **2017**, *18*, 2161−2171.

(206) Lanzalaco, S.; Armelin, E. Poly(N-Isopropylacrylamide) and Copolymers: A Review on Recent Progresses in Biomedical Applications. *Gels* **2017**, *3*, 36.

(207) Lim, K. S.; Schon, B. S.; Mekhileri, N. V.; Brown, G. C. J.; Chia, C. M.; Prabakar, S.; Hooper, G. J.; Woodfield, T. B. F. New Visible-Light Photoinitiating System for Improved Print Fidelity in Gelatin-Based Bioinks. *ACS Biomater. Sci. Eng.* **2016**, *2*, 1752−1762.

(208) Li, C.; Faulkner-Jones, A.; Dun, A. R.; Jin, J.; Chen, P.; Xing, Y.; Yang, Z.; Li, Z.; Shu, W.; Liu, D.; Duncan, R. R. Rapid Formation of a Supramolecular Polypeptide-DNA Hydrogel for In Situ Three-Dimensional Multilayer Bioprinting. *Angew. Chem., Int. Ed.* **2015**, *54*, 3957−3961.

(209) Ifkovits, J. L.; Burdick, J. a. Review: Photopolymerizable and Degradable Biomaterials for Tissue Engineering Applications. *Tissue Eng.* **2007**, *13*, 2369−2385.

(210) Pathak, C. P.; Sawhney, A. S.; Hubbell, J. A. Rapid Photopolymerization of Immunoprotective Gels in Contact with Cells and Tissue. *J. Am. Chem. Soc.* **1992**, *114*, 8311−8312.

(211) Ito, Y. *Photochemistry for Biomedical Applications: From Device Fabrication to Diagnosis and Therapy*; Springer: Singapore, 2018. DOI: 10.1007/978-981-13-0152-0.

(212) Yue, K.; Li, X.; Schrobback, K.; Sheikhi, A.; Annabi, N.; Leijten, J.; Zhang, W.; Zhang, Y. S.; Hutmacher, D. W.; Klein, T. J.; Khademhosseini, A. Structural Analysis of Photocrosslinkable Methacryloyl-Modified Protein Derivatives. *Biomaterials* **2017**, *139*, 163−171.

(213) Hoch, E.; Hirth, T.; Tovar, G. E. M.; Borchers, K. Chemical Tailoring of Gelatin to Adjust Its Chemical and Physical Properties for Functional Bioprinting. *J. Mater. Chem. B* **2013**, *1*, 5675.

(214) Drzewiecki, K. E.; Parmar, A. S.; Gaudet, I. D.; Branch, J. R.; Pike, D. H.; Nanda, V.; Shreiber, D. I. Methacrylation Induces Rapid, Temperature-Dependent, Reversible Self-Assembly of Type-I Collagen. *Langmuir* **2014**, *30*, 11204−11211.

(215) Hoyle, C. E.; Bowman, C. N. Thiol-Ene Click Chemistry. *Angew. Chem., Int. Ed.* **2010**, *49*, 1540−1573.

(216) Bertlein, S.; Brown, G.; Lim, K. S.; Jungst, T.; Boeck, T.; Blunk, T.; Tessmar, J.; Hooper, G. J.; Woodfield, T. B. F.; Groll, J. Thiol−Ene Clickable Gelatin: A Platform Bioink for Multiple 3D Biofabrication Technologies. *Adv. Mater.* **2017**, *29*, 1703404.

(217) Mũnoz, Z.; Shih, H.; Lin, C.-C. Gelatin Hydrogels Formed by Orthogonal Thiol−Norbornene Photochemistry for Cell Encapsulation. *Biomater. Sci.* **2014**, *2*, 1063−1072.

(218) Gramlich, W. M.; Kim, I. L.; Burdick, J. A. Synthesis and Orthogonal Photopatterning of Hyaluronic Acid Hydrogels with Thiol-Norbornene Chemistry. *Biomaterials* **2013**, *34*, 9803−9811.

(219) Ooi, H. W.; Mota, C.; ten Cate, A. T.; Calore, A.; Moroni, L.; Baker, M. B. Thiol−Ene Alginate Hydrogels as Versatile Bioinks for Bioprinting. *Biomacromolecules* **2018**, *19*, 3390.

(220) Xin, S.; Chimene, D.; Garza, J. E.; Gaharwar, A. K.; Alge, D. L. Clickable PEG Hydrogel Microspheres as Building Blocks for 3D Bioprinting. *Biomater. Sci.* **2019**, *7*, 1179−1187.

(221) Jivan, F.; Yegappan, R.; Pearce, H.; Carrow, J. K.; McShane, M.; Gaharwar, A. K.; Alge, D. L. Sequential Thiol-Ene and Tetrazine Click Reactions for the Polymerization and Functionalization of Hydrogel Microparticles. *Biomacromolecules* **2016**, *17*, 3516−3523.

(222) Stichler, S.; Böck, T.; Paxton, N.; Bertlein, S.; Levato, R.; Schill, V.; Smolan, W.; Malda, J.; Teßmar, J.; Blunk, T.; Groll, J. Double Printing of Hyaluronic Acid/Poly(Glycidol) Hybrid Hydrogels with Poly(ε-Caprolactone) for MSC Chondrogenesis. *Biofabrication* **2017**, *9*, 044108.

(223) Yan, M.; Lewis, P. L.; Shah, R. N. Tailoring Nanostructure and Bioactivity of 3D-Printable Hydrogels with Self-Assemble Peptides Amphiphile (PA) for Promoting Bile Duct Formation. *Biofabrication* **2018**, *10*, 035010.

(224) Khanmohammadi, M.; Dastjerdi, M. B.; Ai, A.; Ahmadi, A.; Godarzi, A.; Rahimi, A.; Ai, J. Horseradish Peroxidase-Catalyzed Hydrogelation for Biomedical Applications. *Biomater. Sci.* **2018**, *6*, 1286−1298.

(225) Arai, K.; Tsukamoto, Y.; Yoshida, H.; Sanae, H.; Mir, T. A.; Sakai, S.; Yoshida, T.; Okabe, M.; Nikaido, T.; Taya, M.; Nakamura, M. The Development of Cell-Adhesive Hydrogel for 3D Printing. *Int. J. Bioprinting* **2016**, *2*, 153−162.

(226) Sakai, S.; Ashida, T.; Ogino, S.; Taya, M. Horseradish Peroxidase-Mediated Encapsulation of Mammalian Cells in Hydrogel Particles by Dropping. *J. Microencapsulation* **2014**, *31*, 100−104.

(227) Midha, S.; Ghosh, S. Silk-Based Bioinks for 3D Bioprinting. In *Regenerative Medicine: Laboratory to Clinic*; Springer: Singapore, 2017; p 259.

(228) Compaan, A. M.; Christensen, K.; Huang, Y. Inkjet Bioprinting of 3D Silk Fibroin Cellular Constructs Using Sacrificial Alginate. *ACS Biomater. Sci. Eng.* **2017**, *3*, 1519−1526.

(229) Xu, J.; Liu, Y.; Hsu, S.-h. Hydrogels Based on Schiff Base Linkages for Biomedical Applications. *Molecules* **2019**, *24*, 3005.

(230) Wang, H.; Zhu, D.; Paul, A.; Cai, L.; Enejder, A.; Yang, F.; Heilshorn, S. C. Covalently Adaptable Elastin-Like Protein-Hyaluronic Acid (ELP-HA) Hybrid Hydrogels with Secondary Thermoresponsive Crosslinking for Injectable Stem Cell Delivery. *Adv. Funct. Mater.* **2017**, *27*, 1605609.

(231) Du, Z.; Li, N.; Hua, Y.; Shi, Y.; Bao, C.; Zhang, H.; Yang, Y.; Lin, Q.; Zhu, L. Physiological PH-Dependent Gelation for 3D Printing Based on the Phase Separation of Gelatin and Oxidized Dextran. *Chem. Commun.* **2017**, *53*, 13023−13026.

(232) Dubbin, K.; Hori, Y.; Lewis, K. K.; Heilshorn, S. C. Dual-Stage Crosslinking of a Gel-Phase Bioink Improves Cell Viability and Homogeneity for 3D Bioprinting. *Adv. Healthcare Mater.* **2016**, *5*, 2488−2492.

(233) Mulyasasmita, W.; Cai, L.; Dewi, R. E.; Jha, A.; Ullmann, S. D.; Luong, R. H.; Huang, N. F.; Heilshorn, S. C. Avidity-Controlled Hydrogels for Injectable Co-Delivery of Induced Pluripotent Stem Cell-Derived Endothelial Cells and Growth Factors. *J. Controlled Release* **2014**, *191*, 71−81.

(234) Valot, L.; Martinez, J.; Mehdi, A.; Subra, G. Chemical Insights into Bioinks for 3D Printing. *Chem. Soc. Rev.* **2019**, *48*, 4049−4086.

(235) Wenz, G. An Overview of Host-Guest Chemistry and Its Application to Nonsteroidal Anti-Inflammatory Drugs. *Clin. Drug Invest.* **2000**, *19*, 21−25.

(236) Paolino, M.; Ennen, F.; Lamponi, S.; Cernescu, M.; Voit, B.; Cappelli, A.; Appelhans, D.; Komber, H. Cyclodextrin-Adamantane Host-Guest Interactions on the Surface of Biocompatible Adamantyl-Modified Glycodendrimers. *Macromolecules* **2013**, *46*, 3215−3227.

(237) Highley, C. B.; Rodell, C. B.; Burdick, J. A. Direct 3D Printing of Shear-Thinning Hydrogels into Self-Healing Hydrogels. *Adv. Mater.* **2015**, *27*, 5075−5079.

(238) Ouyang, L.; Highley, C. B.; Rodell, C. B.; Sun, W.; Burdick, J. A. 3D Printing of Shear-Thinning Hyaluronic Acid Hydrogels with Secondary Cross-Linking. *ACS Biomater. Sci. Eng.* **2016**, *2*, 1743−1751.

(239) Rodell, C. B.; Kaminski, A. L.; Burdick, J. A. Rational Design of Network Properties in Guest-Host Assembled and Shear-Thinning Hyaluronic Acid Hydrogels. *Biomacromolecules* **2013**, *14*, 4125−4134.

(240) Jung, H.; Park, J. S.; Yeom, J.; Selvapalam, N.; Park, K. M.; Oh, K.; Yang, J. A.; Park, K. H.; Hahn, S. K.; Kim, K. 3D Tissue Engineered Supramolecular Hydrogels for Controlled Chondrogenesis of Human Mesenchymal Stem Cells. *Biomacromolecules* **2014**, *15*, 707−714.

(241) Park, K. M.; Yang, J. A.; Jung, H.; Yeom, J.; Park, J. S.; Park, K. H.; Hoffman, A. S.; Hahn, S. K.; Kim, K. In Situ Supramolecular Assembly and Modular Modification of Hyaluronic Acid Hydrogels for 3D Cellular Engineering. *ACS Nano* **2012**, *6*, 2960−2968.

(242) Shim, J.-H.; Jang, K.-M.; Hahn, S. K.; Park, J. Y.; Jung, H.; Oh, K.; Park, K. M.; Yeom, J.; Park, S. H.; Kim, S. W.; Wang, J. H.; Kim, K.; Cho, D.-W. Three-Dimensional Bioprinting of Multilayered Constructs Containing Human Mesenchymal Stromal Cells for Osteochondral Tissue Regeneration in the Rabbit Knee Joint. *Biofabrication* **2016**, *8*, 014102.

(243) Jung, H.; Park, K. M.; Yang, J. A.; Oh, E. J.; Lee, D. W.; Park, K.; Ryu, S. H.; Hahn, S. K.; Kim, K. Theranostic Systems Assembled in Situ on Demand by Host-Guest Chemistry. *Biomaterials* **2011**, *32*, 7687−7694.

(244) Oh, E. J.; Park, K.; Kim, K. S.; Kim, J.; Yang, J. A.; Kong, J. H.; Lee, M. Y.; Hoffman, A. S.; Hahn, S. K. Target Specific and Long-Acting Delivery of Protein, Peptide, and Nucleotide Therapeutics Using Hyaluronic Acid Derivatives. *J. Controlled Release* **2010**, *141*, 2−12.

(245) Huettner, N.; Dargaville, T. R.; Forget, A. Discovering Cell-Adhesion Peptides in Tissue Engineering: Beyond RGD. *Trends Biotechnol.* **2018**, *36*, 372.

(246) Chan, V.; Zorlutuna, P.; Jeong, J. H.; Kong, H.; Bashir, R. Three-Dimensional Photopatterning of Hydrogels Using Stereolithography for Long-Term Cell Encapsulation. *Lab Chip* **2010**, *10*, 2062−2070.

(247) Brown, T. E.; Carberry, B. J.; Worrell, B. T.; Dudaryeva, O. Y.; McBride, M. K.; Bowman, C. N.; Anseth, K. S. Photopolymerized Dynamic Hydrogels with Tunable Viscoelastic Properties through Thioester Exchange. *Biomaterials* **2018**, *178*, 496−503.

(248) Lee, J.; Abdeen, A. A.; Zhang, D.; Kilian, K. A. Directing Stem Cell Fate on Hydrogel Substrates by Controlling Cell Geometry, Matrix Mechanics and Adhesion Ligand Composition. *Biomaterials* **2013**, *34*, 8140−8148.

(249) Lutolf, M. P.; Raeber, G. P.; Zisch, A. H.; Tirelli, N.; Hubbell, J. A. Cell-Responsive Synthetic Hydrogels. *Adv. Mater.* **2003**, *15*, 888−892.

(250) Raeber, G. P.; Lutolf, M. P.; Hubbell, J. A. Molecularly Engineered PEG Hydrogels: A Novel Model System for Proteolytically Mediated Cell Migration. *Biophys. J.* **2005**, *89*, 1374−1388.

(251) Fairbanks, B. D.; Schwartz, M. P.; Halevi, A. E.; Nuttelman, C. R.; Bowman, C. N.; Anseth, K. S. A Versatile Synthetic Extracellular Matrix Mimic via Thiol-Norbornene Photopolymerization. *Adv. Mater.* **2009**, *21*, 5005−5010.

(252) Neves, M. I.; Moroni, L.; Barrias, C. C. Modulating Alginate Hydrogels for Improved Biological Performance as Cellular 3D Microenvironments. *Front. Bioeng. Biotechnol.* **2020**, *8*, 665.

(253) Fonseca, K. B.; Maia, F. R.; Cruz, F. A.; Andrade, D.; Juliano, M. A.; Granja, P. L.; Barrias, C. C. Enzymatic, Physicochemical and Biological Properties of MMP-Sensitive Alginate Hydrogels. *Soft Matter* **2013**, *9*, 3283−3292.

(254) Fonseca, K. B.; Bidarra, S. J.; Oliveira, M. J.; Granja, P. L.; Barrias, C. C. Molecularly Designed Alginate Hydrogels Susceptible to Local Proteolysis as Three-Dimensional Cellular Microenvironments. *Acta Biomater.* **2011**, *7*, 1674−1682.

(255) Fonseca, K. B.; Gomes, D. B.; Lee, K.; Santos, S. G.; Sousa, A.; Silva, E. A.; Mooney, D. J.; Granja, P. L.; Barrias, C. C. Injectable MMP-Sensitive Alginate Hydrogels as HMSC Delivery Systems. *Biomacromolecules* **2014**, *15*, 380−390.

(256) da Silva, L. P.; Jha, A. K.; Correlo, V. M.; Marques, A. P.; Reis, R. L.; Healy, K. E. Gellan Gum Hydrogels with Enzyme-Sensitive Biodegradation and Endothelial Cell Biorecognition Sites. *Adv. Healthcare Mater.* **2018**, *7*, 1700686.

(257) Loo, Y.; Hauser, C. A. E. Bioprinting Synthetic Self-Assembling Peptide Hydrogels for Biomedical Applications. *Biomed. Mater.* **2016**, *11*, 014103.

(258) Fonseca, K. B.; Granja, P. L.; Barrias, C. C. Engineering Proteolytically-Degradable Artificial Extracellular Matrices. *Prog. Polym. Sci.* **2014**, *39*, 2010−2029.

(259) Reakasame, S.; Boccaccini, A. R. Oxidized Alginate-Based Hydrogels for Tissue Engineering Applications: A Review. *Biomacromolecules* **2018**, *19*, 3−21.

(260) Gong, Y.; Wang, C.; Lai, R. C.; Su, K.; Zhang, F.; Wang, D. An Improved Injectable Polysaccharide Hydrogel: Modified Gellan Gum for Long-Term Cartilage Regeneration in Vitro. *J. Mater. Chem.* **2009**, *19*, 1968.

(261) Hasany, M.; Thakur, A.; Taebnia, N.; Kadumudi, F. B.; Shahbazi, M.-A.; Pierchala, M. K.; Mohanty, S.; Orive, G.; Andresen, T. L.; Foldager, C. B.; Yaghmaei, S.; Arpanaei, A.; Gaharwar, A. K.; Mehrali, M.; Dolatshahi-Pirouz, A. Combinatorial Screening of Nanoclay-Reinforced Hydrogels: A Glimpse of the "Holy Grail" in Orthopedic Stem Cell Therapy? *ACS Appl. Mater. Interfaces* **2018**, *10*, 34924−34941.

(262) Jamshidi, P.; Ma, P.; Khosrowyar, K.; Smith, A. M.; Grover, L. M. Tailoring Gel Modulus Using Dispersed Nanocrystalline Hydroxyapatite. *J. Exp. Nanosci.* **2012**, *7*, 652−661.

(263) Chimene, D.; Kaunas, R.; Gaharwar, A. K. Hydrogel Bioink Reinforcement for Additive Manufacturing: A Focused Review of Emerging Strategies. *Adv. Mater.* **2020**, *32*, 1902026.

(264) Schuurman, W.; Levett, P. A.; Pot, M. W.; van Weeren, P. R.; Dhert, W. J. A.; Hutmacher, D. W.; Melchels, F. P. W.; Klein, T. J.; Malda, J. Gelatin-Methacrylamide Hydrogels as Potential Biomaterials for Fabrication of Tissue-Engineered Cartilage Constructs. *Macromol. Biosci.* **2013**, *13*, 551−561.

(265) Poldervaart, M. T.; Goversen, B.; de Ruijter, M.; Abbadessa, A.; Melchels, F. P. W.; Öner, F. C.; Dhert, W. J. A.; Vermonden, T.; Alblas, J. 3D Bioprinting of Methacrylated Hyaluronic Acid (MeHA) Hydrogel with Intrinsic Osteogenicity. *PLoS One* **2017**, *12*, No. e0177628.

(266) Kesti, M.; Müller, M.; Becher, J.; Schnabelrauch, M.; D'Este, M.; Eglin, D.; Zenobi-Wong, M. A Versatile Bioink for Three-Dimensional Printing of Cellular Scaffolds Based on Thermally and Photo-Triggered Tandem Gelation. *Acta Biomater.* **2015**, *11*, 162−172.

(267) Włodarczyk-Biegun, M. K.; del Campo, A. 3D Bioprinting of Structural Proteins. *Biomaterials* **2017**, *134*, 180−201.

(268) Ouyang, L.; Yao, R.; Zhao, Y.; Sun, W. Effect of Bioink Properties on Printability and Cell Viability for 3D Bioplotting of Embryonic Stem Cells. *Biofabrication* **2016**, *8*, 035020.

(269) He, Y.; Yang, F.; Zhao, H.; Gao, Q.; Xia, B.; Fu, J. Research on the Printability of Hydrogels in 3D Bioprinting. *Sci. Rep.* **2016**, *6*, 29977.

(270) Ribeiro, A.; Blokzijl, M. M.; Levato, R.; Visser, C. W.; Castilho, M.; Hennink, W. E.; Vermonden, T.; Malda, J. Assessing Bioink Shape Fidelity to Aid Material Development in 3D Bioprinting. *Biofabrication* **2018**, *10*, 014102.

(271) Zhang, Z.; Jin, Y.; Yin, J.; Xu, C.; Xiong, R.; Christensen, K.; Ringeisen, B. R.; Chrisey, D. B.; Huang, Y. Evaluation of Bioink Printability for Bioprinting Applications. *Appl. Phys. Rev.* **2018**, *5*, 041304.

(272) Wüst, S.; Godla, M. E.; Müller, R.; Hofmann, S. Tunable Hydrogel Composite with Two-Step Processing in Combination with Innovative Hardware Upgrade for Cell-Based Three-Dimensional Bioprinting. *Acta Biomater.* **2014**, *10*, 630−640.

(273) Bryant, S. J.; Nuttelman, C. R.; Anseth, K. S. Cytocompatibility of UV and Visible Light Photoinitiating Systems on Cultured NIH/3T3 Fibroblasts in Vitro. *J. Biomater. Sci., Polym. Ed.* **2000**, *11*, 439−457.

(274) Fairbanks, B. D.; Schwartz, M. P.; Bowman, C. N.; Anseth, K. S. Photoinitiated Polymerization of PEG-Diacrylate with Lithium Phenyl-2,4,6-Trimethylbenzoylphosphinate: Polymerization Rate and Cytocompatibility. *Biomaterials* **2009**, *30*, 6702−6707.

(275) Matsunaga, T.; Hieda, K.; Nikaido, O. Wavelength Dependent Formation of Thymine Dimers and (6−4) Photoproducts in DNA by Monochromatic Ultraviolet Light Ranging from 150 to 365 Nm. Photochem. *Photochem. Photobiol.* **1991**, *54*, 403−410.

(276) Wong, D. Y.; Ranganath, T.; Kasko, A. M. Low-Dose, Long-Wave UV Light Does Not Affect Gene Expression of Human Mesenchymal Stem Cells. *PLoS One* **2015**, *10*, e0139307.

(277) Na, K.; Shin, S.; Lee, H.; Shin, D.; Baek, J.; Kwak, H.; Park, M.; Shin, J.; Hyun, J. Effect of Solution Viscosity on Retardation of Cell Sedimentation in DLP 3D Printing of Gelatin Methacrylate/Silk Fibroin Bioink. *J. Ind. Eng. Chem.* **2018**, *61*, 340−347.

(278) Tromayer, M.; Gruber, P.; Markovic, M.; Rosspeintner, A.; Vauthey, E.; Redl, H.; Ovsianikov, A.; Liska, R. A Biocompatible Macromolecular Two-Photon Initiator Based on Hyaluronan. *Polym. Chem.* **2017**, *8*, 451−460.

(279) O'Connell, C. D.; Onofrillo, C.; Duchi, S.; Li, X.; Zhang, Y.; Tian, P.; Lu, L.; Trengove, A.; Quigley, A.; Gambhir, S.; Khansari, A.; Mladenovska, T.; O'Connor, A.; Di Bella, C.; Choong, P. F.; Wallace, G. G. Evaluation of Sterilisation Methods for Bio-Ink Components: Gelatin, Gelatin Methacryloyl, Hyaluronic Acid and Hyaluronic Acid Methacryloyl. *Biofabrication* **2019**, *11*, 035003.

(280) Lorson, T.; Ruopp, M.; Nadernezhad, A.; Eiber, J.; Vogel, U.; Jungst, T.; Lühmann, T. Sterilization Methods and Their Influence on Physicochemical Properties and Bioprinting of Alginate as a Bioink Component. *ACS Omega* **2020**, *5*, 6481−6486.

(281) Rizwan, M.; Chan, S. W.; Comeau, P. A; Willett, T. L.; Yim, E. K.F. Effect of Sterilization Treatment on Mechanical Properties, Biodegradation, Bioactivity and Printability of GelMA Hydrogels. *Biomed. Mater.* **2020**, DOI: 10.1088/1748-605X/aba40c.

(282) Bochenek, M. A.; Veiseh, O.; Vegas, A. J.; McGarrigle, J. J.; Qi, M.; Marchese, E.; Omami, M.; Doloff, J. C.; Mendoza-Elias, J.; Nourmohammadzadeh, M.; Khan, A.; Yeh, C.-C.; Xing, Y.; Isa, D.; Ghani, S.; Li, J.; Landry, C.; Bader, A. R.; Olejnik, K.; Chen, M.; Hollister-Lock, J.; Wang, Y.; Greiner, D. L.; Weir, G. C.; Strand, B. L.; Rokstad, A. M. A.; Lacik, I.; Langer, R.; Anderson, D. G.; Oberholzer, J. Alginate Encapsulation as Long-Term Immune Protection of Allogeneic Pancreatic Islet Cells Transplanted into the Omental Bursa of Macaques. *Nat. Biomed. Eng.* **2018**, *2*, 810−821.

(283) Karajanagi, S. S.; Yoganathan, R.; Mammucari, R.; Park, H.; Cox, J.; Zeitels, S. M.; Langer, R.; Foster, N. R. Application of a Dense Gas Technique for Sterilizing Soft Biomaterials. *Biotechnol. Bioeng.* **2011**, *108*, 1716−1725.

(284) Bernhardt, A.; Wehrl, M.; Paul, B.; Hochmuth, T.; Schumacher, M.; Schütz, K.; Gelinsky, M. Improved Sterilization of Sensitive Biomaterials with Supercritical Carbon Dioxide at Low Temperature. *PLoS One* **2015**, *10*, e0129205.

(285) *Biomaterials*; RegenHu, 2020; https://www.regenhu.com/biomaterials#bioink (accessed 2020-08-26).

(286) *Biomaterials*; RegenHu, 2020; https://www.regenhu.com/biomaterials#osteoink (accessed 2020-08-26).

(287) *Peptide-based Bioinks for 3D Bioprinting: BiogelxTM-INK*; Biogel X, 2018; https://www.biogelx.com/bioink-product-range/ (accessed 2020-08-26).

(288) *PeptInks for Liquid Handling & 3D Bioprinting*; Manchester Biogel, 2020; https://manchesterbiogel.com/products/peptiinks (accessed 2020-08-26).

(289) *Bioinks—Cellink Global*; CellLink Global, 2020; https://www.cellink.com/global/bioinks/ (accessed 2020-08-27,).

(290) *Innovative 3D Matrices for Breakthrough Research*; Advanced BioMatrix. 2020; https://advancedbiomatrix.com/ (accessed 2020-08-27).

(291) GrowInk. *GrowInk Bioinks for 3D Printing*; UPM Biomedicals, 2020; https://www.upmbiomedicals.com/for-life-science/growink/ (accessed 2020-08-27).

(292) Murphy, S. V.; Atala, A. 3D Bioprinting of Tissues and Organs. *Nat. Biotechnol.* **2014**, *32*, 773−785.

(293) Mandrycky, C.; Wang, Z.; Kim, K.; Kim, D. H. 3D Bioprinting for Engineering Complex Tissues. *Biotechnol. Adv.* **2016**, *34*, 422−434.

(294) Skardal, A.; Zhang, J.; Prestwich, G. D. Bioprinting Vessel-like Constructs Using Hyaluronan Hydrogels Crosslinked with Tetrahedral Polyethylene Glycol Tetracrylates. *Biomaterials* **2010**, *31*, 6173–6181.

(295) Smith, C. M.; Stone, A. L.; Parkhill, R. L.; Stewart, R. L.; Simpkins, M. W.; Kachurin, A. M.; Warren, W. L.; Williams, S. K. Three-Dimensional Bioassembly Tool for Generating Viable Tissue-Engineered Constructs. *Tissue Eng.* **2004**, *10*, 1566–1576.

(296) Rezende, R. A.; Bartolo, P. J.; Mendes, A.; Filho, R. M. Rheological Behavior of Alginate Solutions for Biomanufacturing. *J. Appl. Polym. Sci.* **2009**, *113*, 3866–3871.

(297) Smith, C. M.; Christian, J. J.; Warren, W. L.; Williams, S. K. Characterizing Environmental Factors That Impact the Viability of Tissue-Engineered Constructs Fabricated by a Direct-Write Bioassembly Tool. *Tissue Eng.* **2007**, *13*, 373–383.

(298) Knapp, D. M.; Barocas, V. H.; Moon, A. G.; Yoo, K.; Petzold, L. R.; Tranquillo, R. T. Rheology of Reconstituted Type I Collagen Gel in Confined Compression. *J. Rheol.* **1997**, *41*, 971–993.

(299) Fedorovich, N. E.; Schuurman, W.; Wijnberg, H. M.; Prins, H. J.; Van Weeren, P. R.; Malda, J.; Alblas, J.; Dhert, W. J. A. Biofabrication of Osteochondral Tissue Equivalents by Printing Topologically Defined, Cell-Laden Hydrogel Scaffolds. *Tissue Eng., Part C* **2012**, *18*, 33–44.

(300) Nair, K.; Gandhi, M.; Khalil, S.; Yan, K. C.; Marcolongo, M.; Barbee, K.; Sun, W. Characterization of Cell Viability during Bioprinting Processes. *Biotechnol. J.* **2009**, *4*, 1168–1177.

(301) Li, M.; Tian, X.; Zhu, N.; Schreyer, D. J.; Chen, X. Modeling Process-Induced Cell Damage in the Biodispensing Process. *Tissue Eng., Part C* **2010**, *16*, 533–542.

(302) Li, M.; Tian, X.; Schreyer, D. J.; Chen, X. Effect of Needle Geometry on Flow Rate and Cell Damage in the Dispensing-Based Biofabrication Process. *Biotechnol. Prog.* **2011**, *27*, 1777–1784.

(303) Li, H.; Liu, S.; Lin, L. Rheological Study on 3D Printability of Alginate Hydrogel and Effect of Graphene Oxide. *Int. J. Bioprinting* **2016**, *2*, 54–66.

(304) Melchels, F. P. W.; Dhert, W. J. A.; Hutmacher, D. W.; Malda, J. Development and Characterisation of a New Bioink for Additive Tissue Manufacturing. *J. Mater. Chem. B* **2014**, *2*, 2282–2289.

(305) Liu, W.; Heinrich, M. A.; Zhou, Y.; Akpek, A.; Hu, N.; Liu, X.; Guan, X.; Zhong, Z.; Jin, X.; Khademhosseini, A.; Zhang, Y. S. Extrusion Bioprinting of Shear-Thinning Gelatin Methacryloyl Bioinks. *Adv. Healthcare Mater.* **2017**, *6*, 1601451.

(306) Snyder, J.; Rin Son, A.; Hamid, Q.; Wang, C.; Lui, Y.; Sun, W. Mesenchymal Stem Cell Printing and Process Regulated Cell Properties. *Biofabrication* **2015**, *7*, 044106.

(307) Aguado, B. A.; Mulyasasmita, W.; Su, J.; Lampe, K. J.; Heilshorn, S. C. Improving Viability of Stem Cells during Syringe Needle Flow through the Design of Hydrogel Cell Carriers. *Tissue Eng., Part A* **2012**, *18*, 806–815.

(308) Skardal, A.; Zhang, J.; McCoard, L.; Xu, X.; Oottamasathien, S.; Prestwich, G. D. Photocrosslinkable Hyaluronan-Gelatin Hydrogels for Two-Step Bioprinting. *Tissue Eng., Part A* **2010**, *16*, 2675–2685.

(309) Laronda, M. M.; Rutz, A. L.; Xiao, S.; Whelan, K. A.; Duncan, F. E.; Roth, E. W.; Woodruff, T. K.; Shah, R. N. A Bioprosthetic Ovary Created Using 3D Printed Microporous Scaffolds Restores Ovarian Function in Sterilized Mice. *Nat. Commun.* **2017**, *8*, 15261.

(310) Kokkinis, D.; Schaffner, M.; Studart, A. R. Multimaterial Magnetically Assisted 3D Printing of Composite Materials. *Nat. Commun.* **2015**, *6*, 8643.

(311) Billiet, T.; Gevaert, E.; De Schryver, T.; Cornelissen, M.; Dubruel, P. The 3D Printing of Gelatin Methacrylamide Cell-Laden Tissue-Engineered Constructs with High Cell Viability. *Biomaterials* **2014**, *35*, 49–62.

(312) Liu, W.; Heinrich, M. A.; Zhou, Y.; Akpek, A.; Hu, N.; Liu, X.; Guan, X.; Zhong, Z.; Jin, X.; Khademhosseini, A.; Zhang, Y. S. Extrusion Bioprinting of Shear-Thinning Gelatin Methacryloyl Bioinks. *Adv. Healthcare Mater.* **2017**, *6*, 1601451.

(313) Wüst, S.; Müller, R.; Hofmann, S. 3D Bioprinting of Complex Channels—Effects of Material, Orientation, Geometry, and Cell Embedding. *J. Biomed. Mater. Res., Part A* **2015**, *103*, 2558–2570.

(314) Paxton, N. C.; Smolan, W.; Böck, T.; Melchels, F. P. W.; Groll, J.; Juengst, T. Proposal to Assess Printability of Bioinks for Extrusion-Based Bioprinting and Evaluation of Rheological Properties Governing Bioprintability. *Biofabrication* **2017**, *9*, 044107.

(315) Cheng, E.; Yu, H.; Ahmadi, A.; Cheung, K. C. Investigation of the Hydrodynamic Response of Cells in Drop on Demand Piezoelectric Inkjet Nozzles. *Biofabrication* **2016**, *8*, 015008.

(316) Guillotin, B.; Guillemot, F. Cell Patterning Technologies for Organotypic Tissue Fabrication. *Trends Biotechnol.* **2011**, *29*, 183–190.

(317) Barron, J. A.; Wu, P.; Ladouceur, H. D.; Ringeisen, B. R. Biological Laser Printing: A Novel Technique for Creating Heterogeneous 3-Dimensional Cell Patterns. *Biomed. Microdevices* **2004**, *6*, 139–147.

(318) Keriquel, V.; Guillemot, F.; Arnault, I.; Guillotin, B.; Miraux, S.; Amédée, J.; Fricain, J. C.; Catros, S. In Vivo Bioprinting for Computer- and Robotic-Assisted Medical Intervention: Preliminary Study in Mice. *Biofabrication* **2010**, *2*, 014101.

(319) Guillemot, F.; Souquet, A.; Catros, S.; Guillotin, B.; Lopez, J.; Faucon, M.; Pippenger, B.; Bareille, R.; Rémy, M.; Bellance, S.; Chabassier, P.; Fricain, J. C.; Amédée, J. High-Throughput Laser Printing of Cells and Biomaterials for Tissue Engineering. *Acta Biomater.* **2010**, *6*, 2494–2500.

(320) Barron, J. A.; Spargo, B. J.; Ringeisen, B. R. Biological Laser Printing of Three Dimensional Cellular Structures. *Appl. Phys. A: Mater. Sci. Process.* **2004**, *79*, 1027–1030.

(321) Hinczewski, C.; Corbel, S.; Chartier, T. Ceramic Suspensions Suitable for Stereolithography. *J. Eur. Ceram. Soc.* **1998**, *18*, 583–590.

(322) Isenberg, B. C.; DiMilla, P. A.; Walker, M.; Kim, S.; Wong, J. Y. Vascular Smooth Muscle Cell Durotaxis Depends on Substrate Stiffness Gradient Strength. *Biophys. J.* **2009**, *97*, 1313–1322.

(323) Engler, A. J.; Sen, S.; Sweeney, H. L.; Discher, D. E. Matrix Elasticity Directs Stem Cell Lineage Specification. *Cell* **2006**, *126*, 677–689.

(324) Allen, J. L.; Cooke, M. E.; Alliston, T. ECM Stiffness Primes the TGFβ Pathway to Promote Chondrocyte Differentiation. *Mol. Biol. Cell* **2012**, *23*, 3731–3742.

(325) Young, J. L.; Engler, A. J. Hydrogels with Time-Dependent Material Properties Enhance Cardiomyocyte Differentiation in Vitro. *Biomaterials* **2011**, *32*, 1002–1009.

(326) Ribeiro, A. J. S.; Ang, Y.-S.; Fu, J.-D.; Rivas, R. N.; Mohamed, T. M. A.; Higgs, G. C.; Srivastava, D.; Pruitt, B. L. Contractility of Single Cardiomyocytes Differentiated from Pluripotent Stem Cells Depends on Physiological Shape and Substrate Stiffness. *Proc. Natl. Acad. Sci. U. S. A.* **2015**, *112*, 1270–12710.

(327) Boothe, S. D.; Myers, J. D.; Pok, S.; Sun, J.; Xi, Y.; Nieto, R. M.; Cheng, J.; Jacot, J. G. The Effect of Substrate Stiffness on Cardiomyocyte Action Potentials. *Cell Biochem. Biophys.* **2016**, *74*, 527–535.

(328) Wong, L.; Kumar, A.; Gabela-Zuniga, B.; Chua, J.; Singh, G.; Happe, C. L.; Engler, A. J.; Fan, Y.; McCloskey, K. E. Substrate Stiffness Directs Diverging Vascular Fates. *Acta Biomater.* **2019**, *96*, 321–329.

(329) Wang, P.-Y.; Tsai, W.-B.; Voelcker, N. H. Screening of Rat Mesenchymal Stem Cell Behaviour on Polydimethylsiloxane Stiffness Gradients. *Acta Biomater.* **2012**, *8*, 519–530.

(330) Kilian, K. A.; Bugarija, B.; Lahn, B. T.; Mrksich, M. Geometric Cues for Directing the Differentiation of Mesenchymal Stem Cells. *Proc. Natl. Acad. Sci. U. S. A.* **2010**, *107*, 4872–4877.

(331) Yao, X.; Peng, R.; Ding, J. Effects of Aspect Ratios of Stem Cells on Lineage Commitments with and without Induction Media. *Biomaterials* **2013**, *34*, 930–939.

(332) Yang, L.; Gao, Q.; Ge, L.; Zhou, Q.; Warszawik, E. M.; Bron, R.; Lai, K. W. C.; Van Rijn, P. Topography Induced Stiffness Alteration of Stem Cells Influences Osteogenic Differentiation. *Biomater. Sci.* **2020**, *8*, 2638–2652.

(333) Sharma, S.; Goswami, R.; Zhang, D. X.; Rahaman, S. O. TRPV4 Regulates Matrix Stiffness and TGFβ1-Induced Epithelial-Mesenchymal Transition. *J. Cell. Mol. Med.* **2019**, *23*, 761−774.

(334) Lee, S.; Stanton, A. E.; Tong, X.; Yang, F. Hydrogels with Enhanced Protein Conjugation Efficiency Reveal Stiffness-Induced YAP Localization in Stem Cells Depends on Biochemical Cues. *Biomaterials* **2019**, *202*, 26−34.

(335) Ehrbar, M.; Sala, A.; Lienemann, P.; Ranga, A.; Mosiewicz, K.; Bittermann, A.; Rizzi, S. C.; Weber, F. E.; Lutolf, M. P. Elucidating the Role of Matrix Stiffness in 3D Cell Migration and Remodeling. *Biophys. J.* **2011**, *100*, 284−293.

(336) Lv, H.; Li, L.; Sun, M.; Zhang, Y.; Chen, L.; Rong, Y.; Li, Y. Mechanism of Regulation of Stem Cell Differentiation by Matrix Stiffness. *Stem Cell Res. Ther.* **2015**, *6*, 103.

(337) Lalitha Sridhar, S.; Schneider, M. C.; Chu, S.; De Roucy, G.; Bryant, S. J.; Vernerey, F. J. Heterogeneity Is Key to Hydrogel-Based Cartilage Tissue Regeneration. *Soft Matter* **2017**, *13*, 4841−4855.

(338) Morgan, F. L. C.; Moroni, L.; Baker, M. B. Dynamic Bioinks to Advance Bioprinting. *Adv. Healthcare Mater.* **2020**, *9*, 1901798.

(339) Singh, M.; Berkland, C.; Detamore, M. S. Strategies and Applications for Incorporating Physical and Chemical Signal Gradients in Tissue Engineering. *Tissue Eng., Part B* **2008**, *14*, 341−366.

(340) Wang, S.; Wong Po Foo, C.; Warrier, A.; Poo, M. M.; Heilshorn, S. C.; Zhang, X. Gradient Lithography of Engineered Proteins to Fabricate 2D and 3D Cell Culture Microenvironments. *Biomed. Microdevices* **2009**, *11*, 1127−1134.

(341) Byambaa, B.; Annabi, N.; Yue, K.; Trujillo-De Santiago, G.; Alvarez, M. M.; Jia, W.; Kazemzadeh-Narbat, M.; Shin, S. R.; Tamayol, A.; Khademhosseini, A. Bioprinted Osteogenic and Vasculogenic Patterns for Engineering 3D Bone Tissue. *Adv. Healthcare Mater.* **2017**, *6*, 1700015.

(342) Wu, Z.; Su, X.; Xu, Y.; Kong, B.; Sun, W.; Mi, S. Bioprinting Three-Dimensional Cell-Laden Tissue Constructs with Controllable Degradation. *Sci. Rep.* **2016**, *6*, 24474.

(343) Liu, X.; Zuo, Y.; Sun, J.; Guo, Z.; Fan, H.; Zhang, X. Degradation Regulated Bioactive Hydrogel as the Bioink with Desirable Moldability for Microfluidic Biofabrication. *Carbohydr. Polym.* **2017**, *178*, 8−17.

(344) Jia, J.; Richards, D. J.; Pollard, S.; Tan, Y.; Rodriguez, J.; Visconti, R. P.; Trusk, T. C.; Yost, M. J.; Yao, H.; Markwald, R. R.; Mei, Y. Engineering Alginate as Bioink for Bioprinting. *Acta Biomater.* **2014**, *10*, 4323−4331.

(345) Bouhadir, K. H.; Lee, K. Y.; Alsberg, E.; Damm, K. L.; Anderson, K. W.; Mooney, D. J. Degradation of Partially Oxidized Alginate and Its Potential Application for Tissue Engineering. *Biotechnol. Prog.* **2001**, *17*, 945−950.

(346) Cidonio, G.; Glinka, M.; Dawson, J. I.; Oreffo, R. O. C. The Cell in the Ink: Improving Biofabrication by Printing Stem Cells for Skeletal Regenerative Medicine. *Biomaterials* **2019**, *209*, 10−24.

(347) Amit, M.; Carpenter, M. K.; Inokuma, M. S.; Chiu, C. P.; Harris, C. P.; Waknitz, M. A.; Itskovitz-Eldor, J.; Thomson, J. A. Clonally Derived Human Embryonic Stem Cell Lines Maintain Pluripotency and Proliferative Potential for Prolonged Periods of Culture. *Dev. Biol.* **2000**, *227*, 271−278.

(348) Miere, C.; Hewitson, H.; Devito, L.; Wood, V.; Kadeva, N.; Cornwell, G.; Codognotto, S.; Stephenson, E.; Ilic, D. Generation of KCL018 Research Grade Human Embryonic Stem Cell Line Carrying a Mutation in the DMPK Gene. *Stem Cell Res.* **2016**, *16*, 342−344.

(349) Canham, M. A.; Van Deusen, A.; Brison, D. R.; De Sousa, P. A.; Downie, J.; Devito, L.; Hewitt, Z. A.; Ilic, D.; Kimber, S. J.; Moore, H. D.; Murray, H.; Kunath, T. The Molecular Karyotype of 25 Clinical-Grade Human Embryonic Stem Cell Lines. *Sci. Rep.* **2015**, *5*, 17258.

(350) Ye, J.; Bates, N.; Soteriou, D.; Grady, L.; Edmond, C.; Ross, A.; Kerby, A.; Lewis, P. A.; Adeniyi, T.; Wright, R.; Poulton, K. V.; Lowe, M.; Kimber, S. J.; Brison, D. R. High Quality Clinical Grade Human Embryonic Stem Cell Lines Derived from Fresh Discarded Embryos. *Stem Cell Res. Ther.* **2017**, *8*, 128.

(351) Takahashi, K.; Tanabe, K.; Ohnuki, M.; Narita, M.; Ichisaka, T.; Tomoda, K.; Yamanaka, S. Induction of Pluripotent Stem Cells from Adult Human Fibroblasts by Defined Factors. *Cell* **2007**, *131*, 861−872.

(352) Shi, Y.; Inoue, H.; Wu, J. C.; Yamanaka, S. Induced Pluripotent Stem Cell Technology: A Decade of Progress. *Nat. Rev. Drug Discovery* **2017**, *16*, 115−130.

(353) Liu, S.; Yin, N.; Faiola, F. Prospects and Frontiers of Stem Cell Toxicology. *Stem Cells Dev.* **2017**, *26*, 1528−1539.

(354) Bell, C. C.; Lauschke, V. M.; Vorrink, S. U.; Palmgren, H.; Duffin, R.; Andersson, T. B.; Ingelman-Sundberg, M. Transcriptional, Functional, and Mechanistic Comparisons of Stem Cell-Derived Hepatocytes, HepaRG Cells, and Three-Dimensional Human Hepatocyte Spheroids as Predictive in Vitro Systems for Drug-Induced Liver Injury. *Drug Metab. Dispos.* **2017**, *45*, 419−429.

(355) Ma, X.; Liu, J.; Zhu, W.; Tang, M.; Lawrence, N.; Yu, C.; Gou, M.; Chen, S. 3D Bioprinting of Functional Tissue Models for Personalized Drug Screening and in Vitro Disease Modeling. *Adv. Drug Delivery Rev.* **2018**, *132*, 235−251.

(356) Waddington, S. N.; Privolizzi, R.; Karda, R.; O'Neill, H. C. A Broad Overview and Review of CRISPR-Cas Technology and Stem Cells. *Current Stem Cell Reports* **2016**, *2*, 9−20.

(357) Hale, L. J.; Howden, S. E.; Phipson, B.; Lonsdale, A.; Er, P. X.; Ghobrial, I.; Hosawi, S.; Wilson, S.; Lawlor, K. T.; Khan, S.; Oshlack, A.; Quinlan, C.; Lennon, R.; Little, M. H. 3D Organoid-Derived Human Glomeruli for Personalised Podocyte Disease Modelling and Drug Screening. *Nat. Commun.* **2018**, *9*, 5167.

(358) Velasco, S.; Kedaigle, A. J.; Simmons, S. K.; Nash, A.; Rocha, M.; Quadrato, G.; Paulsen, B.; Nguyen, L.; Adiconis, X.; Regev, A.; Levin, J. Z.; Arlotta, P. Individual Brain Organoids Reproducibly Form Cell Diversity of the Human Cerebral Cortex. *Nature* **2019**, *570*, 523−527.

(359) Bruens, L.; Snippert, H. J. G. Expanding the Tissue Toolbox: Deriving Colon Tissue from Human Pluripotent Stem Cells. *Cell Stem Cell* **2017**, *21*, 3−5.

(360) Takebe, T.; Zhang, B.; Radisic, M. Synergistic Engineering: Organoids Meet Organs-on-a-Chip. *Cell. Stem Cell.* **2017**, *21*, 297−300.

(361) Romanazzo, S.; Nemec, S.; Roohani, I. IPSC Bioprinting: Where Are We At? *Materials* **2019**, *12*, 2453.

(362) Carvalho, J. L. Characterization of Decellularized Heart Matrices as Biomaterials for Regular and Whole Organ Tissue Engineering and Initial In-Vitro Recellularization with Ips Cells. *J. Tissue Sci. Eng.* **2012**, *S11*, 002.

(363) Jang, J.; Park, H. J.; Kim, S. W.; Kim, H.; Park, J. Y.; Na, S. J.; Kim, H. J.; Park, M. N.; Choi, S. H.; Park, S. H.; Kim, S. W.; Kwon, S. M.; Kim, P. J.; Cho, D. W. 3D Printed Complex Tissue Construct Using Stem Cell-Laden Decellularized Extracellular Matrix Bioinks for Cardiac Repair. *Biomaterials* **2017**, *112*, 264−274.

(364) Braam, S. R.; Zeinstra, L.; Litjens, S.; Ward-Van Oostwaard, D.; van den Brink, S.; van Laake, L.; Lebrin, F.; Kats, P.; Hochstenbach, R.; Passier, R.; Sonnenberg, A.; Mummery, C. L. Recombinant Vitronectin Is a Functionally Defined Substrate That Supports Human Embryonic Stem Cell Self-Renewal via AVβ5 Integrin. *Stem Cells* **2008**, *26*, 2257−2265.

(365) Baxter, M. A.; Camarasa, M. V.; Bates, N.; Small, F.; Murray, P.; Edgar, D.; Kimber, S. J. Analysis of the Distinct Functions of Growth Factors and Tissue Culture Substrates Necessary for the Long-Term Self-Renewal of Human Embryonic Stem Cell Lines. *Stem Cell Res.* **2009**, *3*, 28−38.

(366) Vitillo, L.; Baxter, M.; Iskender, B.; Whiting, P.; Kimber, S. J. Integrin-Associated Focal Adhesion Kinase Protects Human Embryonic Stem Cells from Apoptosis, Detachment, and Differentiation. *Stem Cell Rep.* **2016**, *7*, 167−176.

(367) Stubb, A.; Guzmán, C.; Närvä, E.; Aaron, J.; Chew, T. L.; Saari, M.; Miihkinen, M.; Jacquemet, G.; Ivaska, J. Superresolution Architecture of Cornerstone Focal Adhesions in Human Pluripotent Stem. *Nat. Commun.* **2019**, *10*, 4756.

(368) Zhao, C.; Lin, K.; Wang, X. Maintenance and Modulation of Stem Cells Stemness Based on Biomaterial Designing via Chemical and Physical Signals. *Applied Materials Today* **2020**, *19*, 100614.

(369) Oldershaw, R. A.; Baxter, M. A.; Lowe, E. T.; Bates, N.; Grady, L. M.; Soncin, F.; Brison, D. R.; Hardingham, T. E.; Kimber, S. J. Directed Differentiation of Human Embryonic Stem Cells toward Chondrocytes. *Nat. Biotechnol.* **2010**, *28*, 1187−1194.

(370) Kelleher, J.; Dickinson, A.; Cain, S.; Hu, Y.; Bates, N.; Harvey, A.; Ren, J.; Zhang, W.; Moreton, F. C.; Muir, K. W.; Ward, C.; Touyz, R. M.; Sharma, P.; Xu, Q.; Kimber, S. J.; Wang, T. Patient-Specific IPSC Model of a Genetic Vascular Dementia Syndrome Reveals Failure of Mural Cells to Stabilize Capillary Structures. *Stem Cell Rep.* **2019**, *13*, 817−831.

(371) Wang, T.; Nimkingratana, P.; Smith, C. A.; Cheng, A.; Hardingham, T. E.; Kimber, S. J. Enhanced Chondrogenesis from Human Embryonic Stem Cells. *Stem Cell Res.* **2019**, *39*, 101497.

(372) Adams, W. J.; Zhang, Y.; Cloutier, J.; Kuchimanchi, P.; Newton, G.; Sehrawat, S.; Aird, W. C.; Mayadas, T. N.; Luscinskas, F. W.; García-Cardeña, G. Functional Vascular Endothelium Derived from Human Induced Pluripotent Stem Cells. *Stem Cell Rep.* **2013**, *1*, 105−113.

(373) Orlova, V. V.; Van Den Hil, F. E.; Petrus-Reurer, S.; Drabsch, Y.; Ten Dijke, P.; Mummery, C. L. Generation, Expansion and Functional Analysis of Endothelial Cells and Pericytes Derived from Human Pluripotent Stem Cells. *Nat. Protoc.* **2014**, *9*, 1514−1531.

(374) Stebbins, M. J.; Gastfriend, B. D.; Canfield, S. G.; Lee, M. S.; Richards, D.; Faubion, M. G.; Li, W. J.; Daneman, R.; Palecek, S. P.; Shusta, E. V. Human Pluripotent Stem Cell−Derived Brain Pericyte−like Cells Induce Blood-Brain Barrier Properties. *Sci. Adv.* **2019**, *5*, No. eaau7375.

(375) Loh, K. M. M.; Chen, A.; Koh, P. W. W.; Deng, T. Z. Z.; Sinha, R.; Tsai, J. M. M.; Barkal, A. A. A.; Shen, K. Y. Y.; Jain, R.; Morganti, R. M. M.; Shyh-Chang, N.; Fernhoff, N. B. B.; George, B. M. M.; Wernig, G.; Salomon, R. E. E. A.; Chen, Z.; Vogel, H.; Epstein, J. A. A.; Kundaje, A.; Talbot, W. S. S.; Beachy, P. A. A.; Ang, L. T. T.; Weissman, I. L. L. Mapping the Pairwise Choices Leading from Pluripotency to Human Bone, Heart, and Other Mesoderm Cell Types. *Cell* **2016**, *166*, 451−467.

(376) Grigoryan, B.; Paulsen, S. J.; Corbett, D. C.; Sazer, D. W.; Fortin, C. L.; Zaita, A. J.; Greenfield, P. T.; Calafat, N. J.; Gounley, J. P.; Ta, A. H.; Johansson, F.; Randles, A.; Rosenkrantz, J. E.; Louis-Rosenberg, J. D.; Galie, P. A.; Stevens, K. R.; Miller, J. S. Multivascular Networks and Functional Intravascular Topologies within Biocompatible Hydrogels. *Science* **2019**, *364*, 458−464.

(377) *ClinicalTrials.gov*; National Library of Medicine (NLM) at the National Institutes of Health (NIH), 2020; https://clinicaltrials.gov/ct2/home (accessed 2020-08-28).

(378) Da Cruz, L.; Fynes, K.; Georgiadis, O.; Kerby, J.; Luo, Y. H.; Ahmado, A.; Vernon, A.; Daniels, J. T.; Nommiste, B.; Hasan, S. M.; Gooljar, S. B.; Carr, A. J. F.; Vugler, A.; Ramsden, C. M.; Bictash, M.; Fenster, M.; Steer, J.; Harbinson, T.; Wilbrey, A.; Tufail, A.; Feng, G.; Whitlock, M.; Robson, A. G.; Holder, G. E.; Sagoo, M. S.; Loudon, P. T.; Whiting, P.; Coffey, P. J. Phase 1 Clinical Study of an Embryonic Stem Cell-Derived Retinal Pigment Epithelium Patch in Age-Related Macular Degeneration. *Nat. Biotechnol.* **2018**, *36*, 328−337.

(379) Schwartz, S. D.; Regillo, C. D.; Lam, B. L.; Eliott, D.; Rosenfeld, P. J.; Gregori, N. Z.; Hubschman, J.-P.; Davis, J. L.; Heilwell, G.; Spirn, M.; Maguire, J.; Gay, R.; Bateman, J.; Ostrick, R. M.; Morris, D.; Vincent, M.; Anglade, E.; Del Priore, L. V.; Lanza, R. Human Embryonic Stem Cell-Derived Retinal Pigment Epithelium in Patients with Age-Related Macular Degeneration and Stargardt's Macular Dystrophy: Follow-up of Two Open-Label Phase 1/2 Studies. *Lancet* **2015**, *385*, 509−516.

(380) Kashani, A. H.; Lebkowski, J. S.; Rahhal, F. M.; Avery, R. L.; Salehi-Had, H.; Dang, W.; Lin, C.-M.; Mitra, D.; Zhu, D.; Thomas, B. B.; Hikita, S. T.; Pennington, B. O.; Johnson, L. V.; Clegg, D. O.; Hinton, D. R.; Humayun, M. S. A Bioengineered Retinal Pigment Epithelial Monolayer for Advanced, Dry Age-Related Macular Degeneration. *Sci. Transl. Med.* **2018**, *10*, No. eaao4097.

(381) Liu, Y.; Xu, H. W.; Wang, L.; Li, S. Y.; Zhao, C. J.; Hao, J.; Li, Q. Y.; Zhao, T. T.; Wu, W.; Wang, Y.; Zhou, Q.; Qian, C.; Wang, L.; Yin, Z. Q. Human Embryonic Stem Cell-Derived Retinal Pigment Epithelium Transplants as a Potential Treatment for Wet Age-Related Macular Degeneration. *Cell Discovery* **2018**, *4*, 50.

(382) Mandai, M.; Watanabe, A.; Kurimoto, Y.; Hirami, Y.; Morinaga, C.; Daimon, T.; Fujihara, M.; Akimaru, H.; Sakai, N.; Shibata, Y.; Terada, M.; Nomiya, Y.; Tanishima, S.; Nakamura, M.; Kamao, H.; Sugita, S.; Onishi, A.; Ito, T.; Fujita, K.; Kawamata, S.; Go, M. J.; Shinohara, C.; Hata, K.; Sawada, M.; Yamamoto, M.; Ohta, S.; Ohara, Y.; Yoshida, K.; Kuwahara, J.; Kitano, Y.; Amano, N.; Umekage, M.; Kitaoka, F.; Tanaka, A.; Okada, C.; Takasu, N.; Ogawa, S.; Yamanaka, S.; Takahashi, M. Autologous Induced Stem-Cell−Derived Retinal Cells for Macular Degeneration. *N. Engl. J. Med.* **2017**, *376*, 1038−1046.

(383) Bantounas, I.; Ranjzad, P.; Tengku, F.; Silajdžić, E.; Forster, D.; Asselin, M. C.; Lewis, P.; Lennon, R.; Plagge, A.; Wang, Q.; Woolf, A. S.; Kimber, S. J. Generation of Functioning Nephrons by Implanting Human Pluripotent Stem Cell-Derived Kidney Progenitors. *Stem Cell Rep.* **2018**, *10*, 766−779.

(384) Qiu, L.; Liao, M.; Chen, A. K.; Wei, S.; Xie, S.; Reuveny, S.; Zhou, Z. D.; Hunziker, W.; Tan, E. K.; Oh, S. K. W.; Zeng, L. Immature Midbrain Dopaminergic Neurons Derived from Floor-Plate Method Improve Cell Transplantation Therapy Efficacy for Parkinson's Disease. *Stem Cells Transl. Med.* **2017**, *6*, 1803−1814.

(385) Yassin, M. A.; Leknes, K. N.; Pedersen, T. O.; Xing, Z.; Sun, Y.; Lie, S. A.; Finne-Wistrand, A.; Mustafa, K. Cell Seeding Density Is a Critical Determinant for Copolymer Scaffolds-Induced Bone Regeneration. *J. Biomed. Mater. Res., Part A* **2015**, *103*, 3649−3658.

(386) Barker, R. A.; Parmar, M.; Studer, L.; Takahashi, J. Human Trials of Stem Cell-Derived Dopamine Neurons for Parkinson's Disease: Dawn of a New Era. *Cell Stem Cell* **2017**, *21*, 569−573.

(387) Studer, L. Strategies for Bringing Stem Cell-Derived Dopamine Neurons to the Clinic—The NYSTEM Trial. *Prog. Brain Res.* **2017**, *230*, 191−212.

(388) Parmar, M.; Grealish, S.; Henchcliffe, C. The Future of Stem Cell Therapies for Parkinson Disease. *Nat. Rev. Neurosci.* **2020**, *21*, 103−115.

(389) Noor, N.; Shapira, A.; Edri, R.; Gal, I.; Wertheim, L.; Dvir, T. 3D Printing of Personalized Thick and Perfusable Cardiac Patches and Hearts. *Adv. Sci.* **2019**, 1900344.

(390) Arai, K.; Murata, D.; Verissimo, A. R.; Mukae, Y.; Itoh, M.; Nakamura, A.; Morita, S.; Nakayama, K. Fabrication of Scaffold-Free Tubular Cardiac Constructs Using a Bio-3D Printer. *PLoS One* **2018**, *13*, e0209162.

(391) Zhang, Y. S.; Arneri, A.; Bersini, S.; Shin, S.-R.; Zhu, K.; Goli-Malekabadi, Z.; Aleman, J.; Colosi, C.; Busignani, F.; Dell'Erba, V.; Bishop, C.; Shupe, T.; Demarchi, D.; Moretti, M.; Rasponi, M.; Dokmeci, M. R.; Atala, A.; Khademhosseini, A. Bioprinting 3D Microfibrous Scaffolds for Engineering Endothelialized Myocardium and Heart-on-a-Chip. *Biomaterials* **2016**, *110*, 45−59.

(392) Wang, Z.; Lee, S. J.; Cheng, H. J.; Yoo, J. J.; Atala, A. 3D Bioprinted Functional and Contractile Cardiac Tissue Constructs. *Acta Biomater.* **2018**, *70*, 48−56.

(393) Liu, J.; He, J.; Liu, J.; Ma, X.; Chen, Q.; Lawrence, N.; Zhu, W.; Xu, Y.; Chen, S. Rapid 3D Bioprinting of in Vitro Cardiac Tissue Models Using Human Embryonic Stem Cell-Derived Cardiomyocytes. *Bioprinting* **2019**, *13*, e00040.

(394) Yu, C.; Ma, X.; Zhu, W.; Wang, P.; Miller, K. L.; Stupin, J.; Koroleva-Maharajh, A.; Hairabedian, A.; Chen, S. Scanningless and Continuous 3D Bioprinting of Human Tissues with Decellularized Extracellular Matrix. *Biomaterials* **2019**, *194*, 1−13.

(395) Liu, J.; He, J.; Liu, J.; Ma, X.; Chen, Q.; Lawrence, N.; Zhu, W.; Xu, Y.; Chen, S. Rapid 3D Bioprinting of in Vitro Cardiac Tissue Models Using Human Embryonic Stem Cell-Derived Cardiomyocytes. *Bioprinting* **2019**, *13*, e00040.

(396) Murphy, W.; Black, J.; Hastings, G. *Handbook of Biomaterial Properties*, 2nd ed.; Springer, 2016; pp 1−676.

(397) Yao, J. Q.; Seedhom, B. B. Mechanical Conditioning Of Articular Cartilage To Prevalent Stresses. *Rheumatology* **1993**, *32*, 956−965.

(398) Nguyen, D.; Haegg, D. A.; Forsman, A.; Ekholm, J.; Nimkingratana, P.; Brantsing, C.; Kalogeropoulos, T.; Zaunz, S.; Concaro, S.; Brittberg, M.; Lindahl, A.; Gatenholm, P.; Enejder, A.; Simonsson, S. Cartilage Tissue Engineering by the 3D Bioprinting of IPS Cells in a Nanocellulose/Alginate Bioink. *Sci. Rep.* **2017**, *7*, 658.

(399) Lam, T.; Dehne, T.; Krüger, J. P.; Hondke, S.; Endres, M.; Thomas, A.; Lauster, R.; Sittinger, M.; Kloke, L. Photopolymerizable Gelatin and Hyaluronic Acid for Stereolithographic 3D Bioprinting of Tissue-Engineered Cartilage. *J. Biomed. Mater. Res., Part B* **2019**, *107*, 2649.

(400) Yeo, M.; Kim, G. Cell-Printed Hierarchical Scaffolds Consisting of Micro-Sized Polycaprolactone (PCL) and Electrospun PCL Nanofibers/Cell-Laden Alginate Struts for Tissue Regeneration. *J. Mater. Chem. B* **2014**, *2*, 314−324.

(401) Duarte Campos, D. F.; Blaeser, A.; Buellesbach, K.; Sen, K. S.; Xun, W.; Tillmann, W.; Fischer, H. Bioprinting Organotypic Hydrogels with Improved Mesenchymal Stem Cell Remodeling and Mineralization Properties for Bone Tissue Engineering. *Adv. Healthcare Mater.* **2016**, *5*, 1336−1345.

(402) Gao, G.; Schilling, A. F.; Hubbell, K.; Yonezawa, T.; Truong, D.; Hong, Y.; Dai, G.; Cui, X. Improved Properties of Bone and Cartilage Tissue from 3D Inkjet-Bioprinted Human Mesenchymal Stem Cells by Simultaneous Deposition and Photocrosslinking in PEG-GelMA. *Biotechnol. Lett.* **2015**, *37*, 2349−2355.

(403) Schuurman, W.; Khristov, V.; Pot, M. W.; van Weeren, P. R.; Dhert, W. J. A.; Malda, J. Bioprinting of Hybrid Tissue Constructs with Tailorable Mechanical Properties. *Biofabrication* **2011**, *3*, 021001.

(404) Mekhileri, N. V.; Lim, K. S.; Brown, G. C. J.; Mutreja, I.; Schon, B. S.; Hooper, G. J.; Woodfield, T. B. F. Automated 3D Bioassembly of Micro-Tissues for Biofabrication of Hybrid Tissue Engineered Constructs. *Biofabrication* **2018**, *10*, 024103.

(405) Stichler, S.; Bock, T.; Paxton, N. C.; Bertlein, S.; Levato, R.; Schill, V.; Smolan, W.; Malda, J.; Tessmar, J.; Blunk, T.; Groll, J. Double Printing of Hyaluronic Acid/Poly(Glycidol) Hybrid Hydrogels with Poly(Epsilon-Caprolactone) for MSC Chondrogenesis. *Biofabrication* **2017**, *9*, 044108.

(406) Yousefi, A.-M.; Hoque, M. E.; Prasad, R. G. S. V; Uth, N. Current Strategies in Multiphasic Scaffold Design for Osteochondral Tissue Engineering: A Review. *J. Biomed. Mater. Res., Part A* **2015**, *103*, 2460−2481.

(407) Park, J. Y.; Choi, J.-C.; Shim, J.-H.; Lee, J.-S.; Park, H.; Kim, S. W.; Doh, J.; Cho, D.-W. A Comparative Study on Collagen Type I and Hyaluronic Acid Dependent Cell Behavior for Osteochondral Tissue Bioprinting. *Biofabrication* **2014**, *6*, 035004.

(408) Choi, Y. J.; Kim, T. G.; Jeong, J.; Yi, H. G.; Park, J. W.; Hwang, W.; Cho, D. W. 3D Cell Printing of Functional Skeletal Muscle Constructs Using Skeletal Muscle-Derived Bioink. *Adv. Healthcare Mater.* **2016**, *5*, 2636−2645.

(409) Laternser, S.; Keller, H.; Leupin, O.; Rausch, M.; Graf-Hausner, U.; Rimann, M. A Novel Microplate 3D Bioprinting Platform for the Engineering of Muscle and Tendon Tissues. *SLAS Technol.* **2018**, *23*, 599−613.

(410) Castilho, M.; Mouser, V.; Chen, M.; Malda, J.; Ito, K. Bi-Layered Micro-Fibre Reinforced Hydrogels for Articular Cartilage Regeneration. *Acta Biomater.* **2019**, *95*, 297−306.

(411) Chai, D. H.; Arner, E. C.; Griggs, D. W.; Grodzinsky, A. J. Av and B1 Integrins Regulate Dynamic Compression-Induced Proteoglycan Synthesis in 3D Gel Culture by Distinct Complementary Pathways. *Osteoarthr. Cartil.* **2010**, *18*, 249−256.

(412) Sakthivel, K.; Kumar, H.; Mohamed, M. G. A.; Talebjedi, B.; Shim, J.; Najjaran, H.; Hoorfar, M.; Kim, K. High Throughput Screening of Cell Mechanical Response Using a Stretchable 3D Cellular Microarray Platform. *Small* **2020**, *16*, 2000941.

(413) Waldman, S. D.; Spiteri, C. G.; Grynpas, M. D.; Pilliar, R. M.; Kandel, R. A. Long-Term Intermittent Shear Deformation Improves the Quality of Cartilaginous Tissue Formed in Vitro. *J. Orthop. Res.* **2003**, *21*, 590−596.

(414) Metcalfe, A. D.; Ferguson, M. W. J. Tissue Engineering of Replacement Skin: The Crossroads of Biomaterials, Wound Healing, Embryonic Development, Stem Cells and Regeneration. *J. R. Soc., Interface* **2007**, *4*, 413−417.

(415) Derr, K.; Zou, J.; Luo, K.; Song, M. J.; Sittampalam, G. S.; Zhou, C.; Michael, S.; Ferrer, M.; Derr, P. Fully Three-Dimensional Bioprinted Skin Equivalent Constructs with Validated Morphology and Barrier Function. *Tissue Eng., Part C* **2019**, *25*, 334−343.

(416) Trasatti, J. P.; Yoo, S.-S.; Singh, G.; Xu, X.; Lee, V.; Tran, T. N.; Dai, G.; Bjornsson, C.; Karande, P. Design and Fabrication of Human Skin by Three-Dimensional Bioprinting. *Tissue Eng., Part C* **2014**, *20*, 473−484.

(417) Pourchet, L. J.; Thepot, A.; Albouy, M.; Courtial, E. J.; Boher, A.; Blum, L. J.; Marquette, C. A. Human Skin 3D Bioprinting Using Scaffold-Free Approach. *Adv. Healthcare Mater.* **2017**, *6*, 1601101.

(418) Pereira, R. F.; Sousa, A.; Barrias, C. C.; Bártolo, P. J.; Granja, P. L. A Single-Component Hydrogel Bioink for Bioprinting of Bioengineered 3D Constructs for Dermal Tissue Engineering. *Mater. Horiz.* **2018**, *5*, 1100−1111.

(419) Kim, B. S.; Lee, J.-S.; Gao, G.; Cho, D.-W. Direct 3D Cell-Printing of Human Skin with Functional Transwell System. *Biofabrication* **2017**, *9*, 025034.

(420) Liu, N.; Huang, S.; Yao, B.; Xie, J.; Wu, X.; Fu, X. 3D Bioprinting Matrices with Controlled Pore Structure and Release Function Guide in Vitro Self-Organization of Sweat Gland. *Sci. Rep.* **2016**, *6*, 34410.

(421) Huang, S.; Yao, B.; Xie, J.; Fu, X. 3D Bioprinted Extracellular Matrix Mimics Facilitate Directed Differentiation of Epithelial Progenitors for Sweat Gland Regeneration. *Acta Biomater.* **2016**, *32*, 170−177.

(422) Abaci, H. E.; Coffman, A.; Doucet, Y.; Chen, J.; Jacków, J.; Wang, E.; Guo, Z.; Shin, J. U.; Jahoda, C. A.; Christiano, A. M. Tissue Engineering of Human Hair Follicles Using a Biomimetic Developmental Approach. *Nat. Commun.* **2018**, *9*, 5301.

(423) Ma, X.; Qu, X.; Zhu, W.; Li, Y. S.; Yuan, S.; Zhang, H.; Liu, J.; Wang, P.; Lai, C. S. E.; Zanella, F.; Feng, G. S.; Sheikh, F.; Chien, S.; Chen, S. Deterministically Patterned Biomimetic Human IPSC-Derived Hepatic Model via Rapid 3D Bioprinting. *Proc. Natl. Acad. Sci. U. S. A.* **2016**, *113*, 2206−2211.

(424) Madden, L. R.; Nguyen, T. V.; Garcia-Mojica, S.; Shah, V.; Le, A. V.; Peier, A.; Visconti, R.; Parker, E. M.; Presnell, S. C.; Nguyen, D. G.; Retting, K. N. Bioprinted 3D Primary Human Intestinal Tissues Model Aspects of Native Physiology and ADME/Tox Functions. *iScience* **2018**, *2*, 156−167.

(425) Homan, K. A.; Kolesky, D. B.; Skylar-Scott, M. A.; Herrmann, J.; Obuobi, H.; Moisan, A.; Lewis, J. A. Bioprinting of 3D Convoluted Renal Proximal Tubules on Perfusable Chips. *Sci. Rep.* **2016**, *6*, 34805.

(426) Bhise, N. S.; Massa, S.; Shin, S. R.; Khademhosseini, A.; Manoharan, V.; Annabi, N.; Atala, A.; Miscuglio, M.; Bishop, C. E.; Calzone, G.; Tamayol, A.; Shupe, T. D.; Ghaderi, M.; Lang, Q.; Dokmeci, M. R.; Shrike Zhang, Y. A Liver-on-a-Chip Platform with Bioprinted Hepatic Spheroids. *Biofabrication* **2016**, *8*, 014101.

(427) Chang, R.; Emami, K.; Wu, H.; Sun, W. Biofabrication of a Three-Dimensional Liver Micro-Organ as an in Vitro Drug Metabolism Model. *Biofabrication* **2010**, *2*, 045004.

(428) Knowlton, S.; Tasoglu, S. A Bioprinted Liver-on-a-Chip for Drug Screening Applications. *Trends Biotechnol.* **2016**, *34*, 681−682.

(429) Lee, H.; Cho, D.-W. One-Step Fabrication of an Organ-on-a-Chip with Spatial Heterogeneity Using a 3D Bioprinting Technology. *Lab Chip* **2016**, *16*, 2618−2625.

(430) Kim, Y.; Kang, K.; Jeong, J.; Paik, S. S.; Kim, J. S.; Park, S. A.; Kim, W. D.; Park, J.; Choi, D. Three-Dimensional (3D) Printing of Mouse Primary Hepatocytes to Generate 3D Hepatic Structure. *Ann. Surg. Treat. Res.* **2017**, *92*, 67−72.

(431) Lee, J. W.; Choi, Y.; Yong, W.; Pati, F.; Shim, J.; Kang, K. S.; Kang, I.-H.; Park, J.; Cho, D.-W. Development of a 3D Cell Printed

Construct Considering Angiogenesis for Liver Tissue Engineering. *Biofabrication* **2016**, *8*, 015007.

(432) Nguyen, D. G.; Funk, J.; Robbins, J. B.; Crogan-Grundy, C.; Presnell, S. C.; Singer, T.; Roth, A. B. Bioprinted 3D Primary Liver Tissues Allow Assessment of Organ-Level Response to Clinical Drug Induced Toxicity In Vitro. *PLoS One* **2016**, *11*, No. e0158674.

(433) Thummel, K. E.; Kunze, K. L.; Shen, D. D. Enzyme-Catalyzed Processes of First-Pass Hepatic and Intestinal Drug Extraction. *Adv. Drug Delivery Rev.* **1997**, *27*, 99−127.

(434) Kizawa, H.; Nagao, E.; Shimamura, M.; Zhang, G.; Torii, H. Scaffold-Free 3D Bio-Printed Human Liver Tissue Stably Maintains Metabolic Functions Useful for Drug Discovery. *Biochem. Biophys. Reports* **2017**, *10*, 186−191.

(435) Norona, L. M.; Nguyen, D. G.; Gerber, D. A.; Presnell, S. C.; LeCluyse, E. L. Modeling Compound-Induced Fibrogenesis In Vitro Using Three-Dimensional Bioprinted Human Liver Tissues. *Toxicol. Sci.* **2016**, *154*, 354−367.

(436) Lee, V. K.; Lanzi, A. M.; Ngo, H.; Yoo, S. S.; Vincent, P. A.; Dai, G. Generation of Multi-Scale Vascular Network System within 3D Hydrogel Using 3D Bio-Printing Technology. *Cell. Mol. Bioeng.* **2014**, *7*, 460−472.

(437) Schöneberg, J.; De Lorenzi, F.; Theek, B.; Blaeser, A.; Rommel, D.; Kuehne, A. J. C.; Kießling, F.; Fischer, H. Engineering Biofunctional in Vitro Vessel Models Using a Multilayer Bioprinting Technique. *Sci. Rep.* **2018**, *8*, 10430.

(438) Skylar-Scott, M. A.; Uzel, S. G. M.; Nam, L. L.; Ahrens, J. H.; Truby, R. L.; Damaraju, S.; Lewis, J. A. Biomanufacturing of Organ-Specific Tissues with High Cellular Density and Embedded Vascular Channels. *Sci. Adv.* **2019**, *5*, No. eaaw2459.

(439) Massa, S.; Sakr, M. A.; Seo, J.; Bandaru, P.; Arneri, A.; Bersini, S.; Zare-Eelanjegh, E.; Jalilian, E.; Cha, B. H.; Antona, S.; Enrico, A.; Gao, Y.; Hassan, S.; Acevedo, J. P.; Dokmeci, M. R.; Zhang, Y. S.; Khademhosseini, A.; Shin, S. R. Bioprinted 3D Vascularized Tissue Model for Drug Toxicity Analysis. *Biomicrofluidics* **2017**, *11*, 044109.

(440) Zhang, Y. S.; Davoudi, F.; Walch, P.; Manbachi, A.; Luo, X.; Dell'Erba, V.; Miri, A. K.; Albadawi, H.; Arneri, A.; Li, X.; Wang, X.; Dokmeci, M. R.; Khademhosseini, A.; Oklu, R. Bioprinted Thrombosis-on-a-Chip. *Lab Chip* **2016**, *16*, 4097−4105.

(441) Dai, X.; Ma, C.; Lan, Q.; Xu, T. 3D Bioprinted Glioma Stem Cells for Brain Tumor Model and Applications of Drug Susceptibility. *Biofabrication* **2016**, *8*, 045005.

(442) Heinrich, M. A.; Bansal, R.; Lammers, T.; Zhang, Y. S.; Michel Schiffelers, R.; Prakash, J. 3D-Bioprinted Mini-Brain: A Glioblastoma Model to Study Cellular Interactions and Therapeutics. *Adv. Mater.* **2019**, *31*, 1806590.

(443) Lee, C.; Abelseth, E.; de la Vega, L.; Willerth, S. M. Bioprinting a Novel Glioblastoma Tumor Model Using a Fibrin-Based Bioink for Drug Screening. *Mater. Today Chem.* **2019**, *12*, 78−84.

(444) Xu, F.; Celli, J.; Rizvi, I.; Moon, S.; Hasan, T.; Demirci, U. A Three-Dimensional in Vitro Ovarian Cancer Coculture Model Using a High-Throughput Cell Patterning Platform. *Biotechnol. J.* **2011**, *6*, 204−212.

(445) Zhao, Y.; Yao, R.; Ouyang, L.; Ding, H.; Zhang, T.; Zhang, K.; Cheng, S.; Sun, W. Three-Dimensional Printing of Hela Cells for Cervical Tumor Model in Vitro. *Biofabrication* **2014**, *6*, 035001.

(446) Langer, E. M.; Allen-Petersen, B. L.; King, S. M.; Kendsersky, N. D.; Turnidge, M. A.; Kuziel, G. M.; Riggers, R.; Samatham, R.; Amery, T. S.; Jacques, S. L.; Sheppard, B. C.; Korkola, J. E.; Muschler, J. L.; Thibault, G.; Chang, Y. H.; Gray, J. W.; Presnell, S. C.; Nguyen, D. G.; Sears, R. C. Modeling Tumor Phenotypes In Vitro with Three-Dimensional Bioprinting. *Cell Rep.* **2019**, *26*, 608−623 e6.

(447) Meng, F.; Meyer, C. M.; Joung, D.; Vallera, D. A.; McAlpine, M. C.; Panoskaltsis-Mortari, A. 3D Bioprinted In Vitro Metastatic Models via Reconstruction of Tumor Microenvironments. *Adv. Mater.* **2019**, *31*, 1806899.

(448) Jiang, T.; Munguia-Lopez, J. G.; Flores-Torres, S.; Grant, J.; Vijayakumar, S.; Leon-Rodriguez, A. De; Kinsella, J. M. Directing the Self-Assembly of Tumour Spheroids by Bioprinting Cellular Heterogeneous Models within Alginate/Gelatin Hydrogels. *Sci. Rep.* **2017**, *7*, 4575.

(449) Zhou, X.; Zhu, W.; Nowicki, M.; Miao, S.; Cui, H.; Holmes, B.; Glazer, R. I.; Zhang, L. G. 3D Bioprinting a Cell-Laden Bone Matrix for Breast Cancer Metastasis Study. *ACS Appl. Mater. Interfaces* **2016**, *8*, 30017−30026.

(450) Wang, X.; Li, X.; Dai, X.; Zhang, X.; Zhang, J.; Xu, T.; Lan, Q. Coaxial Extrusion Bioprinted Shell-Core Hydrogel Microfibers Mimic Glioma Microenvironment and Enhance the Drug Resistance of Cancer Cells. *Colloids Surf., B* **2018**, *171*, 291−299.

(451) Bernal, P. N.; Delrot, P.; Loterie, D.; Li, Y.; Malda, J.; Moser, C.; Levato, R. Volumetric Bioprinting of Complex Living-Tissue Constructs within Seconds. *Adv. Mater.* **2019**, *31*, 1904209.

(452) Adine, C.; Ng, K. K.; Rungarunlert, S.; Souza, G. R.; Ferreira, J. N. Engineering Innervated Secretory Epithelial Organoids by Magnetic Three-Dimensional Bioprinting for Stimulating Epithelial Growth in Salivary Glands. *Biomaterials* **2018**, *180*, 52−66.

(453) Rajkovic, O.; Potjewyd, G.; Pinteaux, E. Regenerative Medicine Therapies for Targeting Neuroinflammation after Stroke. *Front. Neurol.* **2018**, *9*, 734.

(454) Shanjani, Y.; Pan, C. C.; Elomaa, L.; Yang, Y. A Novel Bioprinting Method and System for Forming Hybrid Tissue Engineering Constructs. *Biofabrication* **2015**, *7*, 045008.

(455) de Ruijter, M.; Ribeiro, A.; Dokter, I.; Castilho, M.; Malda, J. Simultaneous Micropatterning of Fibrous Meshes and Bioinks for the Fabrication of Living Tissue Constructs. *Adv. Healthcare Mater.* **2019**, *8*, 1800418.

(456) Miao, S.; Zhu, W.; Castro, N. J.; Nowicki, M.; Zhou, X.; Cui, H.; Fisher, J. P.; Zhang, L. G. 4D Printing Smart Biomedical Scaffolds with Novel Soybean Oil Epoxidized Acrylate. *Sci. Rep.* **2016**, *6*, 27226.

(457) Cui, H.; Liu, C.; Esworthy, T.; Huang, Y.; Yu, Z.; Zhou, X.; San, H.; Lee, S.; Hann, S. Y.; Boehm, M.; Mohiuddin, M.; Fisher, J. P.; Zhang, L. G. 4D Physiologically Adaptable Cardiac Patch: A 4-Month in Vivo Study for the Treatment of Myocardial Infarction. *Sci. Adv.* **2020**, *6*, No. eabb5067.

(458) Hendrikson, W.; Rouwkema, J.; Clementi, F.; van Blitterswijk, C. A.; Fare, S.; Moroni, L. Towards 4D Printed Scaffolds for Tissue Engineering: Exploiting 3D Shape Memory Polymers to Deliver Time-Controlled Stimulus on Cultured Cells. *Biofabrication* **2017**, *9*, 031001.

(459) Goktas, M.; Blank, K. G. Molecular Force Sensors: From Fundamental Concepts toward Applications in Cell Biology. *Adv. Mater. Interfaces* **2017**, *4*, 1600441.

(460) Loebel, C.; Mauck, R. L.; Burdick, J. A. Local Nascent Protein Deposition and Remodelling Guide Mesenchymal Stromal Cell Mechanosensing and Fate in Three-Dimensional Hydrogels. *Nat. Mater.* **2019**, *18*, 883−891.

(461) Khetan, S.; Guvendiren, M.; Legant, W. R.; Cohen, D. M.; Chen, C. S.; Burdick, J. A. Degradation-Mediated Cellular Traction Directs Stem Cell Fate in Covalently Crosslinked Three-Dimensional Hydrogels. *Nat. Mater.* **2013**, *12*, 458−465.

(462) Lancaster, M. A.; Knoblich, J. A. Organogenesis in a Dish: Modeling Development and Disease Using Organoid Technologies. *Science* **2014**, *345*, 1247125−1247125.

(463) Schneeberger, K.; Spee, B.; Costa, P.; Sachs, N.; Clevers, H.; Malda, J. Converging Biofabrication and Organoid Technologies: The next Frontier in Hepatic and Intestinal Tissue Engineering? *Biofabrication* **2017**, *9*, 013001.

(464) Grebenyuk, S.; Ranga, A. Engineering Organoid Vascularization. *Front. Bioeng. Biotechnol.* **2019**, *7*, 39.

(465) Skardal, A.; Murphy, S. V.; Devarasetty, M.; Mead, I.; Kang, H.-W.; Seol, Y.-J.; Shrike Zhang, Y.; Shin, S.-R.; Zhao, L.; Aleman, J.; Hall, A. R.; Shupe, T. D.; Kleensang, A.; Dokmeci, M. R.; Jin Lee, S.; Jackson, J. D.; Yoo, J. J.; Hartung, T.; Khademhosseini, A.; Soker, S.; Bishop, C. E.; Atala, A. Multi-Tissue Interactions in an Integrated Three-Tissue Organ-on-a-Chip Platform. *Sci. Rep.* **2017**, *7*, 8837.

(466) Miri, A. K.; Nieto, D.; Iglesias, L.; Goodarzi Hosseinabadi, H.; Maharjan, S.; Ruiz-Esparza, G. U.; Khoshakhlagh, P.; Manbachi, A.; Dokmeci, M. R.; Chen, S.; Shin, S. R.; Zhang, Y. S.; Khademhosseini,

A. Microfluidics-Enabled Multimaterial Maskless Stereolithographic Bioprinting. *Adv. Mater.* **2018**, *30*, 1800242.

(467) *3D Bioprinting Market by Component (3D Bioprinters (Microextrusion, Inkjet, Laser), Bioink (Natural, Synthetic, Hybrid)), Material (Hydrogel, Living Cells), Application (Skin, Drug Research), End user (Biopharma, Academia) - Global Forecast to 2024*; MarketsandMarkets, 2020; https://www.marketsandmarkets.com/Market-Reports/3d-bioprinting-market-170201787.html?gclid=Cj0KCQjws536BRDTARIsANeUZ5_66uiBvJelGwvGhe5uo6E_t5MhQdScEGFP_EYgiiSbBiYoCserchYaAv_KEALw_wcB (accessed 2020-08-27).

(468) Costa, P. F. Translating Biofabrication to the Market. *Trends Biotechnol.* **2019**, *37*, 1032−1036.

(469) Vijayavenkataraman, S.; Lu, W. F.; Fuh, J. Y. H. 3D Bioprinting − An Ethical, Legal and Social Aspects (ELSA) Framework. *Bioprinting* **2016**, *1−2*, 11−21.